TECHNISCHE UNIVERSITÄT
ILMENAU

Multiple Resource Reuse for Device-to-Device Communication in Future Cellular Networks

PhD Thesis

by

Abubaker Matovu Waswa

Reviewers

Prof. Dr.-Ing. habil. Andreas Mitschele-Thiel

Prof. Dr. rer. nat. Jochen Seitz

Prof. Dr.-Ing. Jens Mückenheim

A dissertation to obtain the academic degree Doktoringenieur (Dr.-Ing.) submitted to the Faculty of Computer Science and Automation, Technische Universität Ilmenau

submitted on: 28.02.2020
defended on: 07.10.2020

urn:nbn:de:gbv:ilm1-2020000437

TECHNISCHE UNIVERSITÄT
ILMENAU

Multiple Resource Reuse for Device-to-Device Communication in Future Cellular Networks

Dissertation

von

Abubaker Matovu Waswa

Gutachter

Prof. Dr.-Ing. habil. Andreas Mitschele-Thiel

Prof. Dr. rer. nat. Jochen Seitz

Prof. Dr.-Ing. Jens Mückenheim

Dissertation zur Erlangung des akademischen Grades Doktoringenieur (Dr.-Ing.)
vorgelegt der Fakultät für Informatik und Automatisierung der Technischen
Universität Ilmenau

eingereicht am: 28.02.2020
verteidigt am: 07.10.2020

urn:nbn:de:gbv:ilm1-2020000437

Abstract

Owing to the further proliferation of new mobile applications, e.g. autonomous driving, automated process control, smart cities/homes, and tactile internet, the number and density of devices requiring wireless connectivity continue to increase. This demands ever more efficient methods for utilizing the available frequency spectrum for cellular networks. To counter this challenge, approaches like spectrum sharing have been proposed as enablers to improve the overall spectral efficiency. Device to device communication (D2D) as an underlaying transmission to the cellular network presents spectral efficiency improvements through the increased sharing of the available cellular spectrum. In D2D, devices in close proximity communicate directly with each other having either minimal or no control from the cellular network.

The third generation partnership project (3GPP) supports, through standardization, the integration of D2D within cellular networks in order to realize the spectral efficiency gains during spectrum sharing and user quality of service (QoS) guarantees. However, the interference between D2D and cellular users during spectrum sharing must be controlled to get these gains in the network. This thesis studies the solutions through which the cellular network's frequency spectrum can be shared with D2D users to concurrently maximize the spectral efficiency and achieve all users' QoS requirements (in terms of threshold signal-to-interference-plus-noise ratio (SINR)).

The thesis is divided into two parts: an analytical study and an algorithmic study. First, the analytical study evaluates the framework for interference management when several D2D users share the cellular network's spectrum. Therein, uniform interference power (UIP) allocation – a scheme where all D2D users contribute equal interference at the base station (BS), is proposed. This scheme is applied to a single-cell scenario with very positive results in improving spectral efficiency although some D2D users are unable to achieve their threshold SINRs.

The main lesson from the analytical study is that spatial separation between users sharing spectrum is important to minimize their mutual interference. So the algorithmic study focuses on D2D-users selection. First, spatial selection criteria are formulated with the objective of identifying multiple D2D users that can share a given cellular user's spectrum to maximize spectral efficiency while all users achieve their threshold SINRs. Thereafter, based on these criteria, two selection algorithms are developed. The first algorithm opportunistically selects D2D users causing the least interference, at given selection instances, to other users sharing the spectrum. The second algorithm randomly selects any D2D users meeting the minimal required spatial separation from other users sharing the spectrum. Both algorithms are presented with very positive results in simulations that consider a single-cell scenario with varying number of users. In a multi-cell scenario, where the experienced inter-cell interference degrades performance, enhancements to both algorithms are applied to achieve the set objectives. These enhancements adapt the selection criteria to: 1) not select cell-edge D2D users and 2) take into account the effects of spectrum sharing between neighbouring cells.

The thesis studies clearly showed that, using appropriate selection criteria, multiple D2D users can share a specific cellular user's spectrum resources to improve the network's spectral efficiency and achieve all users' QoS requirements. These findings together with other existing results on D2D spectrum resource reuse can be the starting point for further academic research and practical implementation.

Zusammenfassung

Aufgrund der stärkeren Verbreitung neuer mobiler Anwendungen, z.B. Autonomes Fahren, automatisierte Prozesssteuerung, intelligente Städte / Wohnen und taktiles Internet, nimmt - die Anzahl und Dichte von Geräten, die drahtlose Verbindungen erfordern, immer weiter zu. Dies erfordert effizientere Verfahren zur Nutzung des verfügbaren Frequenzspektrums für zellulare Netze. Um dieser Herausforderung zu begegnen, wurden Ansätze, wie die gemeinsame Nutzung von Frequenzen, vorgeschlagen, um die gesamte spektrale Effizienz zu verbessern. Die Device-to-Device Kommunikation (D2D) mit paralleler Übertragung zu einem zellularen Netz bietet eine Verbesserung der spektralen Effizienz durch die verstärkte gemeinsame Nutzung des verfügbaren zellularen Spektrums. Mit D2D kommunizieren Geräte in unmittelbarer Nähe direkt miteinander ohne oder mit nur einer minimalen Kontrolle über das Mobilfunknetz.

Das 3rd Generation Partnership Project (3GPP) unterstützt durch Standardisierung die Integration von D2D in Mobilfunknetze, um die spektralen Effizienzgewinne bei der gemeinsamen Nutzung von Frequenzen unter Gewährleistung der Quality of Service (QoS) zu realisieren. Die Interferenzen zwischen D2D und zellularen Benutzern müssen jedoch während der gemeinsamen Nutzung des Spektrums kontrolliert werden, um diese Gewinne im Netzwerk zu erhalten. Die vorliegende Arbeit untersucht Lösungen, mit denen das Frequenzspektrum des Mobilfunknetzes mit D2D-Benutzern geteilt werden kann, welche sowohl die spektrale Effizienz maximieren als auch die QoS-Anforderungen aller Benutzer erfüllen (in Bezug auf das Signal-zu-Rausch-plus-Interferenz Verhältnis (SINR)).

Die vorliegende Arbeit gliedert sich in zwei Teile: eine analytische und eine algorithmische Studie. Zunächst untersucht die analytische Studie den Ansatz für ein Interferenzmanagement, in welchem mehrere D2D-Benutzer das zellulare Spektrum gemeinsam nutzen. Dabei wird die Zuteilung einer einheitlichen Interferenzleistung (UIP) vorgeschlagen – ein Verfahren, bei dem alle D2D-Benutzer mit gleicher Interferenz an der Basisstation (BS) beitragen. Dieses Schema wird auf ein Szenario einer einzelnen Zelle angewendet, welches sehr positive Ergebnisse bei der Verbesserung der spektralen Effizienz erzielt, obwohl einige D2D-Benutzer ihre SINR-Schwellenwerte nicht erreichen können.

Eine wesentliche Erkenntnis aus der analytischen Studie ist, dass eine räumliche Trennung zwischen Benutzern, die das Spektrum gemeinsam nutzen, wichtig ist, um ihre gegenseitige Beeinflussung zu minimieren. Die algorithmische Studie konzentriert sich daher auf die Auswahl geeigneter D2D-Benutzern. Zunächst werden räumliche Auswahlkriterien formuliert mit dem Ziel, mehrere D2D-Benutzer zu identifizieren, die das Spektrum eines bestimmten Mobilfunkbenutzers gemeinsam nutzen können, um die spektrale Effizienz zu maximieren, während alle Benutzer ihre SINR-Schwellenwerte erreichen. Danach werden basierend auf diesen Kriterien zwei Auswahlalgorithmen entwickelt. Der erste Algorithmus wählt opportunistisch D2D-Benutzer aus, die bei bestimmten Auswahlinstanzen die geringste Störung für andere das Spektrum gemeinsam nutzende Benutzer verursachen. Der zweite Algorithmus wählt zufällig alle D2D-Benutzer aus, die räumliche von anderen Benutzern getrennt sind, jedoch das Spektrum gemeinsam nutzen. Beide Algorithmen werden mit sehr positiven Ergebnissen durch Simulationen in einem Szenario einer einzelnen Zelle mit einer unterschiedlichen Anzahl von Benutzern vorgestellt. In einem Szenario mit mehreren Zellen, in welchem die Interferenz zwischen den Zellen die Leistungsfähigkeit beeinträchtigt, werden Verbesserungen an beiden Algorithmen vorgestellt, um die festgelegten Ziele zu erreichen. Diese Verbesserungen

passen die Auswahlkriterien an, um: 1) keine D2D-Benutzer mit Zellenkante auszuwählen und 2) die Auswirkungen der gemeinsamen Nutzung des Frequenzspektrums zwischen benachbarten Zellen zu berücksichtigen.

Die Arbeit zeigt deutlich, dass mithilfe eines geeigneten Auswahlkriteriums mehrere D2D Nutzer in der Lage sind, die gemeinsame Frequenzressource mit zellularen Nutzern zu teilen mit Erhöhung der gesamten spektralen Effizienz und Beibehaltung der QoS Anforderungen aller Nutzer. Die hierbei erbrachten Erkenntnisse können zusammen mit den vorhandenen Ergebnissen als Ausgangspunkt für weitere akademische Forschung sowie einer praktischen Anwendung dienen.

To Aisha, Hibah, Hamim and Hisham
and to my mother Safina Lubega Magala

"Even the smallest changes in our daily routine can create incredible ripple effects that expand our vision of what is possible."

Charles F. Glassman

Acknowledgement

As I conclude my PhD work, I take this opportunity to thank all people and institutions whose unreserved support has enabled me reach this far in the quest for knowledge. I am eternally grateful to the Almighty ALLAH for HIS continued gift of life and good health to undertake the PhD task. This PhD thesis was carried out within the Integrated Communication Systems group as part of the Faculty of Computer Science and Automation. It was financed by the German Academic Exchange Service / Deutscher Akademischer Austauschdienst (DAAD) under the DAAD Research Grants for Doctoral Programmes in Germany.

First, I would like to sincerely thank my supervisor Prof. Andreas Mitschele-Thiel for his spirited guidance and providing me the freedom to exercise my ideas. Secondly, I thank my co-supervisor Prof. Jens Mückenheim for all his valuable advice throughout the PhD period and time to review my thesis. I wish to also thank Prof. Jochen Seitz for accepting to review my thesis as well as being a member of the examination board.

My gratitude is due to Dr. Stephen Mwanje from Nokia Bell Labs, Munich - Germany for the many extensive technical discussions and reviewing my publications. In the same regard, I thank my colleagues in the Integrated Communication Systems group for their critical feedbacks and constructive proposals during our research seminars and workshops. Special thanks for proofreading my complete thesis: Andreas Mitschele-Thiel, Jens Mückenheim and Stephen Mwanje. I would also like to thank our group's administrative team, especially Nicole Sauer and Jürgen Schmidt for their ever friendly assistance with the administrative tasks. They never saved any efforts to help me towards achieving my goals within the group and with whom I always felt at home.

Most importantly, I thank my entire family - my wife Aisha, children, Hibah, Hamim and Hisham, my mother and siblings - for their confidence in my work, patience and unreserved support throughout this time. Above all, Aisha's support and perseverance were fantastic, as she always motivated me to remain persistent.

Contents

List of Figures

List of Tables

CHAPTER 1

Introduction

Contents

The continuous evolution of mobile communication systems has reached the Fifth Generation (5G), which targets support of new applications e.g. autonomous driving using Vehicle-to-Vehicle (V2V) communication, automated process control through Machine Type Communication (MTC), tactile internet and real-time gaming. These new applications arise from the growing need for communication between various existing and new devices, which are redefining different aspects of life on the globe. Currently, 5G envisions an all-connected world where a multitude of devices running given applications will communicate with each other using wireless network technologies. The projections showed that almost 26 billion devices will be connected by 2020 (figure 1.1(a)) [1]. Owing to advances in cellular Internet of Things (IoT) standardization and reduced device costs, the number of IoT devices will exceed mobile phones [2]. Beyond 2020, further forecasts indicate continued exponential growth of device numbers reaching 55 and over 100 billion devices in 2025 and 2030 respectively [3] [4].

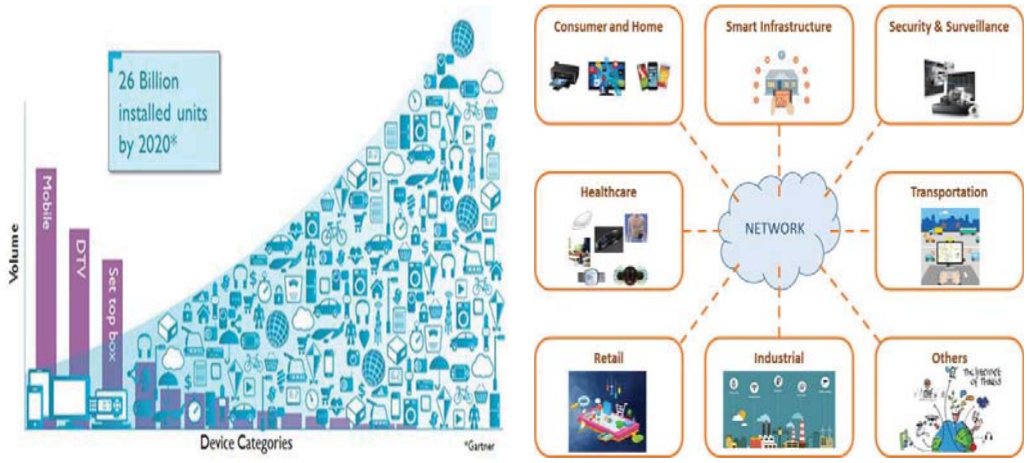

(a) Projections of devices volume.

(b) Applications of Devices.

FIGURE 1.1: Growth in volume and applications of new devices [1].

Figure 1.1(b) depicts some sectors that will benefit from the various applications running on the connected devices. Example applications include:

- Healthcare: remote patient monitoring, telemedicine, drugs delivery using drones, etc.
- Smart Infrastructure: remote metering, smart grids, smart cities, etc.
- Transportation: fleet management, traffic flow, autonomous driving, etc.
- Industrial: automation, process control, collaborative robots, etc

These applications impose demanding Quality of Service (QoS) requirements, e.g. high capacity, ultra-reliability and low latency, necessitating new and efficient techniques of network design and operation. Device-to-Device communication (D2D) presents a potential solution for connectivity of the huge device numbers due to their close proximity and high connection density. In D2D, proximate User Terminals (UTs) directly communicate with each other having either minimal or no involvement (i.e. control) of a network entity/node. The idea of D2D is already realised in the unlicensed spectrum using technologies such as Bluetooth, ZigBee, Wi-Fi direct and Near-Field Communication (NFC). However, the limitations of these technologies, e.g. short range, low throughput, limited spectrum and high interference levels make it increasingly difficult to achieve the new applications' QoS requirements [5]. Cellular networks are able to maintain users' QoS and thus will play a pivotal role in achieving the objectives of an all-connected world. Therefore, D2D promises new advantages and revolutionary opportunities or services once integrated in cellular networks. Some of the network advantages include cellular offloading [6] and multi-hop relaying [7], while the new services such as Intelligent Transport Systems (ITS) utilising vehicular networks [8] and proximity based services [9] will be made possible.

1.1 Motivations

This work is mainly incited by the need for future cellular networks to meet the high capacity demands arising from the new applications while fulfilling their reliability and latency expectations. The Third Generation Partnership Project (3GPP) has broadly classified the applications in three major categories depending on their requirements: enhanced Mobile BroadBand (eMBB) requiring very high data rates, massive Internet of Things (mIoT) demanding for capability to serve increased densities of devices and Ultra-Reliable and Low Latency Communications (URLLC) demanding support of very low latency and very high service availability [10]. These applications present very stringent capacity, reliability and latency requirements on the radio network of cellular systems. In radio networks, these requirements form a triad of competing objectives as shown in figure 1.2 [11]. Typically, operators configure their radio networks to maximize capacity at the expense of reliability and latency as shown by the red triangle. However, efforts to fullfil the stringent reliability and latency demands (e.g. for URLLC applications) adversely affects the capacity (e.g., approximately 70% capacity drop as depicted by the blue triangle). There is need for new strategies that enhance the tradeoffs among these competing requirements to minimize the capacity drop (e.g., to approximately 30%) while meeting the performance demands as shown by the green triangle.

This tradeoff demands significant improvements in spectral efficiency for the network to support the high traffic needs under such rigorous application requirements. The spectrum efficiency improvements are required both on a per user and a per cell basis [12]. The proximity gains granted by D2D presents a unique opportunity of achieving both the reliability and latency requirements while simultaneously enhancing the spectral efficiency [13]. This therefore justifies the need for studies on cellular spectrum sharing by D2D to maximize the network spectral efficiency while simultaneously fulfilling all users QoS requirements.

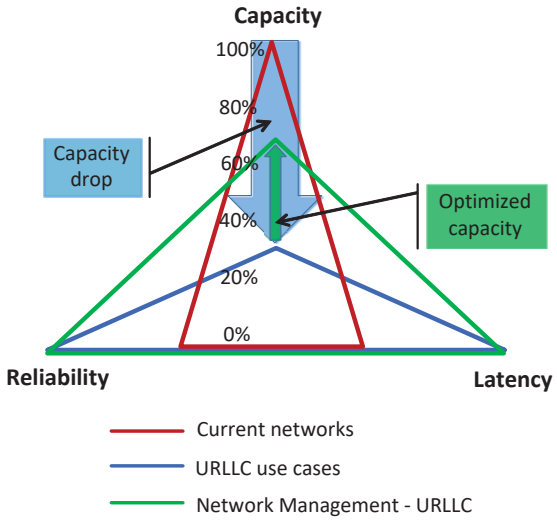

FIGURE 1.2: Tradeoffs among key network requirements [11].

1.2 Scope and Objectives

The admittance of D2D communication in LTE-Advanced (LTE-A) cellular networks as a proximity service is already standardized by 3GPP, starting from release 12 [14]. This initial release specifically targeted the support of public safety use cases e.g. voice communication in emergency situations with or without network coverage. The support of other use cases, e.g. network relay and Vehicle-to-Everything (V2X) communication, is incorporated in the recent release 15 of the standards [15]. The work on network capacity enhancements, which is the the subject of this thesis, will likely be part of the 5G standardization. To alleviate the spectrum deficit in cellular networks, sharing of radio resources for D2D is preferred. This presents high spectral efficiency gains due to increased spectrum reuse by the proximate users. The standard recommends use of the Uplink (UL) spectrum owing to its under-utilization compared to the Downlink (DL) spectrum. Additionally, only the immobile Base Station (BS) is exposed to interference caused by D2D user Terminal (DT)s' transmissions during UL spectrum sharing and the BS has greater capability in handling such interference [16], [17]. Basically, UL spectrum sharing entails the simultanoues use of radio resources by the Cellular user Terminal (CT) while communicating to the BS and DTs directly communicating with each other.

Figure 1.3 illustrates this resource sharing scenario where the solid green and orange lines indicate the desired signals for the cellular and D2D users respectively. The UL spectrum sharing for D2D in cellular networks causes three forms of intra-cell interference shown as dotted lines in the figure:

- **DT-BS Interference (I_D):** The transmissions from a DT transmitter (DT_{Tx}) involved in D2D create interference at the BS during the CT's UL communication (indicated by red dotted lines).

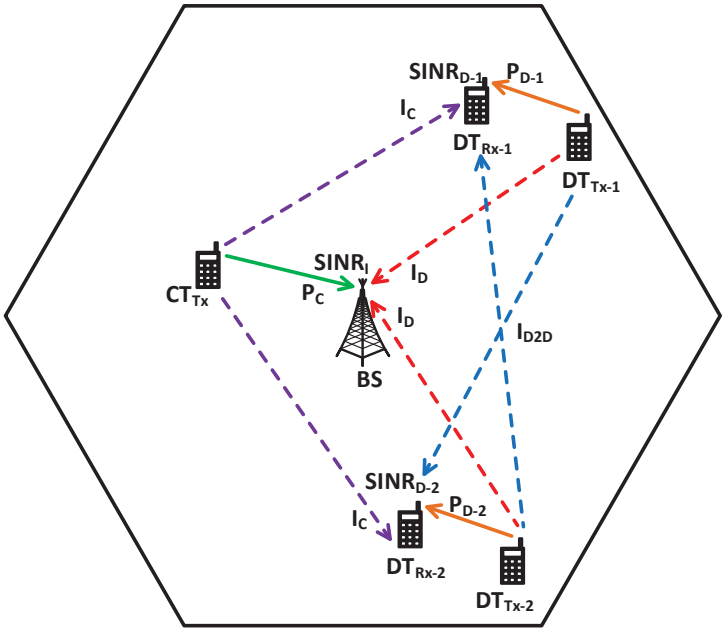

FIGURE 1.3: Intra-cell interference during D2D communication spectrum sharing.

- **CT-DT Interference (I_C):** The CT's transmissions also interfere with the DT receiver (DT_{Rx}) during their D2D interaction (shown as purple dotted lines).
- **DT-DT Interference (I_{D2D}):** In case of multiple D2D pairs sharing spectrum, a given DT_{Tx} causes additional mutual interference with other DT_{Rxs} that are concurrently engaged in D2D (depicted as blue dotted lines).

This inherent intra-cell interference during resource sharing degrades all users' Signal to Interference plus Noise Ratio (SINR)s measured at the BS and DT_{Rxs}. The interference situation is further compounded by Inter-Cell Interference (ICI) from other CTs and DTs also sharing similar resources in neighbouring cells. Consequently, the users' QoS (throughput) and/or network capacity (spectral efficiency) are negatively impacted. However, the low average transmit power used during D2D communication limits the strong interference to close areas surrounding the DT_{Tx}. Therefore, proper sharing of resources with suitable D2D pairs can help minimize this interference and maximize spectral efficiency.

1.2.1 Problem Statement

The focus of this work is to find solutions to the question: "How can the cellular network's spectrum be optimally shared with multiple D2D pairs to maximize the system capacity measured in terms of spectral efficiency?" The optimal spectrum resource sharing should take into consideration the inherent intra- and inter-cell interference so that all users (i.e. CTs and DTs) achieve their QoS requirements. Here, the considered users' QoS requirements are their threshold SINRs since the SINR is a measure of a user's Quality of Experience (QoE) and/or reliability of the communication. The threshold SINR is the minimum user's achieved SINR that guarantees a given throughput and Block Error Rate (BLER).

The core problem in this work is to formulate a D2D resource sharing framework through which intra- and inter-cell interference to all users is minimized and network spectral efficiency maximized. The initial sub-problem is identification of the primary factors facilitating and/or impacting D2D resource sharing. Thereafter, investigation of resource sharing strategies are carried out and algorithms developed. Finally, simulations in a network environment are performed to evaluate performance. The review of state-of-the-art resource sharing approaches will aid the development and evaluation of new optimized strategies.

1.2.2 Proposed Solution

The explored solution ideas to support sharing of the cellular network's spectrum with D2D communication are classified into two major categories:

- **Power Control:** The extent of resource reuse and interference level during spectrum sharing highly depend on the transmit power assigned to users. As such, the initial work focused on examining strategies for appropriate CT and DTs power allocation to facilitate spectrum sharing while maintaining users' QoS. An enhanced users power control scheme based on Uniform Interference Power (UIP) has been considered. The performance results of the UIP scheme proved it's viability in achieving the desired spectral efficiency gains while sharing spectrum with multiple D2D pairs.

- **Smart D2D Users Selection:** Constrained to ensuring that all users achieve their threshold SINRs, selection algorithms that optimize the network's spectral efficiency are required. For the given users transmit power allocations, selection of appropriate D2D pairs to share the cellular network's spectrum has been investigated. Two selection algorithms are considered - one based on opportunistically selecting the least interfering D2D pairs and another chooses D2D pairs in a pseudo-random manner as long as they achieve their SINR thresholds.

1.3 Novelty and Contributions

This thesis' novelty is in the development of a framework that enables multiple D2D pairs to simultaneously share cellular network resources, which are scheduled for conventional CTs communicating with their peers through the BS. The major thesis contributions are divided into three categories: uniform D2D pairs interference power, D2D pairs selection for resource sharing and multiple resources assignment for D2D communication in cellular networks.

1.3.1 Uniform Interference Power from D2D Pairs

A strategy for controlling the intra-cell interference due to radio resource sharing for D2D communication was proposed. Therein, the transmit power of D2D pairs reusing cellular resources is controlled by the BS in a way that each pair contributes the same interference at the BS without negatively impacting the CT's threshold SINR. The proposal is implemented and validated with the Long Term Evolution (LTE) link-level based simulations using MATLAB. The following article has been published with respect to this work:

- A. M. Waswa, D. M. Soleymani, S. Mwanje, J. Mueckenheim, and A. Mitschele-Thiel, "Multiple Resource Reuse for D2D Communication with Uniform Interference in 5G Cellular Networks," in IEEE 28th Annual International Symposium on Personal, Indoor, and Mobile Radio Communications (PIMRC), October 2017, pp. 1–7, Montreal, Canada [18].

1.3.2 D2D Pairs Selection for Resource Sharing

This case considers the scenario where there are multiple D2D pairs that can potentially share a CT's resources. In this case, a subset of those D2D pairs that maximizes the spectral efficiency must be selected. The criteria for selection of multiple D2D pairs allowed to share resources already scheduled for one CT have been formulated. The objective of these criteria is to identify multiple candidate D2D pairs that can share the CT's resources while all users achieve their QoS requirements in terms of threshold SINRs. Based on these criteria, two algorithms: Adaptive Opportunistic Selection (AOS) and Partial Random Selection (PRS) algorithms were developed and validated with MATLAB simulations. The following article has been published on this work:

- A. M. Waswa, S. Mwanje, J. Mueckenheim, and A. Mitschele-Thiel, "Opportunistic and Partial Random Resource Reuse for Multiple D2D Communication in Cellular

Networks," in IEEE 10th International Congress on Ultra Modern Telecommunications and Control Systems (ICUMT 2018), November 2018, pp. 1–7, Moscow, Russia [19].

1.3.3 Multiple Resource Sharing for D2D Communication

This typical network case considers the scenario with multiple CTs and D2D pairs within the cells where some D2D pairs can potentially share any of the available CTs' resources. In this case, several subsets of potential D2D pairs, i.e. one subset per CT's resource, that maximize the total network spectral efficiency must be selected. Concepts and algorithms for coordinating the assignment of available CTs' resources to the D2D pairs' subsets within the network cells have been studied and proposed. The multiple cellular resources scheduled for the CTs within the network provide higher sharing options for D2D pairs to achieve the assignment objectives. The algorithms' major goal is to maximize the network's spectral efficiency while ensuring that all users achieve their threshold SINRs. In this regard, two algorithms: Multi-User Opportunistic (MU-O) and Multi-User Random (MU-R) were developed and enhanced taking into account the multiple resources scheduled for CTs within the cell. MATLAB simulations validated both algorithms in single-cell and multi-cell scenarios. The following paper has been published based on this work:

- A. M. Waswa, S. Mwanje, J. Mueckenheim, and A. Mitschele-Thiel, "QoS-Aware Spectrum Sharing for D2D Communication in Cellular Networks," in 2020 29th European Conference on Networks and Communications (EuCNC), June 2020, pp. 114-119, Dubrovnik, Croatia [20].

1.4 Thesis Organization

The foregoing sections have introduced the major focus of this thesis, the main research question being investigated as well as proposed solutions and the research's contributions. This section presents the organisation of the remaining thesis chapters to guide the different audiences through each chapter's contents.

Chapter 2 introduces the fundamental concepts of D2D when integrated within cellular networks. It gives a brief review of the prerequisite processes to achieve D2D communication with emphasis on radio resource (spectrum) management, whose princples are a necessary background to the discussion of radio resource reuse. It then presents state of the art work on D2D resource reuse highlighting the different strategies adopted to optimize performance through interference mitigation. The chapter concludes with a discussion on potential improvements in the existing shemes and how they can be applied to enhance performance through increased radio resource sharing.

Chapter 3 presents the simulation environment and the required modeling to simulate the typical radio channel charisteristics anticipated in cellular networks. It presents the detailed simulation setup together with respective parameter settings in an LTE link-level simulator based on MATLAB.

Chapter 4 discusses the resource reuse framework of the cellular spectrum for D2D. The discussion starts with an analysis of the constraining factors for resource reuse, which is a prerequisite for the framework development. The analysis considers a single-cell

scenario with one CT, multiple D2D pairs and takes into account their threshold SINRs. This is followed with an investigation into a suitable DT_{Tx} power control strategy to facilitate sharing a given CT's resources by multiple D2D pairs. Finally, the chapter concludes with the development and evaluation of two algorithms for selection of suitable D2D pairs sharing the cellular spectrum while meeting all users QoS (threshold SINRs).

The effectiveness of the D2D pairs selection algorithms in more realistic network scenarios is described in **Chapter 5**. The different aspects of these realistic scenarios include increasing numbers of active CTs and D2D pairs within the network model as well as single-cell and multi-cell environments. The chapter further highlights the necessary algorithms' enhancements to achieve the increased spectral efficiency and users QoS performance objectives. Interestingly, the realistic scenarios enable the algorithms' performance differences to be distinctly observed.

Finally, **Chapter 6** concludes the thesis with highlights of the main achievements and an outlook into future research related to radio resource reuse. Specifically, the achievements highlight the potential of multiple D2D pairs sharing cellular spectrum in enhancing the network capacity while meeting all users QoS requirements. Additionally, an outlook into possible future enhancements for the selection techniques is provided together with hybrid combinations of other resource assignment schemes.

CHAPTER 2

D2D and Resource Reuse: A Review

Contents

D2D in cellular networks first requires an understanding of D2D and cellular networks in their isolated forms before assessing/analysing how the two can seamlessly fit together. This chapter reviews the fundamental aspects of D2D reusing spectrum of the cellular network so as to put the other parts of the thesis into context. Starting with the vital concepts of D2D, section 2.1 discusses D2D benefits, standardization, its application

scenarios and principle of operation. Section 2.2 follows thereafter with a discussion on overlay and underlay D2D modes with respect to the way the cellular spectrum is assigned to D2D pairs. This also highlights the pros and cons of each mode. Section 2.3 presents a review of approaches to mitigate interference during spectrum reuse so as to fully exploit the benefits of D2D. Finally, open research areas that are further addressed by the thesis are presented in section 2.4.

2.1 D2D Communication Concepts

D2D communication is set to revolutionize the design and operation of future cellular networks through a paradigm shift in the way information (i.e. control and data) is exchanged between UTs (i.e. CTs and DTs). Figure 2.1 illustrates the differences between the conventional cellular and D2D communication modes. In the conventional cellular communication mode, CTs always exchange information via a network entity/node, e.g. a BS (figure 2.1(a)). However, in D2D communication mode, the DTs directly exchange information when certain criteria, e.g. DTs' proximity, channel quality between DTs, are met. In this case, either the BS maintains control over the ongoing communication (figure 2.1(b)) or the DTs can autonomously control their direct communication sessions (figure 2.1(c)).

2.1.1 Benefits of D2D

The integration of D2D in cellular networks is motivated by the benefits D2D presents in achieving the performance requirements of both future applications and network operators. Some of the major D2D benefits include:

1. **Proximity gain:** Data exchange among UTs in close range brings the following performance improvements [13]:

   (a) **Low latency -** the direct (i.e. single-hop) data exchange between DTs eliminates the processing delays that would have been imposed by intermediate/relay network nodes. Autonomous driving in V2V communication is a

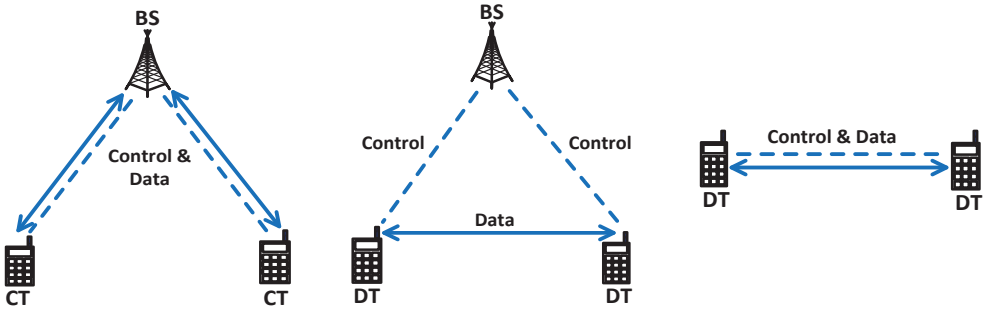

(a) Cellular communication (b) D2D with BS control (c) D2D without BS control

FIGURE 2.1: Conventional cellular and D2D communication modes.

potential beneficiary of the reduced latencies since the mobile vehicles would require very fast exchange of information, e.g. brake signals, to avoid accidents.

(b) **High reliability -** the good radio channel quality between proximate UTs provides a reliable link for exchange of their data. This is especially important for applications like voice and real-time video streaming/gaming where information should be correctly decoded on the first transmission without need for retransmissions.

(c) **High data rate -** proximate DTs experience strong Received Signal Strength (RSS) due to favourable radio propagation conditions, which results in enhanced throughput during their communication. This can benefit aplications like file download that require good data rates to quicky retrieve/download large files.

(d) **Energy efficiency -** close proximity UTs require less transmission power to achieve their desired QoS, which subsequently enhances the network's energy efficiency. Low energy consumption is a key requirement for many remote sensing and metering applications since they have limited energy sources.

(e) **Spectral efficiency -** the lower transmission power of DTs facilitates higher reuse of radio resources since the generated interference is confined to small areas within the cell and can be managed by the cellular network. Additionally, single-hop communication in D2D replaces the two-hop conventional cellular communication, hence saving the network spectrum. Network capacity is thus enhanced through higher number of connected users within the given licensed spectrum.

2. **Traffic off-loading:** The direct traffic among D2D users off-loads cellular networks of user data processing [21]. The network uses the saved processing capacity to handle other vital network tasks e.g. control signaling and also serve higher number of UTs.

3. **Cell coverage extension:** Typically, CTs at the cell edges experience poor RSS due to high Pathloss (PL) and channel fading and also easily fall out of cell coverage area. Such CTs can maintain their communication with the BS by establishing a D2D link with a DT that is in cellular coverage [5]. The DT in proximity of the cell-edge CT acts as a relay node for the CT's data towards the BS. This significantly improves the network's throughput and QoE for cell-edge UTs.

2.1.2 Standardization of D2D

D2D standardization by 3GPP started within release 12 under Proximity-based Services (ProSe) [14]. This initial release focused on defining use cases, deployment scenarios and system architecture enhancements to support D2D over LTE networks. The support of public safety use cases e.g. voice communication in emergency situations with or without network coverage was the main target in release 12. However, support of other use cases e.g. network relay and V2X communication are included in the new release 15 standard [15]. The deployment scenarios are defined based on the network coverage of the DTs, see section 2.1.3.

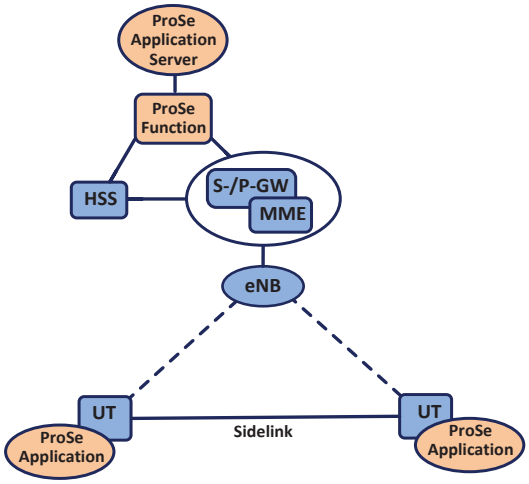

FIGURE 2.2: Simplified ProSe non-roaming network architecture [15]

The support of ProSe in the LTE network required specification of a new node, logical function and interfaces in the system architecture [22], which are described below. Figure 2.2 shows the enhancements and new entities introduced in the LTE network to facilitate ProSe.

1. **ProSe Application Server:** this new third party node, outside the 3GPP scope, stores and manages the applications offering services for ProSe. The ProSe application of ProSe-enabled User Terminal (UT)s communicates with the ProSe Application Server via an application layer interface to download new applications and request services. The ProSe Application Server also stores identities of the ProSe users and maps them to application layer user identities to identify specific users within a given application [23].

2. **ProSe Funtion:** this is a new logical function added to the Evolved Packet Core (EPC) to provide all the relevant network actions required for ProSe. The network related actions include user service provisioning, authorization, charging, security in a specific network and discovery of proximate UTs [24]

3. **Sidelink interface:** this is a new direct interface between UTs that are ProSe-enabled with the addition of the ProSe Application. The ProSe-enabled UTs are subsequently able to discover and directly exchange data with each other via the specified sidelink interface. The sidelink interface is a broadcast (one-to-many) transmission interface that supports group communication. In order to co-exist with both Frequency Division Duplex (FDD) and Time Division Duplex (TDD) LTE (UL/DL) transimissions, the sidelink connectivity is possible in both FDD and TDD spectrum.

The 3GPP standards also specified a new channel structure related to D2D operation (see section 2.1.4), which includes logical channels, transport channels and physical channels/signals [25]. Figure 2.3 illustrates the channel mappings in this new structure. The following channels were defined for the sidelink interface:

1. **sidelink traffic channel (STCH)** is the logical channel carrying user data during ProSe direct communication. This is mapped to the sidelink shared channel (SL-SCH)

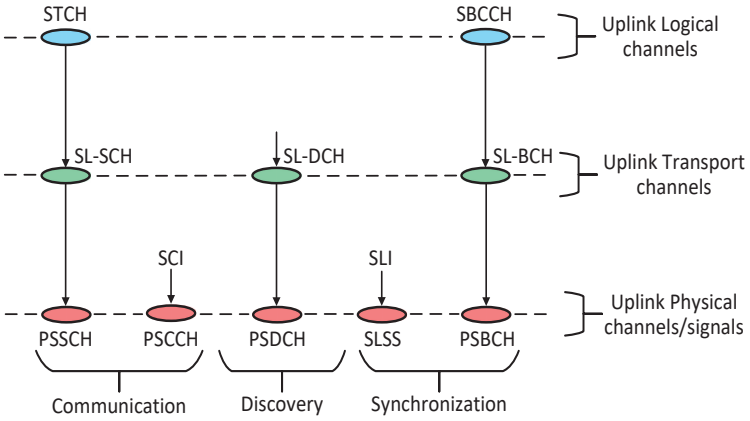

FIGURE 2.3: Sidelink channel structure [26]

transport channel, which is then mapped to the physical sidelink shared channel (PSSCH). Additionally, there exists the physical sidelink control channel (PSCCH) running in parallel to the PSSCH and carries sidelink control information (SCI) that enables the receiving device to correctly detect and decode the PSSCH.

2. **sidelink discovery channel (SL-DCH)** is the transport channel used for ProSe discovery. On the physical layer, SL-DCH is mapped to the physical sidelink discovery channel (PSDCH). There is no logical channel related to ProSe discovery and thus the discovery messages are directly inserted into the SL-DCH transport block on the Media Access Control (MAC) layer.

3. **sidelink broadcast control channel (SBCCH)** is the logical channel used to convey some very basic sidelink related system information for synchronized communication between devices. The SBCCH connects with the corresponding transport channel (sidelink broadcast channel (SL-BCH)) and physical channel (physical sidelink broadcast channel (PSBCH)). The sidelink synchronization signals (SLSS) associated with a specific sidelink identity (SLI) serve as a timing reference for sidelink transmissions and reception for out-of-coverage devices.

2.1.3 D2D Deployment Scenarios

The potential applications utilizing D2D in cellular networks are envisaged to work in varying regions, where network coverage is not always guaranteed. Figure 2.4 illustrates the three major deployment scenarios as specified by 3GPP with respect to network coverage. For each of these scenarios, different applications can utilize D2D to achieve their objectives.

1. **In-coverage:** all DTs are within network coverage and the BS controls their resources (figure 2.4(a)). This scenario is suitable for applications in which DTs have limited mobility e.g. factory automation using MTC, where the factories are located in regions under full cellular network coverage.

2. **Partial coverage:** at least one DT is within network coverage while the other DT is out of coverage (figure 2.4(b)). The BS controls resources used by the in-coverage-DT

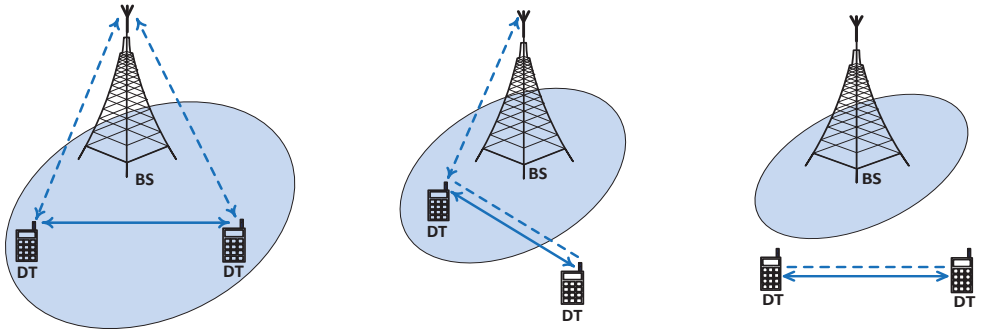

(a) In-coverage (b) Partial coverage (c) Out-of-coverage

FIGURE 2.4: Network coverage scenarios for D2D [27].

while the out-of-coverage-DT uses resources that are either preconfigured or specified by the BS via the in-coverage-DT. This scenario serves mobile user applications in which some DTs enter coverage holes/black spots e.g. in V2V communication.

3. **Out-of-coverage:** all DTs are outside network coverage and utilize preconfigured resources since BS control is not achievable (figure 2.4(c)). The classic application of this scenario is Mission Critical Communication (MCC) services for public safety use cases where the network becomes temporarily out of service due to either emergencies/accidents like fire or natural disasters such as earthquakes, cyclones and floods.

2.1.4 D2D Principle of Operation

The direct data exchange between proximate DTs requires two major operational steps to be realized, i.e. **ProSe discovery** and **ProSe direct communication**. These steps are briefly described below.

1. **ProSe Discovery:**

   This is the first critical step in establishment of a D2D link and is defined as the process where the network and/or UT(s) detects the presence of and identifies other UTs in proximity using radio signals. The failure and/or absence of the ProSe discovery step results in UTs communicating conventionally via the BS. The 3GPP standards specify two types of ProSe discovery: **open** and **restricted discovery** [22].

   In open ProSe discovery, UTs within others proximity are publicly detected and identified without their intervention, i.e. no explicit permission is needed from UTs that are being discovered. This discovery type is suitable for public safety use cases during network outages and emergencies. On the other hand, restricted ProSe discovery requires explicit permission from the UT(s) that is being discovered in order to preserve user's privacy. Restricted ProSe discovery is particularly important for social media applications where anonymous user detection and identification is not desired [28].

Moreover, for each of the above two ProSe discovery types, the discovery process is either network assisted, i.e. **EPC-level** ProSe discovery, or network independent (autonomous), i.e. ProSe **direct** discovery. EPC-level ProSe discovery is a process by which the EPC determines the proximity of two ProSe-enabled UTs and informs them of their proximity. This network assistance is applicable for the in-coverage D2D scenario where the network is aware of all UTs within its coverage. Additionally, EPC-level discovery generates signalling in the network for activating and maintaining UTs' location reporting.

On the other hand, ProSe direct discovery is a procedure employed by ProSe-enabled UTs to discover other ProSe-enabled UTs in their vicinity by using only the capabilities of the UTs with Evolved Universal Terrestrial Radio Access (E-UTRA) technology. This procedure can happen in all D2D deployment scenarios described in section 2.1.3. However, the procedure wastes the UTs' battery due to their continuous transmission or reception of discovery requests.

2. **ProSe Direct Communication:**

This step follows the successful discovery of potential DTs and is defined as a communication between two or more ProSe-enabled UTs in proximity by means of data transmissions using E-UTRA technology via a path (sidelink) not traversing any network node [22]. Depending on the D2D deployment scenario, the BS or discovered UTs perform mode selection, i.e. a decision of data exchange via either conventional cellular or D2D communication, based on given criteria e.g. UTs' proximity [29], higher spectral efficiency/throughput [30] and better energy efficiency [31]. D2D radio bearers are then setup for direct data exchange between the UTs (over sidelink interface) using the assigned radio resources.

In release 12, the 3GPP LTE standard specified two radio resource assignment modes: mode-1 and mode-2 for direct communication via the sidelink for public safety use cases [32]. Mode-1 employs a centralized resource assignment strategy where the BS explicitly allocates radio resources, by means of a scheduling grant, to the DTs. This mode is only possible for the in-coverage D2D scenario owing to its dependence on explicit scheduling grants from the BS. On the other hand, mode-2 is a distributed resource assignment strategy where the DTs autonomously select radio resources for their sidelink communication and is thus possible in both in-coverage and out-of-coverage scenarios. Release 14 of the standard further specified two modes: mode-3 and mode-4 (similar to mode-1 and mode-2 respectively) to support direct communication (via the sidelink interface) for V2V use cases [33].

Moreover, device synchronization is also required to ensure that sidelink transmissions take place within the given time-frequency resources to avoid interference to/from other UTs involved in either direct or cellular communication. The sidelink synchronization can either be network dependent, where UTs under network coverage use the ordinary cell synchronisation signals of the serving cell, or autonomous, where UTs use special SLSS transmited by another UT [26].

2.2 Radio Resource Management (RRM) for D2D

Radio Resource Management (RRM) is important in cellular networks like LTE to ensure efficient use of radio resources as well as meeting the users' QoS requirements. The BS, i.e. evolved NodeB (eNB) in LTE, carries out the RRM role in the network by scheduling the available resources to users depending on their radio channel conditions and QoS requirements. LTE employs the Orthogonal Frequency Division Multiplexing (OFDM) scheme where a given network operator's licensed spectrum is split into a number of sub-carriers (of 15 kHz sub-carrier spacing) and assigned to UTs for a predetermined time duration. These assignments are referred to as Resource Blocks (RB)s and the scheduling function within the BS allocates these RBs to UTs upon request. The number, N_{RB}, of available RBs for a given network ranges from 6 to 100 depending on the licensed system bandwidth [26].

The RB is the smallest assignable radio resource handled by the BS scheduler and comprises of 12 consecutive sub-carriers of 0.5 milliseconds (ms) duration, i.e. one slot. Given the 15 kHz sub-carrier spacing, the minimum allocated bandwidth to a UT is 180 kHz. Each slot is further split in time to accommodate either 7 or 6 OFDM symbols in case of normal or extended Cyclic Prefix (CP), respectively. One OFDM symbol forms the Resource Element (RE), i.e. smallest unit of resource for transmission of user data or control information. Figure 2.5 illustrates the described RBs and REs as defined in LTE standards with the normal CP. Two slots of 1 ms duration make up a subframe, which subsequently constitutes part of the generic LTE physical layer frame of 10 ms duration (i.e. a set of 10 subframes).

In the UL, Single Carrier Frequency Division Multiple Access (SC-FDMA) is applied where user data and reference signals are multiplexed together in a similar transmission structure as shown in figure 2.5. The SC-FDMA implementation in LTE uses an OFDM

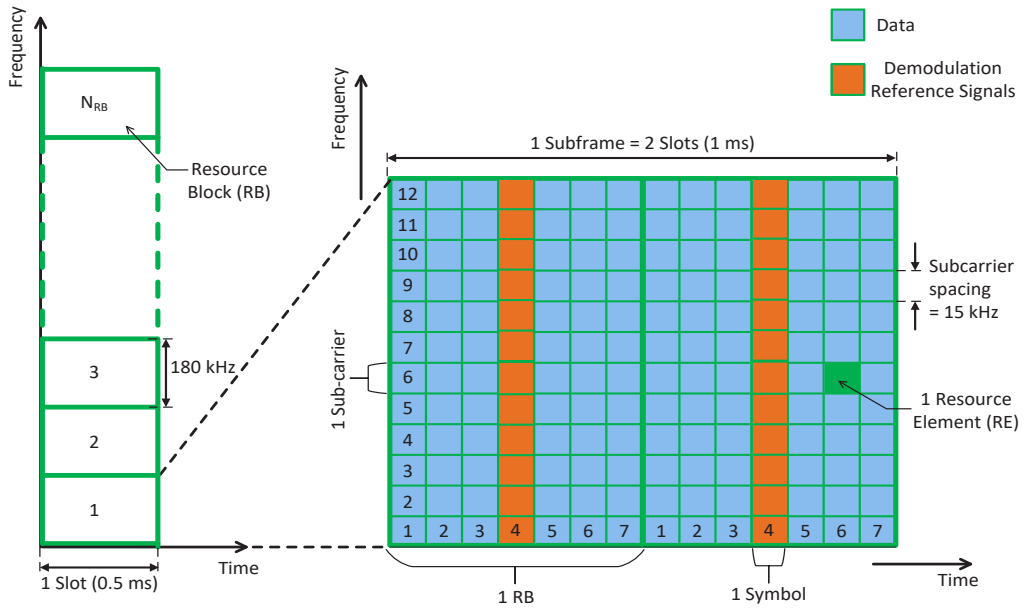

FIGURE 2.5: RB and RE as defined for the LTE uplink with normal cyclic prefix [34]

front-end preceded by a Discrete Fourier Transform (DFT) precoder, which is referred to as either DFT-Precoded OFDM or DFT-spread OFDM (DFTS-OFDM). This usage of the DFTS-OFDM on the UL allows for orthogonal separation of UL transmissions in the frequency domain [26]. The Demodulation Reference Signals (DM-RS) are important in ensuring coherent signal demodulation at the receiving devices. For PSDCH, PSCCH and PSSCH demodulation, the DM-RS are transmitted in either the 4^{th} symbol of the slot in normal CP or the 3^{rd} symbol of the slot in extended CP. The sidelink DM-RS sequence length equals the size (i.e. number of sub-carriers) of the assigned RBs to a UT (see figure 2.5).

The classification of D2D within cellular networks is based on how the network's RBs are allocated for D2D use. Two modes of assigning RBs for D2D within the LTE network, i.e. overlay (dedicated) and underlay (shared) mode, are proposed and described in the following subsections.

2.2.1 Overlay D2D: Dedicated Mode

Overlay D2D is the orthogonal (dedicated) use of RBs by CTs and DTs within the cell for their respective communication. Figure 2.6 demonstrates the overlay D2D principle of RRM in cellular networks. This mode requires reserving a percentage of the network's RBs, originally used by only CTs, for DTs involved in D2D as illustrated in figure 2.6(a). The proportion of reserved RBs, i.e. μ%, may be dynamically adjusted based on the cell load and network operator's CTs/DTs priority policy. Figure 2.6(b) shows that overlay D2D experiences no intra-cell interference due to the orthogonality in RBs assignment and therefore the CTs and DTs achieve high data rates due to the favourable radio channel conditions. This mode is also simple to implement since the BS doesnot need to manage/coordinate any interference within the cell.

However, the low cell spectral efficiency of overlay D2D due to no spectrum reuse requires a surplus of RBs (i.e. during low cell-load) to be allocated to CTs and DTs within the cell. The surplus RBs may not always be available amidst the high demand for network

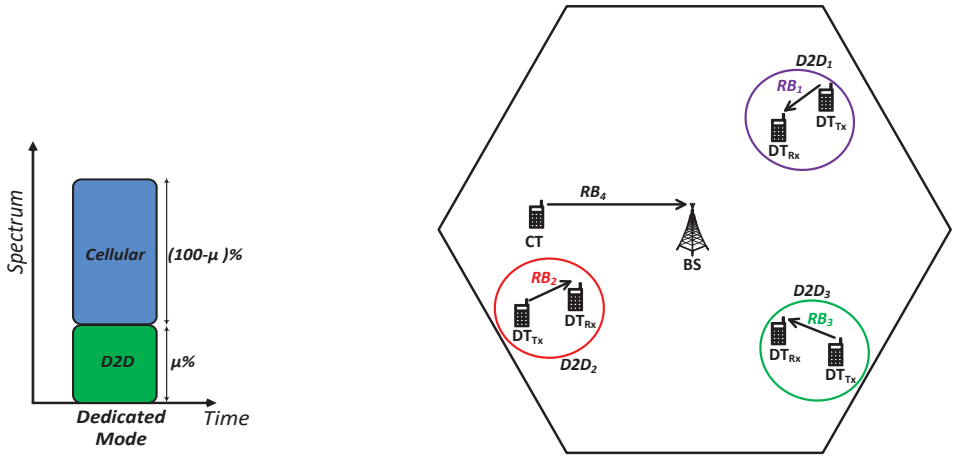

(a) Spectrum assignment

(b) Example for RBs assignment in dedicated mode

FIGURE 2.6: Overlay D2D RRM.

capacity due to growing number of UTs. Additionally, spectrum reusability, by DTs communicating with low transmit power, is not fully exploited in this mode.

2.2.2 Underlay D2D: Shared Mode

Underlay D2D is the reuse of the same RBs for both cellular and D2D communication within the network cells. Figure 2.7 demonstrates the underlay D2D principle of RRM in cellular networks. In this mode, the CTs and DTs within the cell share all the available network's RBs as illustrated in figure 2.7(a). The BS non-orthogonally allocates RBs to UTs within the cell such that a given CT in UL communication and DTs involved in D2D simultaneously use the same RBs as shown in figure 2.7(b). Note that the BS still allocates RBs to CTs within the cell in an orthogonal manner as per the LTE standards. This mode is more spectrally efficient compared to overlay D2D due to the increased resource utilization [35]. The capacity demands by D2D can be fulfilled by a fully loaded cell while employing this mode.

However, as illustrated in figure 2.7(b), the extent of RBs sharing is limited by the intra- and inter-cell interference from other CTs and DTs communicating over the same RBs. Therefore, the system (e.g. the BS that is responsible for RRM) has to carefully control/coordinate this interference to minimize the impact on the UTs' QoS.

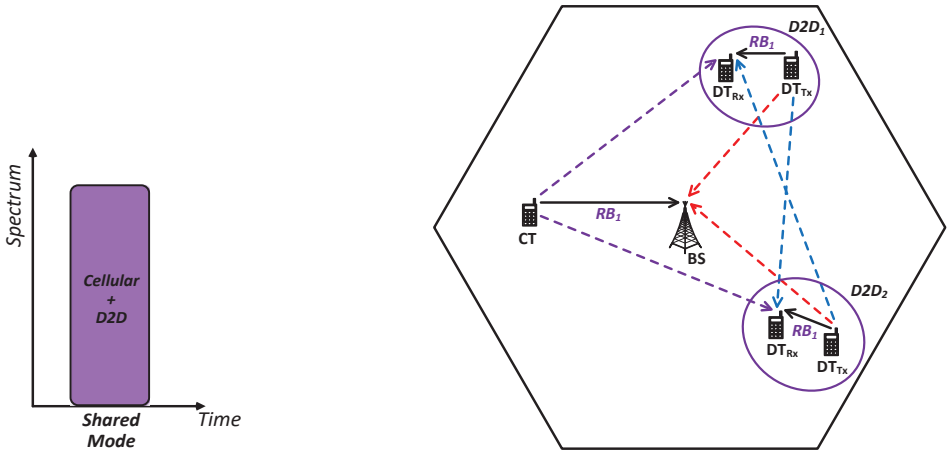

(a) Spectrum assignment

(b) Example for reuse of UL RBs

FIGURE 2.7: Underlay D2D RRM.

2.3 D2D Interference Mitigation: State of the Art

Owing to the improved spectral efficiency delivered by spectrum sharing, underlay D2D continues to attract more research interest than overlay D2D. This interest has mainly focused on combating the inherent interference problem that arises due to spectrum sharing in order to fully exploit the promised capacity gains. As discussed in section 1.2, the extent of spectrum sharing is limited by the intra-cell interference that arises when D2D pairs reuse the cellular spectrum. This intra-cell interference coupled

with ICI severely degrade the SINRs of UTs that share spectrum. Subsequently, the UTs' throughput and network spectral efficiency is reduced when the interference situation is not well managed during spectrum sharing.

A number of interference mitigation strategies are proposed in the literature and these fall into five categories namely: 1) power control and resource allocation, 2) distance-based resource allocation, 3) fractional frequency reuse, 4) graph theory and 5) game theory. A review of these strategies is presented in the following sub-sections.

2.3.1 Power Control and Resource Allocation

Power control is a mechanism for optimally setting the UTs' transmit power to maximize throughput performance and/or minimize interference. In [36] and [37] a Particle Swarm Optimization (PSO) approach is presented to set the CT and multiple DTs transmit power while sharing RBs in a way to maximize system throughput. The sharing of the CT's RB is limited to a single DT in this case. The authors adopted PSO owing to its ability to search locally for an optimal solution of UTs' power settings. In [38] and [39], authors set the DT transmit power in a way not to exceed the preset interference margin at the BS determined by the CT's transmit power. The interference margin was created by assigning the CT with higher transmit power than would be necessary in case of no RB sharing.

The authors in [40] and [41] employ a resource allocation scheme that ensures that the CT's QoS is guaranteed by limiting severe interference towards the BS during RB sharing. Resource allocation also seeks to achieve efficient utilization of assigned RBs by aligning the UTs transmit power to maximize system throughput. [41] presents formulations for the number of DTs, within a multi-cell system, allowed to share the CT's RBs. Thereafter, a Blind Admission Control (BAC) scheme that randomly selects these DTs is proposed and evaluated in terms of spectral efficiency. The BAC scheme uses the LTE Open Loop Fractional Power Control (OFPC) strategy for allocating the CT's transmit power such that it avails a given interference margin at the BS. The D2D pairs transmit power is allocated such that the DT_{Rxs} have a fixed RSS. Spectral efficiency improvements are observed with the BAC scheme while the CT's QoS is maintained.

However, it is observed that most power control and resource allocation shemes focused on maximizing system throughput with little or no emphasis on CT and DTs QoS requirements. An attempt to include the UTs' QoS requirements only considered guaranteeing the CT's QoS and ignoring that of DTs with whom RBs are shared. This resulted in the DTs going into outage once their QoS requirements (e.g. threshold SINRs) are not achieved.

2.3.2 Distance-based Resource Allocation

The authors in [42], [43], [44] and [45] also suggested minimizing interference by selecting DTs that are furthest away from the BS and/or CT to share RBs. In [42] and [43], multiple DTs were considered to share a given CT's RB with the objective of maximizing system throughput. However, [44] and [45] considered only a single DT sharing a CT's RB and formulated the minimum separation distance of the DT from the BS and/or CT in order to guarantee their QoS.

The schemes in [46] and [47] extended the distance-based solution by defining an Interference Limited Area (ILA), within which the DT is not allowed to reuse the CT's RB to limit the interference between them. Although the solutions achieved higher throughput and UTs QoS, the BS requires information on all UTs' locations and/or Channel Quality Indicator (CQI) between them. Such information creates signaling overhead in the network. To limit the signaling overhead, [48] and [49] proposed heuristic algorithms that either gradually allowed multiple DTs, one at a time to share a CT's RB or gradually removed worst performing DTs from sharing a CT's RB with the objective to maximize system throughput.

2.3.3 Fractional Frequency Reuse (FFR)

In [50] and [51] the Fractional Frequency Reuse (FFR) technique for coordination of interference from DTs towards CTs has been presented. Figure 2.8 illustrates how the FFR technique operates. In this technique, the available network spectrum is partitioned into four sub-spectrum parts, labelled F_1, F_2, F_3 and F_4 in the ratio f_1:f_2:f_3:f_4, as shown in figure 2.8(a). Each of the network's cells are then split into two regions: inner region that is closer to the BS and outer region that extends towards the cell edges. The CTs in all cells' inner regions are allocated orthogonal RBs from F_1 sub-spectrum, while CTs in the outer region of adjacent cells are allocated orthogonal RBs from F_2, F_3 and F_4 sub-spectrums as illustrated in figure 2.8(b). To manage D2D interference during RB reuse, DTs located in the inner region reuse RBs from the sub-spectrums assigned to CTs in outer region of neighbouring cells (either F_2 or F_3 or F_4), while DTs located in the outer region reuse RBs from the sub-spectrum assigned to CTs in the inner region (F_1). Additionally, this technique only allows a single DT to reuse RBs assigned to a given CT in order to avoid severe interference due to increased RB reuse.

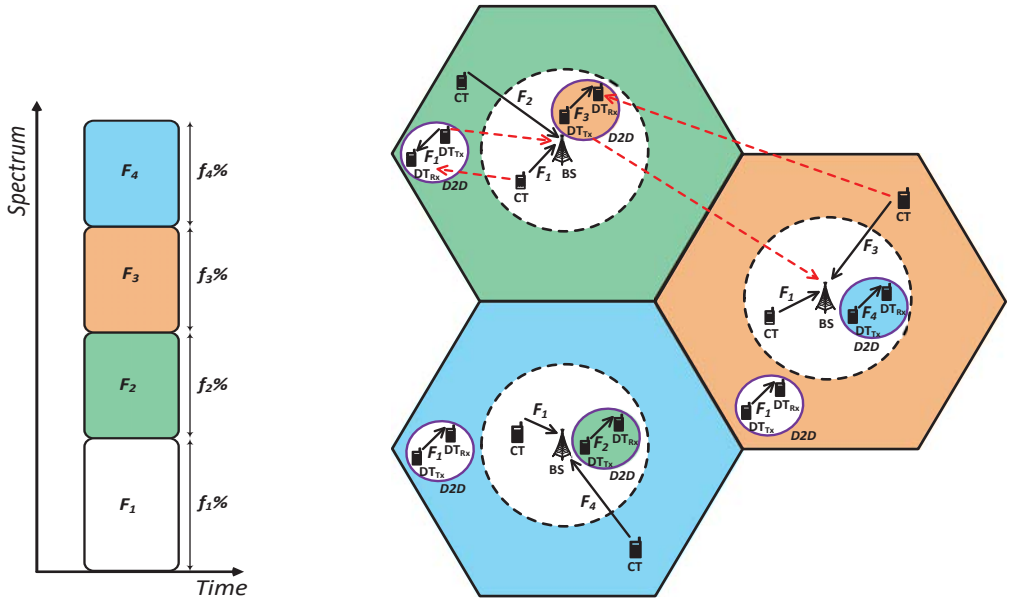

(a) UL spectrum partitioning

(b) Example UL spectrum assignment for D2D

FIGURE 2.8: FFR scheme for D2D in cellular networks.

Based on the CT and DT QoS requirements, i.e. threshold SINRs, authors in [50] formulate the radius of the inner region and extend the FFR technique to a multi-cells scenario. The solution in [51] combines FFR with power control and RB allocation techniques and evaluate the aggregated solution in a single-cell scenario. Although the FFR technique enhances the spectral efficiency and achieves the CT/DT threshold SINRs, it limits the extent of reuse for assigned CT RBs to a single DT.

2.3.4 Graph Theory

The authors in [52] and [53] propose graph coloring and bipartite graph matching techniques to share RBs taking into account the computational complexity of finding an optimal solution. Figure 2.9 illustrates the graph theory techniques for D2D resource sharing in cellular networks. A graph is constructed comprising of: 1) vertices that are grouped in two sets, i.e. a set of CTs to which RBs are already scheduled and a set of DTs requesting for RB allocations and 2) edges that connect the different vertices in the two sets. In graph colouring, illustrated in figure 2.9(a), the vertices in the CTs set are given predefined colours while vertices in the DTs set are coloured differently depending on their suitability to share the CTs' RBs. A match of the colours in the two sets indicates that the DT shares a given CT's RB. Figure 2.9(b) shows the bipartite graph matching technique where the edges connecting vertices in the two sets are given different weights, W_{mn}. These weights indicate the preference of the DT sharing the given CT's RB. The vertice colours in graph colouring and edge weights in the bipartite graph are defined according to different criteria, e.g. achievable throughput (network capacity), outage probability (interference levels), energy efficiency and transmission delay.

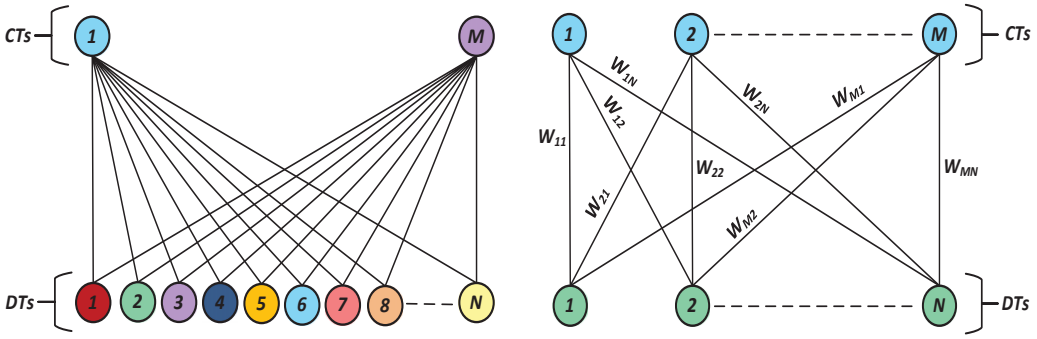

(a) Graph colouring (b) Bipartite graph

FIGURE 2.9: Graph theory techniques for D2D resource sharing.

The weakness of graph colouring techniques is their requirement for information on all radio channel conditions between the BS and DTs sharing the CT's RBs. This increases signalling in the network especially with high number of CTs and DTs. Additionally, the considered number of DTs is at most equal to that of CTs resulting in only a single DT sharing a given CT's RB.

2.3.5 Game Theory

A Stackelberg game theoretical approach to coordinate the interference to BS and DTs is presented in [54] and [55]. This approach applys a seller-buyers hierarchical struture in assignment of RBs. The BS being the owner of RBs in the network acts as the RB-seller in the game by setting the interference price for the CT RBs based on their measured interference margin. The set interference price defines the maximum transmit power a DT is allowed to use while sharing the CT's RB. A higher price means that a lower maximum transmit power is utilized by the DT sharing RBs. On the other hand, the DTs are controlled by the BS for interference management and thus are the RB-buyers whose chosen actions in setting their transmit power seek to maximize their individual payoffs in terms of throughput. These actions should also consider the prices announced by the BS. The RB-buyers compete for the CTs RBs according to their prices decided by the BS.

The authors in [55] further enhance the interference pricing to allow for a Differentiated Pricing Scheme (DPS). The BS sells RBs to multiple DTs using an interference margin determined by the CT's transmit power. The BS' goal in selling RBs is to maximize its revenue charged from the DTs sharing the RBs while keeping within the interference margin (i.e. guaranteeing the CT's SINR). In the DPS scheme, the BS sets different prices for each DT wishing to share the RB based on the interference it causes at the BS. Lower prices are set for DTs causing less interference compared with the DTs having greater interference. Based on the set prices, the DTs competitively adapt their transmit powers to maximize their throughput. The approach converges to an equilibrium with limited iteration and also enhhances the system throughput while ensuring that the CTs QoS was achieved.

2.4 Open Research Areas

The existing research has so far focused on a single D2D pair sharing a given CT's RB(s) and managing the subsequent interference between DTs and CTs. However, owing to the proximity gain of D2D where DTs have low transmit powers, it is possible for multiple D2D pairs to share the CT's RB while having tolerable interference. This proposition provides various RBs assignment options for UTs (i.e. CTs and DTs) within the network. Figure 2.10 shows the generalized RBs assignment in a cellular network with underlay D2D. Here, the UTs are categorized in four sets, namely:

1. **Idle UTs:** these are registered in the network and are not assigned any RBs since they have no requirement to transmit data in a given instant.

2. **Non-reuse UTs:** depending on the operator policy to provide highly reliable communication these UTs are assigned orthogonal RB(s) based on their traffic requirements. This is the overlay D2D mode.

3. **Single-reuse UTs:** here only a single DT shares a given CT's RB(s) while managing the interference between them. Depending on the DT's traffic requirements, several RBs of only a single CT can be shared.

4. **Multi-reuse UTs:** here multiple DTs share a given CT's RB(s) in order to improve the network capacity by utilizing the D2D proximity gain. Management of increased

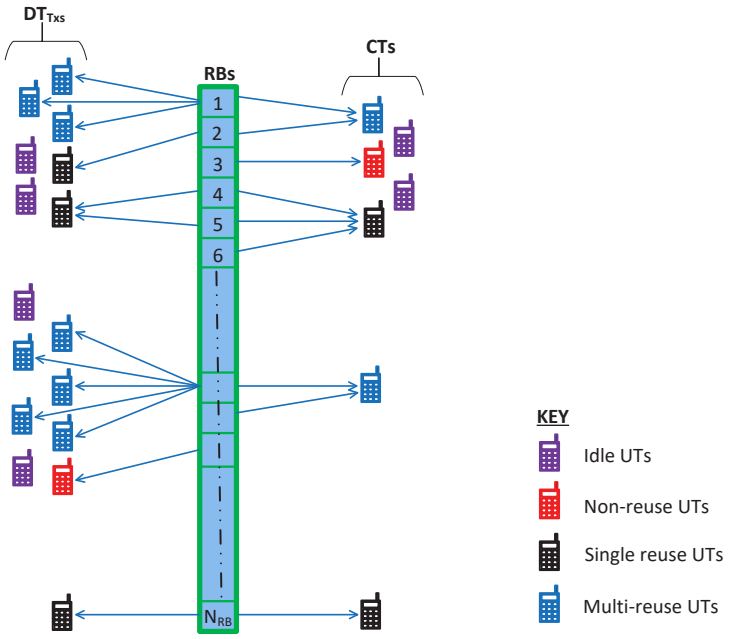

FIGURE 2.10: Generalized RBs assignment problem for D2D in cellular networks.

mutual interference between the multiple UTs sharing RBs is required for this category.

The last category (i.e. multi-reuse UTs) promises to alleviate the capacity deficit in future cellular networks that will serve a massive number of devices (UTs). However, new considerations have to be taken into account to achieve this and some of these are discussed in the following sub-sections.

2.4.1 Prioritization of all UTs QoS

Most published work has prioritized the CTs QoS during resource sharing with DTs. This has resulted in DTs either not achieving their data rate requirements or going into outage due to severe interference from either the CT or other DT_{Txs} during resource sharing in cellular networks. There is therefore a need to equally prioritize the DTs' QoS along with that of CTs.

2.4.2 Standardized D2D Pairs Power Control

The investigated power control schemes in section 2.3.1 focused on limiting the DTs transmit power in order to avoid severe interference at the BS. This also disregarded the DTs' QoS, which may lead to their poor performance especially given the kind of applications that will adopt D2D. Further, the DTs are expected to fall back to the conventional cellular communication in case their D2D links become infeasible. Therefore, using the already standardized power control techniques, e.g. the LTE open-loop and closed-loop power control, would simplify D2D integration in cellular networks if they are adopted.

2.4.3 D2D Pairs Selection for Resource Reuse

The distance-based approach in section 2.3.2 evaluated scenarios where only a single DT shared the CT RB, which are simpler. However, the more complicated scenarios involving multiple DTs should be studied by formulating the threshold reuse distances between all UTs so that criteria for sharing RBs are derived. The required reuse distances include: 1) DT_{Txs}-BS, 2) CT-DT_{Rxs} and 3) other DT_{Txs}-DT_{Rx}. These reuse distances should take into account both the CT and DTs QoS requirements (threshold SINRs). The reuse distances form the basis of the D2D pairs selection criteria to share the CT resources.

These open research challenges provide the background for the work undertaken in the following chapters of this thesis.

CHAPTER 3

Models and Assumptions

Contents

D2D communication is a new concept whose integration into existing cellular networks requires its promised performance gains to be validated in a simple, accurate and cost effective manner. Currently, only prototypes without known implementations of D2D in cellular networks exist. Therefore, the performance validations are carried out using either analytical techniques or advanced system/network level simulators that are in most cases a modification of existing LTE-based simulator packages.

This chapter describes the simulation environment for the proposed algorithms developed in this work, which seek to improve the cell spectral efficiency when several D2D pairs (DTs) are allowed to reuse UL radio resources already scheduled by the base station (BS) for the cellular users (CTs) in an LTE network. First, section 3.1 introduces the evaluation method followed with the applied network model for simulations using MATLAB software in section 3.2. Sections 3.3 to 3.5 provide the related model assumptions, applied parameters that influence system performance and users distribution in the network. Section 3.6 concludes this chapter with the simulation setup.

3.1 Evaluation Method

Owing to the fast evolution of cellular network technologies and limited D2D implementations, the thesis sequentially uses analytical and simulation techniques to assess system performance during resource reuse by several D2D pairs within existing cellular networks.

Analytically, two performance metrics: a global and individual user metric, are used to study the impacting factors on system performance. Specifically, the global metric is the total cell spectral efficiency while the individual user metric is the achieved SINRs for the CTs and DTs. Thereafter, an LTE network scenario is modeled that uses the proposed UL resource assignment algorithms and parameter settings to approximate an operational cellular network. This is then simulated using a MATLAB based LTE simulator to validate the performance results achieved in the analytical studies.

3.2 Network Model

The simulations are based on an LTE cellular network operating within band 7 spectrum (i.e. 2.6 GHz band) [56] and consisting of either one (01) or seven (07) cells, with each cell served by a single omni-directional BS placed at the center. The single-cell (1-cell) scenario is used as a proof of concept for the resource assignment algorithms and can be easily extended to the more realistic multi-cell (7-cells) network scenario. The geographical cellular coverage is modelled as a hexagonal grid shown in figure 3.1, with each cell having a radius of $200m$. Each cell serves two sets of users within its coverage area: *a*) convetional cellular users in set $\mathcal{CT} = \{1, \ldots, M\}$ and *b*) D2D user pairs in set $\mathcal{DT} = \{1, \ldots, N\}$. The CTs are located a distance, R_{C_i}, $(\forall i \in \mathcal{CT})$ from the BS while each D2D pair is comprised of a $\mathrm{DT_{Tx}}$ located a distance, R_{D_j}, $(\forall j \in \mathcal{DT})$ from the BS and a $\mathrm{DT_{Rx}}$ which is at a random separation distance, R_{D2D_j}, from it's respective $\mathrm{DT_{Tx}}$.

The performance evaluations for the reuse of UL spectrum in this thesis consider two cases: 1) single-cell simulations that evaluate performance of an isolated cell, e.g. the center cell in figure 3.1 and 2) multi-cell simulations that provide a realistic network evaluation with all other neighbouring network cells shown in figure 3.1.

3.3 Network Model Assumptions

The following assumptions are considered for the above network model:

1. Each BS is aware of all CTs' and DTs' locations within its cellular coverage area through measurements, e.g. Global Positioning System (GPS) and their communication modes, i.e. cellular and D2D modes respectively, have already been determined.

2. Owing to the projected massive number of devices in future cellular networks, the number of DTs is taken to be much higher than that of CTs (i.e. $N \gg M$). This therefore means that the assignment problem during UL resource reuse is not merely a simple one-to-one mapping (i.e. pairing) problem but rather a one-to-many assignment problem.

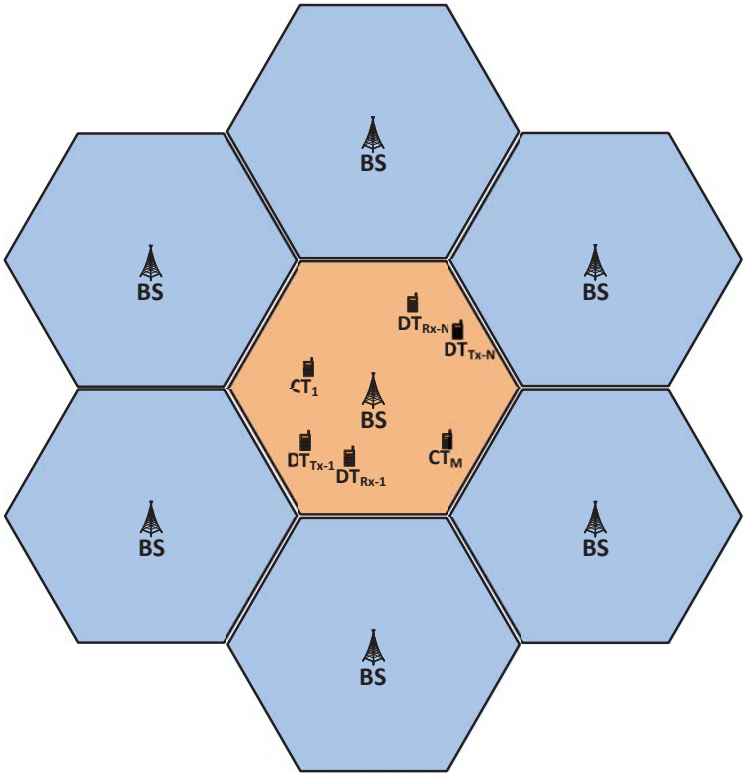

FIGURE 3.1: Simulation network layout

3. The cellular network is fully loaded, i.e. all the available UL RBs have been scheduled for CTs within the cell and thus the D2D pairs have to share (reuse) the scheduled RBs. For simplicity, a single RB is scheduled for each CT, such that the number of available RBs per cell is equal to the number of CTs in each cell. The D2D pairs assignment to the RB scheduled for different CTs is independent of each RB.

4. All CTs and D2D pairs have full buffer traffic.

5. The RB scheduling for all CTs has already been accomplished by the BS, i.e. RB scheduling for CTs is outside the scope of this thesis.

6. The scheduler applies Inter-Cell Interference Coordination (ICIC) techniques to minimize ICI from CTs using similar RBs in neighbouring cells. Thus, the RBs experiencing high ICI are excluded from the candidate RBs to be shared with D2D pairs.

7. All users in each set, i.e. $\mathcal{CT}$ and $\mathcal{DT}$, have uniform target Signal to Noise Ratio (SNR) and threshold SINR requirements. Additionally, the same noise power, $\mathcal{N}$, is experienced at each of the respective receivers. Equation 3.1 shows that $\mathcal{N}$ in dB is a product of the thermal noise, $\mathcal{N}_o$, and receiver noise figure, NF in the linear domain. Given the receiver's thermal noise power density, n_o, of $-174\,dBm/Hz$, NF of $5\,dB$ [57, table A.2.1.1.4-3] and RB bandwidth, B_{RB}, of $180\,kHz$, the noise power is computed accordingly.

$$\mathcal{N} = \mathcal{N}_o \cdot NF = n_o \cdot B_{RB} \cdot NF \equiv -116\,dBm \tag{3.1}$$

8. The applied parameters notation in this network model together with some default values are given in table 3.1. The settings of the given default values are discussed in sections 3.4 and 3.5.

Table 3.1: Parameters notation

Parameter	**Symbol**	**Default value**
Carrier frequency	f_c	2.6 GHz
Cell radius	R_{cell}	200 m
Number of CTs per cell	M	variable 1 or 10
Number of D2D pairs per cell	N	variable 40, 50 or 500
BS antenna gain	G_B	5 dBi
UT antenna gain	G_{UT}	0 dBi
Channel gain (i^{th} CT $\Leftrightarrow$ BS)	G_{C_i}	
Channel gain (j^{th} $\mathrm{DT_{Tx}}$ $\Leftrightarrow$ BS)	G_{D_jB}	
Channel gain (j^{th} $\mathrm{DT_{Tx}}$ $\Leftrightarrow$ j^{th} $\mathrm{DT_{Rx}}$)	G_{D2D_j}	
Channel gain (i^{th} CT $\Leftrightarrow$ j^{th} $\mathrm{DT_{Rx}}$)	$G_{C_iD_j}$	
Channel gain (l^{th} $\mathrm{DT_{Tx}}$ $\Leftrightarrow$ j^{th} $\mathrm{DT_{Rx}}$)	$G_{D2O_{lj}}$	
Distance (i^{th} CT $\Leftrightarrow$ BS)	R_{C_i}	
Distance (j^{th} $\mathrm{DT_{Tx}}$ $\Leftrightarrow$ BS)	R_{D_j}	
Distance (j^{th} $\mathrm{DT_{Tx}}$ $\Leftrightarrow$ j^{th} $\mathrm{DT_{Rx}}$)	R_{D2D_j}	
Distance (i^{th} CT $\Leftrightarrow$ j^{th} $\mathrm{DT_{Rx}}$)	$R_{C_iD_j}$	
Distance (l^{th} $\mathrm{DT_{Tx}}$ $\Leftrightarrow$ j^{th} $\mathrm{DT_{Rx}}$)	$R_{D2O_{lj}}$	
Path loss exponent (UT $\Leftrightarrow$ BS)	α_b	3.67
Path loss exponent (UT $\Leftrightarrow$ UT)	α_u	4.33
Propagation constant (UT $\Leftrightarrow$ BS)	c_b	-33.49 dB
Propagation constant (UT $\Leftrightarrow$ UT)	c_u	-19.80 dB
Noise power	$\mathcal{N}$	-116 dBm
Threshold SINR for CTs	Γ_C^{th}	6 dB
Target SNR for CTs	Γ_C^{target}	12 dB
Threshold SINR for DTs	Γ_D^{th}	15 dB
Target SNR for DTs	Γ_D^{target}	25 dB
Transmit power for i^{th} CT	P_{C_i}	
Minimum/maximum CT transmit power	$\mathcal{P}_C^{min}$ / $\mathcal{P}_C^{max}$	-40 / 23 dBm
Transmit power for j^{th} DT	P_{D_j}	
Minimum/maximum DT transmit power	$\mathcal{P}_D^{min}$ / $\mathcal{P}_D^{max}$	-40 / 23 dBm
Shadow fading standard deviation	σ_{sf}	4 dB
Monte-Carlo simulation runs	MC	10^4

3.4 Radio Propagation Models

The achieved users' SINRs are derived from the received desired and interfering signal strengths at the respective receivers. Therefore, it is important to make use of reliable radio propagation models to estimate the received signal strength in simulation studies. Equation 3.2 shows that the received signal strength, P_{Rx} is directly proportional to the user transmit power, P_{Tx}, transmitter and receiver antenna gains, G_{Tx} and G_{Rx} respectively, and radio channel gain, G_{ch} between the communicating entities. The BS and UT antenna gains are specified by 3GPP as 5 dBi and 0 dBi respectively [57, table A.2.1.1.4-3].

$$P_{Rx} = P_{Tx} \cdot G_{Tx} \cdot G_{Rx} \cdot G_{ch} \tag{3.2}$$

3.4.1 Users Transmit Power

Power control algorithms are used in cellular networks to determine the appropriate users' transmit power to achieve their desired SINRs for reliable communication. The CTs and DTs transmit power is standardised by 3GPP with the minimum and maximum set at -40 and 23 dBm respectively [56] [58].

3.4.2 Radio Channel Charateristics

The radio channel gain, G_{ch}, is a key characteristic of any wireless channel, which is highly dynamic over both time and frequency. The variations of channel gain between any two communicating entities is a random variable accounting for two main effects: pathloss and fading as given by equation 3.3.

$$G_{ch} = c \cdot r^{-\alpha} \cdot |h|^2 \tag{3.3}$$

where c is the propagation constant, r is the distance between communicating entities, α is the pathloss exponent and $|h|^2$ represents the fading effects.

Pathloss (PL): The 3GPP standards define pathloss models for the radio channel between users (CTs and DTs) and the BS [57, table B.1.2.1-1]. In this work, the Urban Micro hexagonal cell Non Line-Of-Sight (UMi-NLOS) channel model, given in equation 3.4, is used for all channels from either CTs or DTs towards the BS.

$$PL_{\text{BS}} = 36.7log_{10}(r) + 22.7 + 26log_{10}(f_c) \tag{3.4}$$

with the PL defined in decibel (dB), distance, r in meters and carrier frequency, f_c in GHz.

The indoor cellular network channel models are also observed to be valid for D2D communication, especially in indoor situations [59]. Therefore, the Indoor Hotspot Non Line-Of-Sight (InH-NLOS) channel model is assumed in this work for channels between different DTs and also from CTs towards DTs [57, table B.1.2.1-1] as given by equation 3.5.

$$PL_{\text{DT}} = 43.3log_{10}(r) + 11.5 + 20log_{10}(f_c) \tag{3.5}$$

The default values of constants c and α in the linear domain PL model of equation 3.3 are derived from the dB domain PL models in equations 3.4 and 3.5. Additionally, a

minimum separation, R_{min} of 10 m, between communicating entities is specified for the validity of the above two PL models.

Fading: This is the variation of experienced attenuation of the radio wave signal strength due to multipath propagation and shadowing effects. Multipath propagation effects arise when a given radio signal takes several different paths from the transmitter to a receiver. This could be due to either reflections from large objects or scattering at small objects. The constructive and destructive interference of these multipath signals leads to signal strength variations that are frequency dependent. On the other hand, the shadowing effects are usually frequency independent and occur when radio signals are completely blocked by larger objects (e.g. buildings and hills) from reaching the receiver. In this work, the adopted shadow fading model is log-normally distributed with 0 dB mean and 4 dB of standard deviation [57, table B.1.2.1-1]. The fast fading effects arising from multipath propagation are not considered throughout this study.

3.5 Cells and Users Distribution

The cells-distribution over the geographical network coverage area is as shown in figure 3.1. The CTs and $\text{DT}_{\text{Tx}s}$ are uniformly distributed within each cell's coverage area around the BS. This distribution entails that the Cumulative Distribution Function (CDF) for the CTs' and $\text{DT}_{\text{Tx}s}$' distance, r ($0 \leq r \leq R_{max}$) from the BS is expressed as the ratio of the circular area, $\pi \cdot r^2$ to the cellular coverage area, $\pi \cdot R_{max}^2$ [60]. The CDF derivative with respect to r gives the Probability Density Function (PDF), $f(r)$, as shown in equation 3.6.

$$f(r) = \begin{cases} \dfrac{2r}{R_{max}^2} & \text{if } \; R_{min} < r \leq R_{max} \\ 0 & \text{Otherwise} \end{cases} \tag{3.6}$$

where R_{min} is the minimum distance, set to 10 m, between the communicating entities in accordance with the channel model requirements in section 3.4.2 and R_{max} is the maximum distance, set to R_{cell}, between the CTs/$\text{DT}_{\text{Tx}s}$ and the BS. The CTs' and $\text{DT}_{\text{Tx}s}$' distance from the BS is thus distributed over the interval $[R_{min}, R_{cell}]$. Theoretically, the PDF in equation 3.6 is only valid for $R_{min} = 0$. However, if $R_{min} \ll R_{max}$ the deviation is practically very small and can be ignored. Further, the angle θ between the x-axis and the line from the BS to the CTs/DT_{Tx} is uniformly distributed over the interval $[0, 2\pi]$.

The separation between the DT_{Rx} and the DT_{Tx} for the D2D pairs is also uniformly distributed as given by equation 3.6 above with R_{max} set to R_{D2D}. The DT_{Rx}-DT_{Tx} separation, R_{D2D_j}, between any given D2D pair is thus distributed over the interval $[R_{min}, R_{D2D}]$.

3.6 Simulation Setup

Each simulation run is always initiated with the distribution of a specified number of users (CTs and D2D pairs) within the each cell. Using the CTs and DTs locations, channel gains amongst all users are derived from the adopted pathloss and shadow fading models in table 3.1. Thereafter, RB assignment to the D2D users and transmit power

allocations (as discussed in chapters 4 and 5) are done before carrying out spectral efficiency and achieved SINR performance computations on a snapshot basis. Therefore, this simulation setup together with the model assumptions and parameters form the basis for evaluation of the proposed ideas and algorithms in the subsequent chapters.

CHAPTER 4

Single Resource Assignment Problem

Contents

The reuse of cellular radio resources for D2D communication (i.e. underlay D2D mode) is seen as one way to improve resource utilization (spectral efficiency) and thus, enhances the network capacity. However, reuse of radio resources by both CTs and D2D users leads to intra-cell interference for which solutions are required to keep it below given threshold levels. One advantage of the required proximity for D2D is the significantly lower average transmit power of the DTs compared to the CT. A significant level of interference caused by a given D2D pair during resource reuse is expected to be limited to a restricted area surrounding the D2D pair. Similarly, for cellular communication

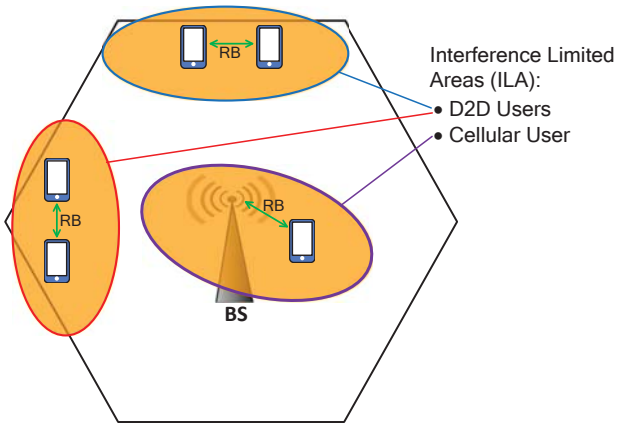

FIGURE 4.1: Spatial RB reuse for cellular and D2D communication [61].

links, the area experiencing high interference depends on the CT's transmit power and its location from the serving BS, as will be discussed later in this chapter.

Figure 4.1 illustrates an example of radio resource reuse within a cell where two D2D pairs and one cellular user are sharing resources (i.e. RBs). The circles around users demarcate areas of high interference, i.e. interference limited area (ILA) [46], within which resource reuse is not permitted. Thus, spatial separation of the different ILAs to avoid their overlap is crucial to ensure minimal intra-cell interference among users sharing the radio resources. Additionally, depending on the size of the different users' ILAs, higher number of multiple D2D pairs are allowed to share resources within a given cell, further boosting the overall network spectral efficiency and/or capacity. The reuse of RBs, scheduled for a single CT, by multiple D2D pairs within the cell forms the basis of this chapter.

The chapter begins with a feasibility analysis of multiple D2D pairs sharing RBs scheduled for a single CT in section 4.1. This is followed with a review of impacting factors that influence the network performance objectives under set constraints in section 4.2. Thereafter, section 4.3 presents a power allocation scheme, in which the BS controls the intra-cell interference, as well as an analysis of the scheme's performance.

Next, the sections 4.4 and 4.5 introduce a framework for spatial resource reuse by multiple D2D pairs within a single cell while achieving SINR thresholds of both cellular and D2D users. Here, two novel algorithms with a selection criteria for chosing the suitable D2D pairs permitted to share a resource are proposed and their performance is also evaluated. Section 4.6 concludes the chapter with key learnings from sharing a single CT's resources by multiple D2D pairs.

4.1 Analytical Model for D2D Reuse of UL Resources

This section formulates and analyses the factors that should be taken into consideration for resource reuse by multiple users engaged in D2D communication. Figure 4.2 shows a single cell scenario that is considered in this analysis. The scenario is comprised of one CT and multiple D2D pairs under the BS' coverage (figure 4.2(a)). The BS shares

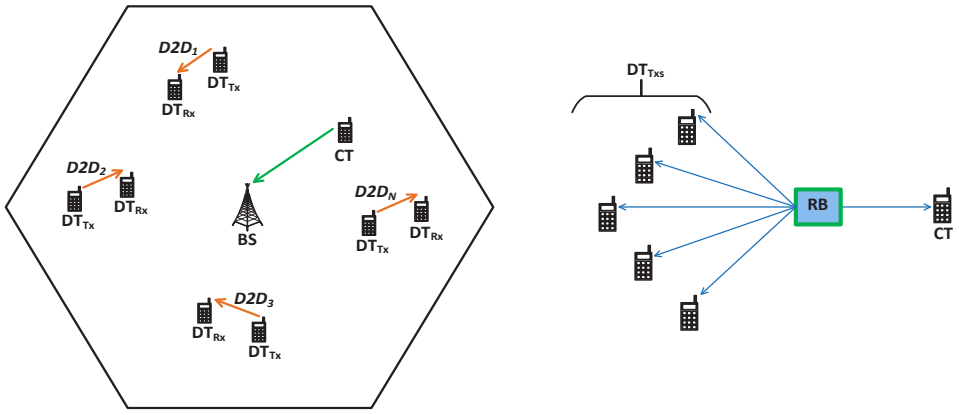

(a) CT and D2D users distribution in a single cell (b) Multiple DT_{Txs} sharing the RB with CT

FIGURE 4.2: Uplink resource sharing by multiple D2D pairs.

a single RB already scheduled for use by the CT with multiple D2D users within the cell (figure 4.2(b)). Since reuse of a single CT's RB is considered in this chapter, the subscripts on all parameters related to the CT as given in table 3.1 are dropped.

The objective of D2D sharing the CT's RB is to maximize the total cell spectral efficiency, η, of the network while ensuring that the SINR thresholds of both CT and D2D users are met. The total cell spectral efficiency, measured in bits per second per Hertz (bps/Hz), is defined as the aggregate throughput achieved by the different communicating entities per given allocated spectrum bandwidth in the cell. In this analysis, η is formulated as the summation of the individual UTs' spectral efficiency using Shannon's capacity formula as given in equation 4.1.

$$\eta = log_2(1 + \Gamma_C) + \sum_{j=1}^{N} log_2(1 + x_j \Gamma_{D_j}) \tag{4.1}$$

where Γ_C and Γ_{D_j} are the SINRs at the BS and the j^{th} DT_{Rx} respectively and x_j is a binary variable that indicates whether the j^{th} D2D user shares or doesnot share the CT's RB, i.e. x_j is set to 1 when a RB scheduled for the CT is shared with the j^{th} D2D user and 0 otherwise.

Equation 4.1 shows that the total cell spectral efficiency can be maximized by either increasing Γ_C and Γ_{D_j} (i.e. utilizing higher users' transmit power) for a very limited number of users sharing resources or sharing the CT resources with higher number $\mathcal{X}$ (given by equation 4.2) of D2D users having lower transmit power. The logarithmic nature of equation 4.1 makes having higher $\mathcal{X}$ preferable to increasing Γ_C and Γ_{D_j} for given users' threshold SINRs. However, $\mathcal{X}$ cannot be increased indefinitely due to the higher mutual interference among users sharing resources. Therefore an optimal $\mathcal{X}$ (i.e. $\mathcal{X}^{max}$) that maximizes the total cell spectral efficiency while achieving users' threshold SINRs should be estimated.

$$\mathcal{X} = \sum_{j=1}^{N} x_j \tag{4.2}$$

The reuse of the CT's UL RBs for D2D brings about DT_{Tx} - BS interference as well as CT - DT_{Rx} interference. Additionally, a DT_{Rx} of a given D2D pair will also experience interference from other DT_{Txs} when more than one D2D pair reuse the CT's RB. The SINRs, Γ_C at the BS and Γ_{D_j} at the j^{th} DT_{Rx} given by equations 4.3a and 4.3b respectively, should at least equal their threshold values.

$$\Gamma_C = \frac{P_C G_C}{\sum_{j=1}^{N} x_j P_{D_j} G_{D_j B} + \mathcal{N}} \geq \Gamma_C^{th} \tag{4.3a}$$

$$\Gamma_{D_j} = \frac{x_j P_{D_j} G_{D2D_j}}{P_C G_{CD_j} + \left(\sum_{l=1, l\neq j}^{N} x_l P_{D_l} G_{D2O_{lj}} \right) + \mathcal{N}} \geq \Gamma_D^{th} \tag{4.3b}$$

The expression $\left(\sum_{l=1, l\neq j}^{N} x_l P_{D_l} G_{D2O_{lj}} \right)$ in equation 4.3b represents the mutual interference from other DT_{Txs} reusing the same RB onto the j^{th} DT_{Rx} and can be rewritten as,

$$\sum_{l=1, l\neq j}^{N} x_l P_{D_l} G_{D2O_{lj}} = \sum_{l=1}^{N} x_l P_{D_l} G_{D2O_{lj}} - x_j P_{D_j} G_{D2D_j} \tag{4.4}$$

The following assumptions are considered in this analysis to estimate $\mathcal{X}^{max}$ (i.e. optimal number of D2D users that can share the CT resources while meeting all users' SINR requirements):

1. Average channel gains between communicating entities are used to determine RSS values due to the uniform user distribution within the cell.

2. Shadow fading is ignored such that the radio channel is invariant during data transmission periods and thus the distance-based pathloss models determine the average channel gains among users sharing resources.

3. The CT and multiple D2D users sharing the RB just achieve their threshold SINRs.

4. Only intra-cell interference due to RB reuse is considered in the single cell scenario.

In order to meet the CT's threshold SINR requirements during RB sharing, the BS controls the CT's transmit power by scaling it up using an interference margin factor, k, $\left(\forall k \in \{\mathbb{R}^+; k > 1\}\right)$. This factor compensates for the expected interference when other DT_{Txs} share the CT's RB. Therefore, this control of CT's transmit power leads to a higher SNR, Γ_C^{SNR} of $k\Gamma_C^{th}$ at the BS when no D2D users share the CT's RB. From this, the minimum CT transmit power required to allow DT_{Txs} to reuse its RB is formulated in equation 4.5.

$$\frac{P_C G_C}{\mathcal{N}} = k\Gamma_C^{th} = \Gamma_C^{SNR} \tag{4.5a}$$

$$k = \frac{\Gamma_C^{SNR}}{\Gamma_C^{th}} = \frac{P_C G_C}{\mathcal{N}\Gamma_C^{th}} > 1 \tag{4.5b}$$

From equations 4.3a and 4.5a, the maximum interference at the BS from all $\mathrm{DT_{Tx}}$'s sharing the CT's RB must satisfy the condition (in equation 4.6) that:

$$\sum_{j=1}^{N} x_j P_{D_j} G_{D_j B} \leq \left(\frac{\Gamma_C^{SNR}}{\Gamma_C^{th}} - 1\right)\mathcal{N} \tag{4.6}$$

Using average channel gains in equations 4.5b and 4.6, the average CT and $\mathrm{DT_{Tx}}$ transmit powers, $\overline{P}_C$ and $\overline{P}_D$ respectively are obtained in equations 4.7a and 4.7b.

$$\overline{P}_C > \frac{\mathcal{N}\Gamma_C^{th}}{\mathbb{E}[G_C]} \tag{4.7a}$$

$$\overline{P}_D \leq \frac{1}{\mathcal{X}} \frac{\left(\frac{\Gamma_C^{SNR}}{\Gamma_C^{th}} - 1\right)\mathcal{N}}{\mathbb{E}[G_{DB}]} \tag{4.7b}$$

where $\overline{P}_C$ and $\overline{P}_D$ should be within the UTs' transmit power bounds (equation 4.8) as per the 3GPP standards requirements [56].

$$\mathcal{P}_C^{min} \leq \overline{P}_C \leq \mathcal{P}_C^{max} \tag{4.8a}$$

$$\mathcal{P}_D^{min} \leq \overline{P}_D \leq \mathcal{P}_D^{max} \tag{4.8b}$$

Lemma 4.1. *Since the DT_{Tx} transmit power defined in equation 4.7b decreases with increasing $\mathcal{X}$ and given the $\mathcal{P}_D^{min}$ transmit power bound, the maximum number, $\mathcal{X}_C^{max}$, of D2D users allowed to reuse the CT's RB while meeting the CT's SINR threshold is given in equation 4.9.*

$$\mathcal{X} \leq \frac{1}{\mathcal{P}_D^{min}} \frac{\left(\frac{\Gamma_C^{SNR}}{\Gamma_C^{th}} - 1\right)\mathcal{N}}{\mathbb{E}[G_{DB}]} \equiv \mathcal{X}_C^{max} \tag{4.9}$$

Lemma 4.2. *Additionally, using equations 4.3b, 4.4, 4.7a and 4.7b, the maximum number, $\mathcal{X}_D^{max}$ of D2D users allowed to reuse the RB while meeting the DT_{Rx}' threshold SINRs can be derived as in equation 4.10.*

$$\frac{\frac{\left(\frac{\Gamma_C^{SNR}}{\Gamma_C^{th}}-1\right)\mathcal{N}}{\mathcal{X}} \frac{\mathbb{E}[G_{D2D}]}{\mathbb{E}[G_{DB}]}}{\Gamma_C^{SNR}\mathcal{N}\frac{\mathbb{E}[G_{CD}]}{\mathbb{E}[G_C]} + \left(\frac{\Gamma_C^{SNR}}{\Gamma_C^{th}} - 1\right)\mathcal{N}\frac{\mathbb{E}[G_{D2O}]}{\mathbb{E}[G_{DB}]} - \frac{\left(\frac{\Gamma_C^{SNR}}{\Gamma_C^{th}}-1\right)\mathcal{N}}{\mathcal{X}} \frac{\mathbb{E}[G_{D2D}]}{\mathbb{E}[G_{DB}]} + \mathcal{N}} \geq \Gamma_D^{th} \tag{4.10a}$$

$$\mathcal{X} \leq \frac{\left(\frac{\Gamma_C^{SNR}}{\Gamma_C^{th}} - 1\right)\frac{(1+\Gamma_D^{th})}{\Gamma_D^{th}}\frac{\mathbb{E}[G_{D2D}]}{\mathbb{E}[G_{DB}]}}{\Gamma_C^{SNR}\frac{\mathbb{E}[G_{CD}]}{\mathbb{E}[G_C]} + \left(\frac{\Gamma_C^{SNR}}{\Gamma_C^{th}} - 1\right)\frac{\mathbb{E}[G_{D2O}]}{\mathbb{E}[G_{DB}]} + 1} \equiv \mathcal{X}_D^{max} \tag{4.10b}$$

Since the channel gain has two independent random variable components (as given in equation 3.3), its average value is given as:

$$\mathbb{E}[G] = c\mathbb{E}[r^{-\alpha}]\mathbb{E}[|h|^2] \tag{4.11}$$

With the assumed invariance of the radio channel during the transmission period (i.e. $\mathbb{E}[|h|^2] = 1$), only the pathloss component is taken into consideration. The average

channel gain is thus derived in equation 4.12 using equation 3.6 as described in [41].

$$\mathbb{E}[G] = c\mathbb{E}[r^{-\alpha}] = c\int_{R_{min}}^{R_{max}} r^{-\alpha} f(r)dr \tag{4.12a}$$

$$\mathbb{E}[G] = \frac{2c}{R_{max}^2(\alpha-2)}\left(R_{min}^{-(\alpha-2)} - R_{max}^{-(\alpha-2)}\right) \tag{4.12b}$$

In equation 4.13, the respective average channel gains required to compute $\mathcal{X}_C^{max}$ and $\mathcal{X}_D^{max}$ are formulated using equation 4.12b as follows:

$$\mathbb{E}[G_{D2D}] = \frac{2c_u}{R_{D2D}^2(\alpha_u-2)}\left(R_{min}^{-(\alpha_u-2)} - R_{D2D}^{-(\alpha_u-2)}\right) \tag{4.13a}$$

$$\mathbb{E}[G_{DB}] = \frac{2c_b}{R_{D}^2(\alpha_b-2)}\left(R_{min}^{-(\alpha_b-2)} - R_{D}^{-(\alpha_b-2)}\right) \tag{4.13b}$$

$$\mathbb{E}[G_{C}] = \frac{2c_b}{R_{C}^2(\alpha_b-2)}\left(R_{min}^{-(\alpha_b-2)} - R_{C}^{-(\alpha_b-2)}\right) \tag{4.13c}$$

$$\mathbb{E}[G_{CD}] = \frac{2c_u}{R_{CD}^2(\alpha_u-2)}\left(R_{min}^{-(\alpha_u-2)} - R_{CD}^{-(\alpha_u-2)}\right) \tag{4.13d}$$

$$\mathbb{E}[G_{D2O}] = \frac{2c_u}{R_{D2O}^2(\alpha_u-2)}\left(R_{min}^{-(\alpha_u-2)} - R_{D2O}^{-(\alpha_u-2)}\right) \tag{4.13e}$$

Finally, the maximum number, $\mathcal{X}^{max}$, of D2D pairs that can share the CT's RB in the cell while meeting the SINR constraints in equation 4.3 is given by $\min\left\{\mathcal{X}_C^{max}, \mathcal{X}_D^{max}\right\}$. The total cell spectral efficiency, η, is then computed from equation 4.1 using $\mathcal{X}^{max}$ and the threshold SINRs Γ_C^{th} and Γ_D^{th}. The following section numerically studies the parameters that have direct impact on the total cell spectral efficiency through affecting the value of $\mathcal{X}^{max}$.

4.2 Analytical Model Results for D2D Resource Reuse

The formulated maximum number, $\mathcal{X}^{max}$ of D2D pairs that can share the CT's RB in section 4.1 facilitates the analysis of total cell spectral efficiency constraining parameters. These parameters are classified in two categories: CT and D2D constraints. Table 4.1 shows the default values used in this analysis together with those in table 3.1.

Table 4.1: Analysis parameters

Parameter	**Symbol**	**Default value**
Minimum user separation	R_{min}	10 m
CT $\Leftrightarrow$ BS distance	R_C	200 m
DT_{Tx} $\Leftrightarrow$ BS distance	R_D	200 m
D2D pair separation	R_{D2D}	20 m
CT $\Leftrightarrow$ DT_{Rx} distance	R_{CD}	400 m
Inter DT_{Tx} $\Leftrightarrow$ DT_{Rx} distance	R_{D2O}	400 m
CT Transmit power	P_C	23 dBm

Note: In the following analysis, the distances R are normalized with respect to the cell radius (i.e. normalized R, $R^{norm.} = \frac{R}{R_{cell}}$).

4.2.1 CT Constraints

Figure 4.3 shows how the CT's transmit power and CT-BS distance affect the cell spectral efficiency through impacting $\mathcal{X}^{max}$.

CT Transmission Power (P_C):

The CT transmit power, P_C is important in defining the achieved CT SNR, Γ_C^{SNR} and interference margin factor, k (equation 4.5a) at the BS. The variation of P_C (in the range $\mathcal{P}_C^{min}$ to $\mathcal{P}_C^{max}$) while keeping other factors (e.g. CT-BS channel gain) constant determines the extent to which the scheduled RB can be reused by other D2D pairs. Figure 4.3(a) shows a linear relationship between Γ_C^{SNR} and P_C, in the dB domain,

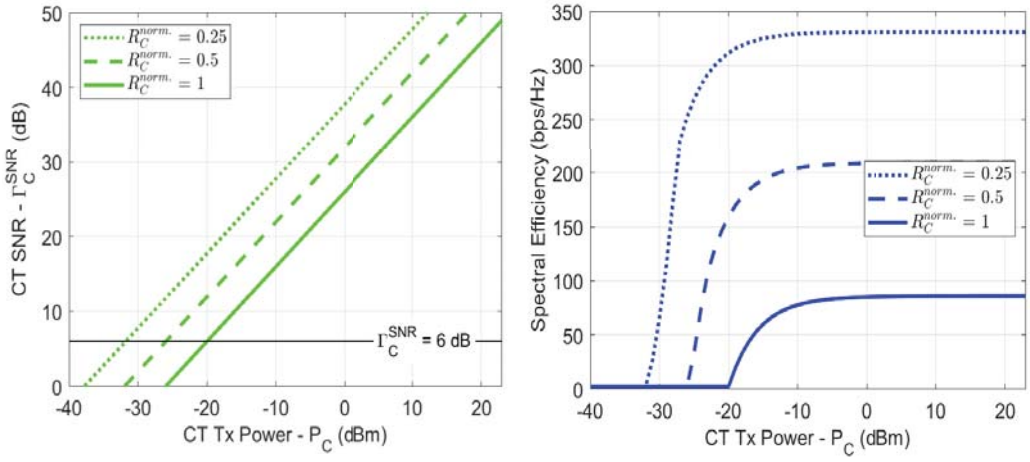

(a) CT SNR dependency on P_C

(b) Spectral efficiency dependency on P_C

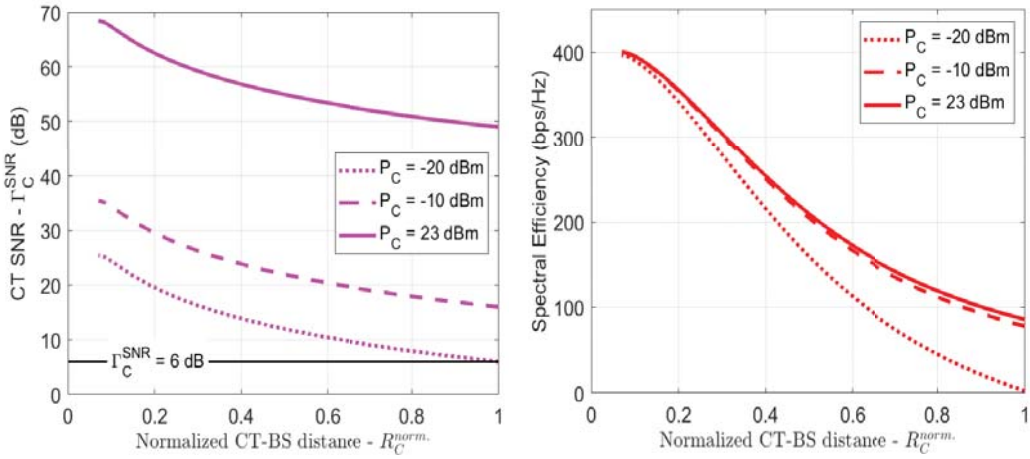

(c) CT SNR dependency on R_C

(d) Spectral efficiency dependency on R_C

FIGURE 4.3: Impact of CT constraints cell spectral efficiency.

for three normalized CT-BS distances (i.e. $R_C^{norm.} = 0.25, 0.5$ and 1). For a given P_C, higher Γ_C^{SNR} is achieved with smaller $R_C^{norm.}$ due to greater CT-BS channel gain when the CT is closer to the BS. Figure 4.3(b) shows the impact of varying P_C on the achieved cell spectral efficiency for $R_C^{norm.} = 0.25, 0.5$ and 1. Low values of P_C (for which $\Gamma_C^{SNR} \leq \Gamma_C^{th} = 6$ dB in figure 4.3(a)) result in constant spectral efficiency i.e. only the CT contributes to the achieved spectral efficiency since k is small ($k \leq 1$) and thus no RB reuse is allowed as per equation 4.9.

Further increase of P_C, such that $\Gamma_C^{SNR} > \Gamma_C^{th} = 6$ dB in figure 4.3(a) leads to a rapid increase in spectral efficiency but quickly saturates when P_C results in $\Gamma_C^{SNR} > 20$ dB. This saturation is due to the very high mutual interference between the many D2D pairs sharing the RB. Therefore, high values for P_C are preferred for the CT whose scheduled RBs are shared with other multiple D2D pairs to improve the cell spectral efficiency. The spectral efficiency performance is higher for smaller $R_C^{norm.}$ with a given P_C due to greater Γ_C^{SNR} that provides a larger interference margin.

CT-BS Distance (R_C):

The second parameter with direct impact on the interference margin, k is the CT's radio channel gain, G_C, towards the BS (see equation 4.5a), which depends on R_C. Typically, radio channel gains reduce with increasing distance between communicating parties. Figure 4.3(c) shows that Γ_C^{SNR} decreases with increasing R_C when P_C is set to three values (i.e. $P_C = -20, -10$ and 23 dBm). Consequently, the interference margin decreases with increasing R_C for a fixed P_C hence leading to lower number, $\mathcal{X}_C^{max}$, of D2D pairs sharing the RB. As discussed above, increasing P_C results in higher Γ_C^{SNR} and interference margin, k.

Figure 4.3(d) shows the impact of varying R_C on the achieved cell spectral efficiency for $P_C = -20, -10$ and 23 dBm. There is marginal impact on spectral efficiency for P_C settings above -10 dBm. The cell spectral efficiency decreases with increasing R_C due to the decreasing interference margin. This result illustrates that depending on R_C, different number, $\mathcal{X}^{max}$, of D2D pairs can share the CT's RB to increase the cell spectral efficiency while achieving all users' threshold SINRs. Therefore, sharing resources of CTs closer to the BS is more desirable to maximize spectral efficiency.

4.2.2 D2D Constraints

Figure 4.4 illustrates the impact of D2D pairs related parameters, i.e. D2D separation, R_{D2D}, and DT_{Tx}-BS distance, R_D, on the cell spectral efficiency through affecting $\mathcal{X}^{max}$ while all users achieve their threshold SINRs.

D2D Separation (R_{D2D}):

Figure 4.4(a) shows the cell spectral efficiency variation with increasing $R_{D2D}^{norm.}$ for three different DT_{Tx}-BS distances (i.e. $R_D^{norm.} = 0.5$, 0.75 and 1). The cell spectral efficiency decreases exponentially with increasing R_{D2D} reaching a steady value of only the CT's spectral efficiency when $R_{D2D}^{norm.}$ is approximately greater than 0.4. This negative impact on cell spectral efficiency is attributed to the decreasing D2D pair gain, G_{D2D} with higher R_{D2D} and hence reduces the number, $\mathcal{X}_D^{max}$, of D2D pairs that share the CT's RB as given in equation 4.10b. Additionally, better cell spectral efficiency is achieved for

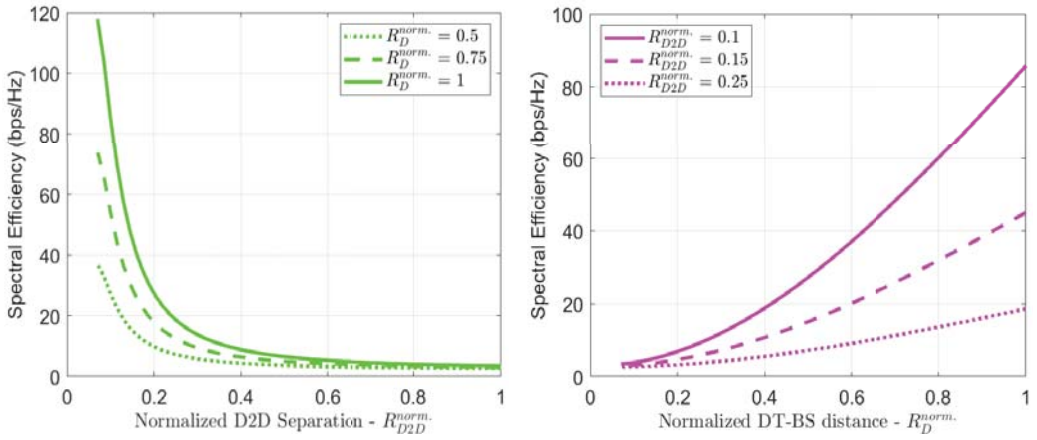

(a) Spectral efficiency dependency on R_{D2D} (b) Spectral efficiency dependency on R_D

FIGURE 4.4: Impact of DT constraints on cell spectral efficiency.

TABLE 4.2: Maximum number of D2D pairs sharing a given RB

$\mathcal{X}^{max}$ D2D pairs		$R_{D2D}^{norm.}$ 0.1	0.15	0.25
P_C (dBm)	-15	11	5	2
	-10	14	7	2
	23	**16**	8	3

higher values of DT_{Tx}-BS distance, $R_D^{norm.}$, due to lower G_{DB} that results in reduced interference at the BS from D2D pairs during RB sharing.

Table 4.2 shows the maximum number, $\mathcal{X}^{max}$, of D2D pairs that maximize the spectral efficiency while achieving their threshold SINRs for different settings of P_C and $R_{D2D}^{norm.}$. The results show a decrease of $\mathcal{X}^{max}$ when either P_C decreases or $R_{D2D}^{norm.}$ increases. The maximum of 16 D2D pairs sharing the CT's RB is realised with $P_C = 23$ dBm and $R_{D2D}^{norm.} = 0.1$. Therefore, in order to achieve the high spectral efficiency gains during reuse of cellular UL spectrum, D2D pairs whose DTs are in close proximity of not more than 10% of the cell radius (i.e. $20m$) are the preferred choice. This D2D separation is adopted in the remaining part of the thesis.

DT_{Tx}-BS Distance (R_D):

Figure 4.4(b) shows the variation of cell spectral efficiency with $R_D^{norm.}$ for three cases of D2D separations (i.e. $R_{D2D}^{norm.} = 0.1$, 0.15 and 0.25). Increasing R_D results in higher cell spectral efficiency performance for each case, with the $R_{D2D}^{norm.} = 0.1$ case presenting the best performance. The increase of $R_D^{norm.}$ deteriorates the DTs-BS channel gains, G_{DB}, and thus reduces the observed DT_{Tx}-BS interference due to RB reuse for D2D communication. This results in higher number, $\mathcal{X}^{max}$ (see equations 4.9 and 4.10b), of D2D pairs sharing the cellular spectrum and thus improves the cell spectral efficiency. This demonstrates that D2D pairs further away from the BS present higher opportunities in achieving better spectral efficiency performance compared to their counterparts located near the BS.

4.3 Uniform Interference Power (UIP) Scheme for D2D

The users transmission power is a major factor in the spectral efficiency performance during resource reuse for D2D communication. As discussed in section 4.2.1, the CT's transmit power, P_C is increased in order to accommodate the reuse of its RB by multiple D2D pairs. It is also equally important that the transmit power of the D2D pairs reusing the cellular resources is adapted to ensure that the resultant interference is kept within the interference margin set by P_C. The following sections discuss transmit power allocation strategy for D2D pairs in the proposed UIP scheme together with the scheme's performance in a single cell scenario.

4.3.1 UIP Transmit Power Allocation Strategy

Different from the analytical model in section 4.1, users are typically randomly distributed within the cellular network with varying distances to the BS as well as between themselves. In such circumstances, for given P_{D_j} of $\mathrm{DT_{Tx}}s$, the BS experiences different levels of interference while sharing resources with multiple D2D pairs. A UIP scheme is proposed for D2D while reusing the cellular uplink spectrum resources [18]. In this scheme, the CT transmit power, P_C is set to $\mathcal{P}_C^{max}$ to provide the maximum interference margin using equation 4.5b while P_{D_j} of all $\mathrm{DT_{Tx}}s$ reusing the RB is controlled (assigned) by the BS in such a way that each $\mathrm{DT_{Tx}}$ contributes the same (uniform) interference at the BS as other $\mathrm{DT_{Tx}}s$ sharing the RB. In order to keep within the interference margin set by P_C, the number, $\mathcal{X}$, of D2D pairs reusing the RB equally share the acceptable interference given in equation 4.6 at the BS. The transmit power assigned to each $\mathrm{DT_{Tx}}$ is then computed using equation 4.14 below.

$$P_{D_j} G_{D_j B} \leq \frac{\left(\frac{\Gamma_C^{SNR}}{\Gamma_C^{th}} - 1\right)\mathcal{N}}{\mathcal{X}} \tag{4.14a}$$

$$P_{D_j} = \frac{1}{\mathcal{X}} \frac{\left(\frac{\Gamma_C^{SNR}}{\Gamma_C^{th}} - 1\right)\mathcal{N}}{G_{D_j B}} \tag{4.14b}$$

This $\mathrm{DT_{Tx}}$ transmit power allocation strategy ensures that $\mathrm{DT_{Tx}}s$ with higher channel gains towards the BS (i.e. $\mathrm{DT_{Tx}}s$ located closer to the BS) are assigned less transmit power as compared to those with lower $\mathrm{DT_{Tx}}$-BS channel gains. The UIP transmit power assignment scheme for $\mathrm{DT_{Tx}}s$ is different from that applied in the analytical model where the $\mathrm{DT_{Tx}}s$ were assigned uniform power, $\overline{P}_D$, based on average channel gain towards the BS. The following section evaluates the performance of the proposed UIP scheme.

4.3.2 UIP Performance Evaluation

The performance analysis of the UIP scheme is divided into three parts consisting of: 1) total cell spectral efficiency, 2) CT outage probability and 3) achieved DTs' SINRs. The simulations were carried out in a single isolated cell enviroment with one CT and variable number of multiple D2D pairs uniformly distributed within the cell, which are then allocated transmit power using the UIP scheme. Table 4.3 gives the additional

TABLE 4.3: UIP simulation parameters

Parameter	Symbol	Default value
Number of CTs	M	1
Number of DTs	N	variable 1 - 40
CT transmit power	$P_C = \mathcal{P}_C^{max}$	23 dBm
max. D2D pair separation	$R_{D2D} = 0.1R_{cell}$	20 m

simulation parameters used in this evaluation together with other parameters given in section 3.3.

The UIP scheme performance is compared with the BAC scheme in the state of the art [41] (discussed in section 2.3.1), where the CT's transmit power is also increased to provide an interference margin using the LTE OFPC. For a suitable comparative analysis, the same P_C is used for both the UIP and BAC schemes. However, in the BAC scheme, each $\mathrm{DT_{Tx}}$ transmit power is set by applying a channel inversion power control algorithm which maintains a fixed RSS of $-78\ dBm$ at the respective $\mathrm{DT_{Rx}}$ for a given D2D pair. The set $\mathrm{DT_{Txs}}$ transmit power, P_{D_j}, should be within the limits $\{P_D^{min}, P_D^{max}\}$ for both the UIP and BAC schemes.

Total Cell Spectral Efficiency

Figure 4.5 shows the average total cell spectral efficiency as a function of the number of D2D pairs sharing the CT's RB for the UIP and BAC schemes. With fewer number of D2D pairs sharing the given RB, the difference in performance between the two schemes is observed to be relatively small with the UIP scheme being better. This is attributed to the low mutual interference between the D2D pairs sharing the RB in both schemes. However, with increasing number of D2D pairs sharing the RB, the UIP scheme increasingly outperforms the BAC scheme. Its is observed that the BAC scheme

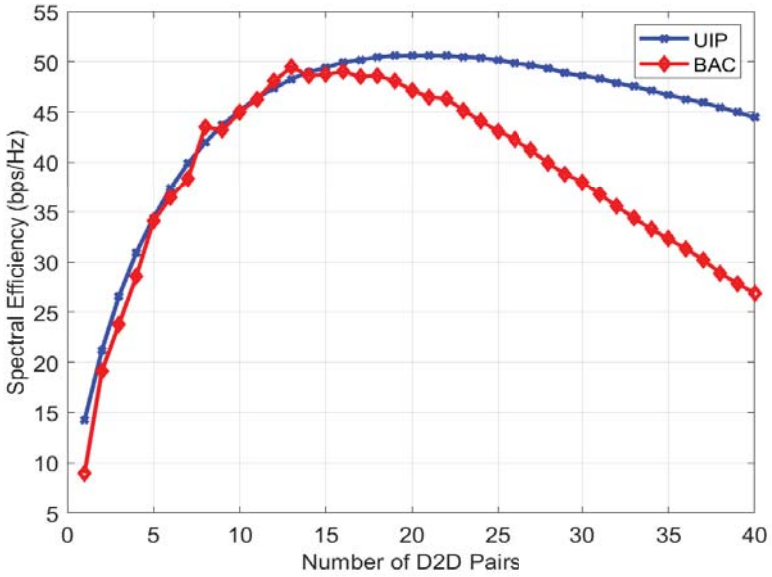

FIGURE 4.5: Spectral efficiency versus number of D2D pairs.

achieves maximum spectral efficiency with $\mathcal{X} = 16$ D2D pairs sharing the CT's RB, which is similar to the analytical result in section 4.2.2 whereas the UIP scheme reaches its maximum when $\mathcal{X}$ is approximately 21 D2D pairs. This difference in $\mathcal{X}$ for UIP compared to the analytical results is due to the control of $\mathrm{DT}_{\mathrm{Tx}s}$ transmit power in relation to that of the CT whose RB is shared.

Further increase of $\mathcal{X}$ up to 40 results in a decrease of the spectral efficiency for both schemes due to increased mutual interference between D2D pairs sharing a RB. A 10% performance difference between the two schemes is observed when 21 D2D pairs share the CT's RB and this difference increases to approximately 65% when $\mathcal{X} = 40$. This result shows that the UIP scheme performs better than the BAC scheme by allowing more D2D pairs to share the CT's RB and hence improves the total cell spectral efficiency. The achieved maximum total cell spectral efficiency for the UIP scheme (i.e. 50 bps/Hz) is observed to be over 20 times that of the conventional CT when it achieves its threshold SINR (i.e. 2.32 bps/Hz) while its RB is not reused by any D2D pairs. However, the achieved maximum total cell spectral efficiency for the UIP and BAC schemes is approximately 40% below the analytical results. This is because the analytical study assumed that all $\mathcal{X}$ D2D pairs sharing the RB achieved their threshold SINRs, which is not necessarily the case for both UIP and BAC schemes as discussed below.

CT Outage Probability with flexible number of DTs

Figure 4.6 compares the CT outage probability of the UIP and BAC schemes as the number of D2D pairs sharing the CT's RB is increased. The CT is considered to go into outage once its achieved SINR during RB sharing with the D2D pairs goes below Γ_C^{th}. Here, the outage probability was computed as the ratio of the number of times the CT goes into outage to the number of simulation runs for a given number of D2D pairs sharing the CT's RB. The UIP scheme results show that the CT does not experience any outage because the $\mathrm{DT}_{\mathrm{Tx}s}$ transmit power is controlled based on P_C in order not to exceed the set interference margin. However, the BAC scheme experiences higher CT outage with increasing number of D2D pairs sharing the RB. This is because the $\mathrm{DT}_{\mathrm{Tx}s}$ transmit power allocation in this scheme is independent of P_C. Therefore, as the number of D2D pairs sharing the RB increases, the CT experiences more interference leading to

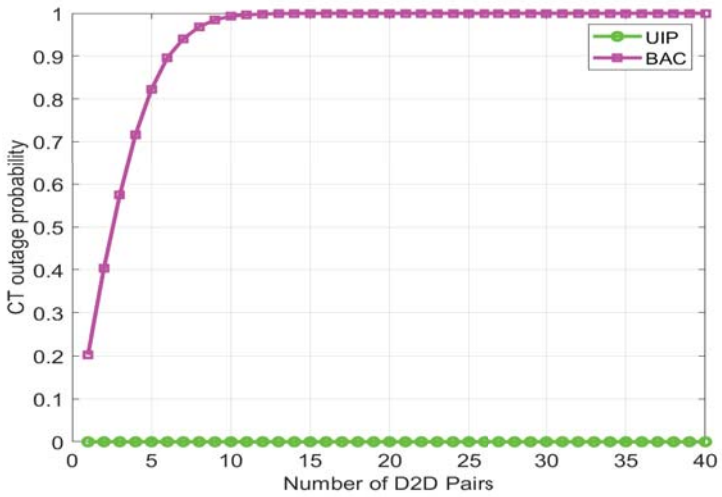

FIGURE 4.6: CT outage probability versus number of D2D pairs.

its outage. The BAC scheme should thus share the CT's RB with very limited number of D2D pairs to minimize CT outage.

DTs' SINRs with fixed number of DTs

Figure 4.7 shows the CDF of the $DT_{Rxs'}$ achieved SINRs when 16 and 21 D2D pairs reuse the RB allocated to the CT for the UIP and BAC schemes. It is observed that DT_{Rxs} achieve higher SINRs with low number of D2D pairs sharing the CT's RB. For example, with 16 D2D pairs, approximately 40% of the DT_{Rxs} achieve SINRs above the 15 dB threshold as compared to approximately 30% of the DT_{Rxs} with 21 D2D pairs. This is attributed to the low mutual interference between the D2D pairs with lower number of D2D pairs sharing the CT's RB. Additionally, the UIP scheme presents better SINR performance than the BAC scheme with more DT_{Rxs} achieving higher SINRs. Although almost the same proportion of DT_{Rxs} achieve the SINR threshold of 15 dB for both schemes, there are more DT_{Rxs} achieving higher SINRs (e.g. above 30 dB) in the UIP scheme. This difference in SINR performance is due to stronger mutual interference between D2D pairs arising from higher transmit power allocations in the BAC scheme compared with UIP.

This result demonstrates that not all D2D pairs in the cell are eligible to share the CT's RB due to their failure (e.g. approximately 60% of D2D pairs) to achieve Γ_D^{th}. Therefore, appropriate selection algorithms are required to ensure that the selected D2D pairs sharing the CT's RB achieve their threshold SINRs while improving the total cell spectral efficiency.

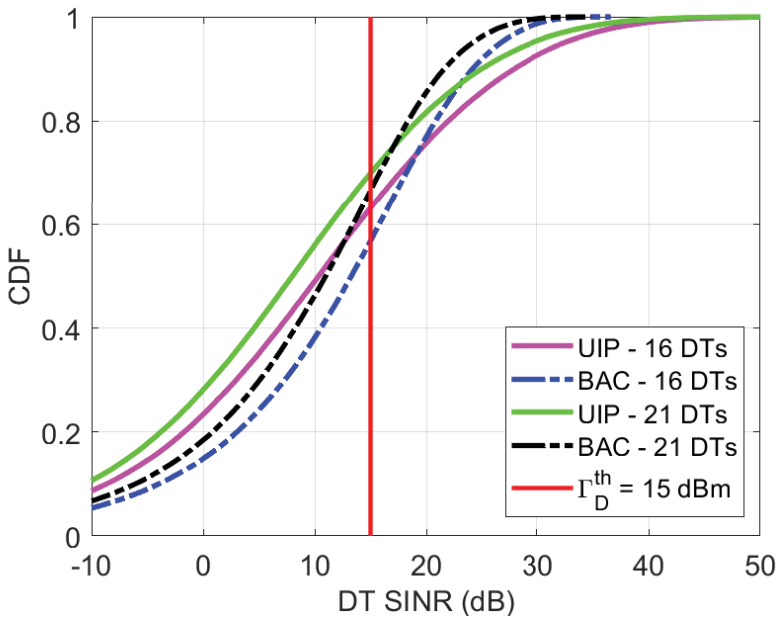

FIGURE 4.7: DT_{Rx} SINR performance.

4.4 Resource Reuse Regions

The spatial resource reuse by multiple D2D pairs within a cell requires specific determination of the different ILA sizes as described in this chapter's introduction. The ILA sizes aid in identification of the reuse and/or no-reuse regions within the cell where other potential D2D pairs are either admitted or not admitted to share a RB. Figure 4.8 illustrates the different RB reuse regions within a given cell from both the CT and D2D user's perspective. To ensure reliable communication from the CT to BS (figure 4.8(a) shows the CT user's perspective), the $\mathrm{DT_{Txs}}$ sharing the RB should be outside the red-dotted circles centered around the BS. Increasing the number of $\mathrm{DT_{Txs}}$ sharing the RB results in a bigger circle that defines the ILA (i.e. the circle size expands from B_1 to B_2 in this example where the increase is from 1 to 2 $\mathrm{DT_{Txs}}$ reusing a RB). Therefore, the RB reuse region where all $\mathrm{DT_{Txs}}$ should be located to guarantee the CT's achievement of Γ_C^{th} is outside the bigger circle. The ILA size increase ensures that the resultant interference from the existing and additional D2D pairs sharing a RB is tolerable for the CT to realize Γ_C^{th}. Accordingly, increased number of D2D users reusing a CT's RBs must be further away from the BS to keep within the CT's interference margin.

Similarly, from the D2D pair's perspective (figure 4.8(b) where a given D2D pair reuses a RB), the CT and other $\mathrm{DT_{Txs}}$ sharing the RB should be outside the blue-dotted circles cetered around the $\mathrm{DT_{Rx}}$. The size of these ILA circles also expands (e.g. from D_1 to D_2 in this illustration) with increasing number of D2D pairs sharing the RB. Typically, due to DTs proximity, the transmit power of $\mathrm{DT_{Txs}}$ is less than that used by the CT. This results in a given $\mathrm{DT_{Rx}}$ experiencing lower interference from each of the other $\mathrm{DT_{Txs}}$ than from the CT during RB sharing. Correspondingly, the ILA size around a $\mathrm{DT_{Rx}}$ is smaller for the other $\mathrm{DT_{Txs}}$ sharing the RB compared to that of the CT.

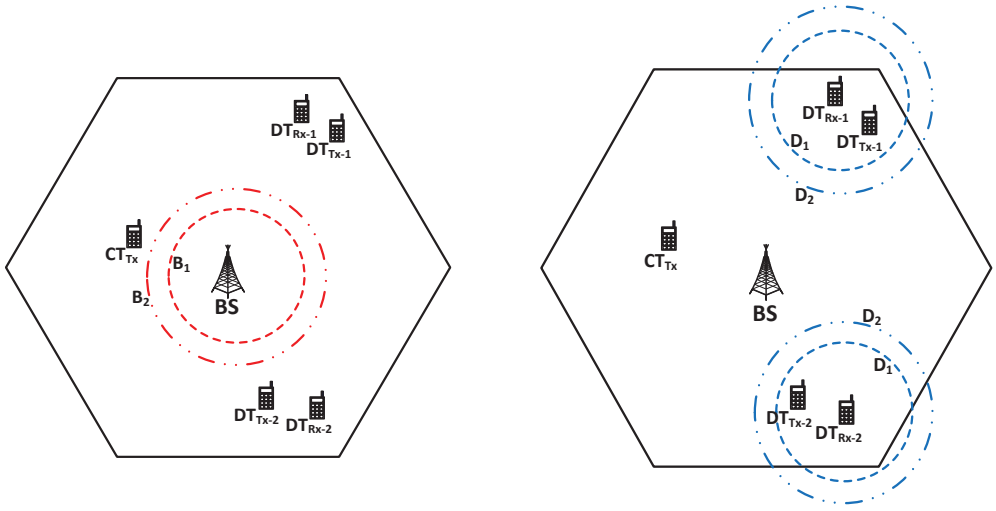

(a) RB reuse region from CT perspective

(b) RB reuse region from D2D perspective

FIGURE 4.8: D2D users resource reuse regions.

Consequently, during sharing of the CT's RB within a cell, three reuse distances are important in defining the size of the ILA circles that are centered around either the BS or $\mathrm{DT_{Rx}}$:

1. DT_{Tx}-BS reuse distance, $R^{reuse}_{D_j}$;
2. CT-DT_{Rx} reuse distance, $R^{reuse}_{CD_j}$;
3. DT_{Tx}-DT_{Rx} reuse distance, $R^{reuse}_{D2O_{lj}}$.

These distances depend on the users' performance requirements e.g. threshold SINRs, their transmit power allocation strategy and the actual channel gains among the communicating entities. Two known LTE power control strategies: fixed SNR target (Fixed SNR Target (FST)) and closed-loop (Closed Loop power control (CL)) power control are considered to formulate these reuse distances.

The following sections formulate the ILA sizes based on given network and/or UT performance requirements to establish the resource reuse regions within the cell using FST and CL strategies. Three assumptions are utilized in the formulations:

1. the radio channel is invariant during data transmission period, i.e. shadow fading is ignored and therefore channel gains between communicating entities are determined by the distance-based pathloss models;
2. the limiting case in a single-cell scenario occurs when all interferers are equidistant from a given receiver with which the RB is shared; and
3. the maximum separation, R_{D2D} between DTs in any given D2D pair should not exceed 10% of the cell radius, R_{cell} to benefit from DTs' proximity as discussed in section 4.2.2.

4.4.1 Fixed SNR Target Power Control (FST)

In LTE, FST power control fully compensates the signal pathloss between any two communicating entities and thus guarantees a given RSS level at the respective receiver [62]. This strategy only considers system noise effects and ignores any experienced interference while assigning users' transmit powers. Accordingly, a fixed SNR is achieved at the corresponding receiver and applying the FST power control strategy for all users, the CT and DTs' transmit powers are obtained in a distributed manner using equation 4.15.

$$\frac{P_C G_C}{\mathcal{N}} = \Gamma_C^{target} \tag{4.15a}$$

$$\frac{P_{D_j} G_{D2D_j}}{\mathcal{N}} = \Gamma_D^{target} \tag{4.15b}$$

where Γ_C^{target} and Γ_D^{target} are the target SNRs for the CT and DTs, respectively.

The users' target SNRs are set such that they are greater than their required threshold SINRs. This makes their respective communication more resilient to the impending intra-cell interference during RB sharing due to the incorporated interference margin for each user by the FST strategy. Therefore, with this strategy, all users' transmit powers are higher than the amount that is required to achieve their threshold SINRs and also within the minimum and maximum UT's power limits given in table 3.1.

Lemma 4.3. *Given the CT and DTs' target SNRs and threshold SINRs while employing the FST strategy, the reuse distances defining the ILAs are such that:*

$$R_{D_j}^{reuse} \geq \left(\mathcal{X}\frac{1}{\mathcal{I}_C^{max}}\right)^{\frac{1}{\alpha}} R_{D2D} \equiv R_{D_\mathcal{X}}^{FST} \tag{4.16a}$$

$$R_{CD_j}^{reuse} \geq \left(\mathcal{X}\frac{\Gamma_C^{target}}{\Gamma_D^{target}}\frac{1}{\mathcal{I}_{D_j}^{max}}\right)^{\frac{1}{\alpha}} R_C \equiv R_{CD_\mathcal{X}}^{FST} \tag{4.16b}$$

$$R_{D2O_{lj}}^{reuse} \geq \left(\mathcal{X}\frac{1}{\mathcal{I}_{D_j}^{max}}\right)^{\frac{1}{\alpha}} R_{D2D} \equiv R_{D2O_\mathcal{X}}^{FST} \tag{4.16c}$$

where;

$$\mathcal{I}_C^{max} = \frac{\Gamma_C^{target} - \Gamma_C^{th}}{\Gamma_D^{target}\Gamma_C^{th}} \qquad \textit{and} \qquad \mathcal{I}_{D_j}^{max} = \frac{\Gamma_D^{target} - \Gamma_D^{th}}{\Gamma_D^{target}\Gamma_D^{th}}$$

Proof. From equations 4.3a and 4.15, the condition that multiple $\mathrm{DT_{Txs}}$ should satisfy in order to share a RB allocated to the CT while achieving Γ_C^{th} is formulated in equation 4.17.

$$\frac{\Gamma_C^{target}}{\Gamma_D^{target}\sum\limits_{j=1}^{N}\frac{x_j G_{D_jB}}{G_{D2D_j}} + 1} \geq \Gamma_C^{th} \tag{4.17a}$$

$$\sum_{j=1}^{N}\frac{x_j G_{D_jB}}{G_{D2D_j}} \leq \mathcal{I}_C^{max} \tag{4.17b}$$

where

$$\mathcal{I}_C^{max} = \frac{\Gamma_C^{target} - \Gamma_C^{th}}{\Gamma_D^{target}\Gamma_C^{th}}$$

is the maximum allowed cumulative interference at the BS due to RB reuse.

Furthermore, using equations 4.3b and 4.15, the other additional condition for selecting multiple D2D pairs sharing the CT's RB (i.e. $x_{j/l} = 1$) is formulated in equation 4.18.

$$\frac{\Gamma_D^{target}}{\Gamma_C^{target}\frac{G_{CD_j}}{G_C} + \Gamma_D^{target}\sum\limits_{l=1,l\neq j}^{N}\frac{x_l G_{D2O_{lj}}}{G_{D2D_l}} + 1} \geq \Gamma_D^{th} \tag{4.18a}$$

$$\frac{\Gamma_C^{target}}{\Gamma_D^{target}}\frac{G_{CD_j}}{G_C} + \sum_{l=1,l\neq j}^{N}\frac{x_l G_{D2O_{lj}}}{G_{D2D_l}} \leq \mathcal{I}_{D_j}^{max} \tag{4.18b}$$

where

$$\mathcal{I}_{D_j}^{max} = \frac{\Gamma_D^{target} - \Gamma_D^{th}}{\Gamma_D^{target}\Gamma_D^{th}}$$

is the maximum allowed cumulative interference at the j^{th} $\mathrm{DT_{Rx}}$ during RB reuse.

Given that the radio channel is assumed to be invariant during data transmission (i.e. $|h|^2 = 1$ in equation 3.3), the distance between communicating entities is a good measure of the channel gain. Therefore, equations 4.17b and 4.18b are rewritten as in equation 4.19.

$$\sum_{j=1}^{N} x_j \left(\frac{R_{D2D_j}}{R_{D_j}}\right)^{\alpha} \leq \mathcal{I}_C^{max} \tag{4.19a}$$

$$\frac{\Gamma_C^{target}}{\Gamma_D^{target}} \left(\frac{R_C}{R_{CD_j}}\right)^{\alpha} + \sum_{l=1, l\neq j}^{N} x_l \left(\frac{R_{D2D_l}}{R_{D_{lj}}}\right)^{\alpha} \leq \mathcal{I}_{D_j}^{max} \tag{4.19b}$$

where R_{CD_j} and $R_{D2O_{lj}}$ are the distances from the: 1) CT to j^{th} $\mathrm{DT_{Rx}}$ and 2) l^{th} $\mathrm{DT_{Tx}}$ to j^{th} $\mathrm{DT_{Rx}}$, respectively.

Using equation 4.19a and taking the limiting case scenario where all the selected $\mathcal{X}$ D2D pairs sharing the same RB have maximum separation, R_{D2D} and are equidistant from the BS (i.e. each $\mathrm{DT_{Tx}}$ contributes the same amount of interference at the BS), the minimum distance, $R_{D_{\mathcal{X}}}^{FST}$, that $\mathrm{DT_{Tx}}s$ should be away from the BS in order to achieve Γ_C^{th} is obtained in equation 4.20.

$$R_{D_j}^{reuse} \geq \left(\mathcal{X}\frac{1}{\mathcal{I}_C^{max}}\right)^{\frac{1}{\alpha}} R_{D2D} \equiv R_{D_{\mathcal{X}}}^{FST} \tag{4.20}$$

Similarly, considering another limiting case scenario where all other $\mathrm{DT_{Tx}}s$ sharing the CT's RB are equidistant from a given $\mathrm{DT_{Rx}}$ (i.e. each $\mathrm{DT_{Tx}}$ is contributing the same amount of interference at the $\mathrm{DT_{Rx}}$), equation 4.19b is further simplified in 4.21.

$$\frac{\Gamma_C^{target}}{\Gamma_D^{target}} \left(\frac{R_C}{R_{CD_j}}\right)^{\alpha} + (\mathcal{X}-1)\left(\frac{R_{D2D}}{R_{D2O_{lj}}}\right)^{\alpha} \leq \mathcal{I}_{D_j}^{max} \tag{4.21}$$

The first and second terms on the left hand side of equation 4.21 represent the contributions to the total amount of interference at the j^{th} $\mathrm{DT_{Rx}}$ by the CT and other $\mathrm{DT_{Tx}}s$ respectively. This shows that each $\mathrm{DT_{Rx}}$ has up to $\mathcal{X}$ interfering users within the cell. Letting the CT's interference contribution to equal that of just one $\mathrm{DT_{Tx}}$ aids in finding the minimum distance, $R_{CD_{\mathcal{X}}}^{FST}$, the CT should be from a given $\mathrm{DT_{Rx}}$ (as given in equation 4.22).

$$\frac{\Gamma_C^{target}}{\Gamma_D^{target}} \left(\frac{R_C}{R_{CD_j}}\right)^{\alpha} = \left(\frac{R_{D2D}}{R_{D2O_{lj}}}\right)^{\alpha} \tag{4.22a}$$

$$\mathcal{X}\frac{\Gamma_C^{target}}{\Gamma_D^{target}} \left(\frac{R_C}{R_{CD_j}}\right)^{\alpha} \leq \mathcal{I}_{D_j}^{max} \tag{4.22b}$$

$$R_{CD_j}^{reuse} \geq \left(\mathcal{X}\frac{\Gamma_C^{target}}{\Gamma_D^{target}}\frac{1}{\mathcal{I}_{D_j}^{max}}\right)^{\frac{1}{\alpha}} R_C \equiv R_{CD_{\mathcal{X}}}^{FST} \tag{4.22c}$$

Finally, substituting 4.22c in 4.22a, gives the minimum distance, $R^{FST}_{D2O_{\mathcal{X}}}$, the other $\mathrm{DT_{Txs}}$ should be from a given $\mathrm{DT_{Rx}}$ with which a RB is shared, as in equation 4.23.

$$R^{reuse}_{D2O_{lj}} \geq \left(\mathcal{X}\frac{1}{\mathcal{I}^{max}_{D_j}}\right)^{\frac{1}{\alpha}} R_{D2D} \equiv R^{FST}_{D2O_{\mathcal{X}}} \tag{4.23}$$

■

4.4.2 Closed Loop Power Control (CL)

The CL scheme allocates users' transmit powers by taking into account their measured interference and either fully or partially compensates for the pathloss between communicating entities [63]. Applying the CL power control strategy for all users, the CT and $\mathrm{DT_{Txs}}$ transmit powers are updated accordingly depending on the pathloss, noise and interference situation due to RB sharing. In contrast to the FST strategy in section 4.4.1, this approach avoids unnecessarily high users' transmit powers that would cause higher interference to other users sharing the RB within the cell. Correspondingly, applying CL strategy ensures that users achieve their threshold SINRs with just sufficient transmit powers. Additionally, given that D2D communication occurs between proximate DTs and given the requirement to limit mutual interference among users during RB sharing, a lower target transmit power, $\mathcal{P}^{target}_{D}$ is recommended for $\mathrm{DT_{Txs}}$ and should be less than $\mathcal{P}^{max}_{D}$ specified by 3GPP.

Lemma 4.4. *Given the CT and DTs' threshold SINRs and their respective maximum/-target transmit power bounds while employing the CL strategy, the reuse distances defining the ILAs are such that:*

$$R^{reuse}_{D_j} \geq \left(\mathcal{X}\frac{c\Gamma^{th}_{C}\mathcal{P}^{target}_{D}}{c\mathcal{P}^{max}_{C}R^{-\alpha}_{C} - \mathcal{N}\Gamma^{th}_{C}}\right)^{\frac{1}{\alpha}} \equiv R^{CL}_{D_{\mathcal{X}}} \tag{4.24a}$$

$$R^{reuse}_{CD_j} \geq \left(\mathcal{X}\frac{c\Gamma^{th}_{D}\mathcal{P}^{max}_{C}}{c\mathcal{P}^{target}_{D}R^{-\alpha}_{D2D} - \mathcal{N}\Gamma^{th}_{D}}\right)^{\frac{1}{\alpha}} \equiv R^{CL}_{CD_{\mathcal{X}}} \tag{4.24b}$$

$$R^{reuse}_{D2O_{lj}} \geq \left(\mathcal{X}\frac{c\Gamma^{th}_{D}\mathcal{P}^{target}_{D}}{c\mathcal{P}^{target}_{D}R^{-\alpha}_{D2D} - \mathcal{N}\Gamma^{th}_{D}}\right)^{\frac{1}{\alpha}} \equiv R^{CL}_{D2O_{\mathcal{X}}} \tag{4.24c}$$

Proof. As can be observed in equations 4.3a and 4.3b, each user has up to $\mathcal{X}$ interfering users within the cell. Taking the limiting case scenario where all the selected $\mathcal{X}$ D2D pairs have maximum separation, R_{D2D} and are equidistant from the BS (i.e. each $\mathrm{DT_{Tx}}$ contributes the same amount of interference at the BS), equation 4.3a is rewritten as in equation 4.25 below.

$$P_C G_C \geq \mathcal{X}\Gamma^{th}_{C} P_{D_j} G_{D_j B} + \mathcal{N}\Gamma^{th}_{C} \tag{4.25}$$

Furthermore, considering another limiting case scenario where: 1) all other $\mathrm{DT_{Txs}}$ sharing the CT's RB are equidistant from a given $\mathrm{DT_{Rx}}$ (i.e. each of the other $\mathrm{DT_{Txs}}$ is contributing the same amount of interference at a given $\mathrm{DT_{Rx}}$) and 2) the CT's contribution to interference at the $\mathrm{DT_{Rx}}$ is equal to that of just one other $\mathrm{DT_{Tx}}$,

equation 4.3b is also simplified in equation 4.26.

$$P_{D_j}G_{D2D_j} \geq \Gamma_D^{th}\Big(P_C G_{CD_j} + (\mathcal{X}-1)P_{D_l}G_{D2O_{lj}} + \mathcal{N}\Big) \tag{4.26a}$$

$$P_C G_{CD_j} = P_{D_l}G_{D2O_{lj}} \tag{4.26b}$$

$$P_{D_j}G_{D2D_j} \geq \mathcal{X}\Gamma_D^{th}P_C G_{CD_j} + \mathcal{N}\Gamma_D^{th} \tag{4.26c}$$

Equations 4.25 and 4.26c show two regions bounded by straight lines. Since P_C and P_{D_j} are coupled together (i.e. depend on each other) in these equations, there is need to find the intersection of these two regions [53]. An intersection point with positive values of both P_C and P_{D_j} is only achievable when the gradient of the line in 4.26c is greater than that of the line in 4.25, i.e.;

$$\frac{G_{D2D_j}}{\mathcal{X}\Gamma_D^{th}G_{CD_j}} > \frac{\mathcal{X}\Gamma_C^{th}G_{D_jB}}{G_C} \tag{4.27}$$

The intersection point $(P_{D_j}^t, P_C^t)$, illustrated in figure 4.9, can be obtained by simultaneously solving 4.25 and 4.26c with the inequality signs replaced by the equal signs, and hence given in equation 4.28 below.

$$P_{D_j}^t = \left(\frac{\mathcal{X}\Gamma_C^{th}\Gamma_D^{th}G_{CD_j} + \Gamma_D^{th}G_C}{G_C G_{D2D_j} - \mathcal{X}^2\Gamma_C^{th}\Gamma_D^{th}G_{CD_j}G_{D_jB}}\right)\mathcal{N} \tag{4.28a}$$

$$P_C^t = \left(\frac{\mathcal{X}\Gamma_C^{th}\Gamma_D^{th}G_{D_jB} + \Gamma_C^{th}G_{D2D_j}}{G_C G_{D2D_j} - \mathcal{X}^2\Gamma_C^{th}\Gamma_D^{th}G_{CD_j}G_{D_jB}}\right)\mathcal{N} \tag{4.28b}$$

The shaded area in figure 4.9 represents other possible transmit power combinations for the CT and $\mathrm{DT}_{\mathrm{Txs}}$ that satisfy upper bound constraints in equations 4.8a and 4.8b.

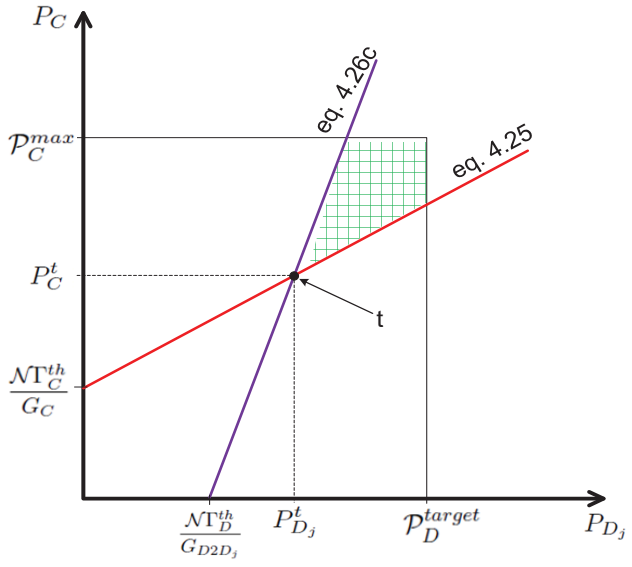

FIGURE 4.9: CT and D2D pairs transmit power allocation

With all other parameters being constant, $P^t_{D_j}$ and P^t_C are observed to depend on G_{D_jB} and G_{CD_j}. The values of G_{D_jB} and G_{CD_j} that satisfy the maximum/target transmit power bounds are obtained by constraining $P^t_{D_j}$ and P^t_C in equation 4.28 to respectively be less than their maximum/target values. i.e.

$$P^t_{D_j} = \left(\frac{\mathcal{X}\Gamma^{th}_C\Gamma^{th}_D G_{CD_j} + \Gamma^{th}_D G_C}{G_C G_{D2D_j} - \mathcal{X}^2\Gamma^{th}_C\Gamma^{th}_D G_{CD_j} G_{D_jB}}\right)\mathcal{N} \leq \mathcal{P}^{target}_D \tag{4.29a}$$

$$P^t_C = \left(\frac{\mathcal{X}\Gamma^{th}_C\Gamma^{th}_D G_{D_jB} + \Gamma^{th}_C G_{D2D_j}}{G_C G_{D2D_j} - \mathcal{X}^2\Gamma^{th}_C\Gamma^{th}_D G_{CD_j} G_{D_jB}}\right)\mathcal{N} \leq \mathcal{P}^{max}_C \tag{4.29b}$$

Solving 4.29 simultaneously generates two quadratic inequalities of the variables $\mathcal{X}G_{D_jB}$ and $\mathcal{X}G_{CD_j}$ given in equation 4.30.

$$\mathcal{A}_1(\mathcal{X}G_{D_jB})^2 + \mathcal{B}_1(\mathcal{X}G_{D_jB}) - \mathcal{C}_1 \leq 0 \tag{4.30a}$$

$$\mathcal{A}_2(\mathcal{X}G_{CD_j})^2 + \mathcal{B}_2(\mathcal{X}G_{CD_j}) - \mathcal{C}_2 \leq 0 \tag{4.30b}$$

where;

$$\begin{aligned}
\mathcal{A}_1 &= \Gamma^{th}_C\Gamma^{th}_D\mathcal{P}^{target}_D \\
\mathcal{A}_2 &= \Gamma^{th}_C\Gamma^{th}_D\mathcal{P}^{max}_C \\
\mathcal{B}_1 &= \left(\mathcal{N}\Gamma^{th}_C\Gamma^{th}_D + \Gamma^{th}_C\mathcal{P}^{target}_D G_{D2D_j} - \Gamma^{th}_D\mathcal{P}^{max}_C G_C\right) \\
\mathcal{B}_2 &= \left(\mathcal{N}\Gamma^{th}_C\Gamma^{th}_D + \Gamma^{th}_D\mathcal{P}^{max}_C G_C - \Gamma^{th}_C\mathcal{P}^{target}_D G_{D2D_j}\right) \\
\mathcal{C}_1 &= G_{D_{jj}}\left(\mathcal{P}^{max}_C G_C - \mathcal{N}\Gamma^{th}_C\right) \\
\mathcal{C}_2 &= G_C\left(\mathcal{P}^{target}_D G_{D2D_j} - \mathcal{N}\Gamma^{th}_D\right)
\end{aligned}$$

Since the channel gains should be greater than zero, only the positive roots of the above quadratic inequalities are considered to obtain G_{D_jB} and G_{CD_j} as given in equation 4.31.

$$G_{D_jB} \leq \frac{1}{\mathcal{X}}\left(\frac{\mathcal{P}^{max}_C G_C - \mathcal{N}\Gamma^{th}_C}{\Gamma^{th}_C\mathcal{P}^{target}_D}\right) \tag{4.31a}$$

$$G_{CD_j} \leq \frac{1}{\mathcal{X}}\left(\frac{\mathcal{P}^{target}_D G_{D2D_j} - \mathcal{N}\Gamma^{th}_D}{\Gamma^{th}_D\mathcal{P}^{max}_C}\right) \tag{4.31b}$$

Additionally, the condition (equation 4.32) that $G_{D2O_{lj}}$ should satisfy to meet the $\mathrm{DT}_{\mathrm{Txs}}$ target transmit power bounds is obtained using equations 4.26b, 4.28 and 4.31.

$$G_{D2O_{lj}} \leq \frac{1}{\mathcal{X}}\left(\frac{\mathcal{P}^{target}_D G_{D2D_j} - \mathcal{N}\Gamma^{th}_D}{\Gamma^{th}_D\mathcal{P}^{target}_D}\right) \tag{4.32}$$

Assuming similar radio channel model for all communicating entities and that the distance between them is a good measure of the channel gain (i.e. $|h|^2 = 1$ in equation 3.3), the

reuse distances for the CL strategy are obtained in equation 4.33.

$$R_{D_j}^{reuse} \geq \left(\mathcal{X} \frac{c\Gamma_C^{th}\mathcal{P}_D^{target}}{c\mathcal{P}_C^{max} R_C^{-\alpha} - \mathcal{N}\Gamma_C^{th}} \right)^{\frac{1}{\alpha}} \equiv R_{D_{\mathcal{X}}}^{CL} \tag{4.33a}$$

$$R_{CD_j}^{reuse} \geq \left(\mathcal{X} \frac{c\Gamma_D^{th}\mathcal{P}_C^{max}}{c\mathcal{P}_D^{target} R_{D2D}^{-\alpha} - \mathcal{N}\Gamma_D^{th}} \right)^{\frac{1}{\alpha}} \equiv R_{CD_{\mathcal{X}}}^{CL} \tag{4.33b}$$

$$R_{D2O_{lj}}^{reuse} \geq \left(\mathcal{X} \frac{c\Gamma_D^{th}\mathcal{P}_D^{target}}{c\mathcal{P}_D^{target} R_{D2D}^{-\alpha} - \mathcal{N}\Gamma_D^{th}} \right)^{\frac{1}{\alpha}} \equiv R_{D2O_{\mathcal{X}}}^{CL} \tag{4.33c}$$

■

The reuse distances defining respective ILAs in equations 4.16 and 4.24 are the basis of the distance-based criteria for selecting the D2D pairs to share the RB scheduled for a given CT. The equations 4.16 and 4.24 show that the criteria become more stringent with increasing $\mathcal{X}$ irrespective of the power control strategy employed. However, the stringency is proportional to $\mathcal{X}^{\frac{1}{\alpha}}$ with all other parameters kept constant. These distances define the boundaries for the 'no-reuse' and/or 'reuse' regions within the cell (see figure 4.8) when a RB already scheduled for the CT is shared with multiple D2D pairs.

4.5 D2D Pairs Selection Algorithms

In a cellular network, the D2D pairs that can potentially share the RB scheduled for a given CT are typically randomly distributed throughout the cell. Typically, not all D2D pairs may be allowed to share the same resources due to the high interference between them as explained in this chapter's introduction. As such, selection algorithms are required to identify the appropriate D2D pairs allowed to reuse the cellular resources. In this regard, two algorithms, i.e. Adaptive Opportunistic Selection (AOS) and Partial Random Selection (PRS) are proposed [19]. These algorithms utilize the formulated reuse distances in section 4.4 to select D2D pairs permitted to share resources. Both algorithms are assumed to be executed centrally by the BS since it is the sole entity responsible for scheduling resources to the CT in the cellular network. The major objective of these algorithms is to maximize the total cell spectral efficiency (as given in equation 4.1).

Figure 4.10 provides the generic sequence of events for the proposed algorithms. Initially, network parameters (e.g. threshold SINRs, maximum/target UT's transmit power, etc) are defined as inputs to the algorithms. Thereafter, users (i.e. CT and D2D pairs) are distributed within the cell and initializations are carried out for the previous spectral efficiency, $\eta_{prev.}$ and extent of RB resue, $\mathcal{X}$. The $\eta_{prev.}$ and $\mathcal{X}$ are initialized to the CT's spectral efficiency, η_C and 1, respectively.

Next, depending on the applied power control strategy, the reuse distance limits are computed using either equation 4.16 or 4.24. These reuse distance limits are used to select the appropriate D2D pair to share the CT's RB using either AOS or PRS scheme. Thereafter, a new spectral efficiency, η_{new} is computed to be used in the decision for further RB sharing. When $\eta_{new} > \eta_{prev.}$, the recently selected D2D pair is added to others allowed to share the RB and the D2D pair selection is repeated in a loop that updates the reuse distance limits after incrementing $\mathcal{X}$ by 1. Otherwise the loop is exited when $\eta_{new} < \eta_{prev.}$ and the algorithms are terminated.

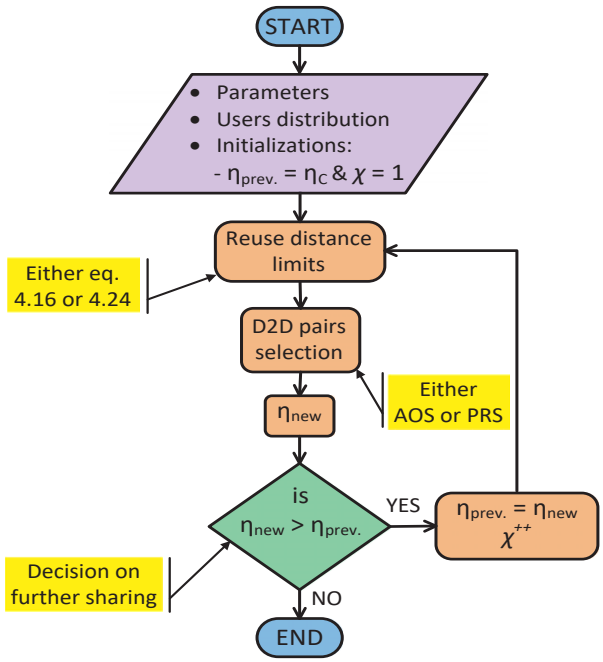

FIGURE 4.10: D2D pairs selection algorithms flow chart.

The following sections describe each of the proposed algorithms in further details and discuss their performance in a single cell scenario.

4.5.1 Adaptive Opportunistic Selection (AOS)

The AOS algorithm is a greedy D2D pairs selection algorithm that subsequently selects the best D2D pairs to share the CT's RB to maximize the total cell spectral efficiency. The basic idea of the AOS algorithm is that the best D2D pairs are those that cause the least interference to other users sharing the RB and thus allow all users (i.e. CT and D2D pairs) to achieve their threshold SINRs. Accordingly, cell-edge D2D pairs with the least channel gains between them and their interferers are the most suitable choice for RB reuse. The inverse relationship between channel gain and distance (section 3.4.2) makes D2D pairs that are further apart from each other preferable in sharing a RB. The distances between the selected D2D pairs and other users sharing the RB should at least be greater than the reuse distances as specified in section 4.4.

Algorithm 4.1 shows that the selection of the best D2D pair for sharing a RB is based on selecting a pair outside the ILAs and results in maximum increase of cell spectral efficiency. The algorithm is initialized with system parameters, users distribution and the CT's spectral efficency as the initial cell spectral efficiency. The best selected D2D pair, at a given selection instant, is one with maximum aggregated distance from all other interfering users (i.e. those with whom the same RB is shared) after satisfying the reuse distances in equations 4.16 and 4.24 (**line 7 and 9**). The parameters w_1, w_2 and w_3 represent the weights, which measure the significance of the respective distances. For simplification purposes, equal weights are assumed in this system analysis (i.e. $w_1 = w_2 = w_3 = 1$). In case of the first D2D user sharing a RB (i.e. $\mathcal{X} = 1$ - **line 6**), the BS and DT_{Rx} only experience interference from a single user within the cell.

Algorithm 4.1: AOS algorithm for D2D pairs sharing a scheduled CT RB

1: Given: a) parameters $\leftarrow \Gamma_D^{target}$, Γ_D^{th}, Γ_C^{target}, Γ_C^{th}, $\mathcal{P}_C^{max}$, $\mathcal{P}_D^{target}$, α
   b) Distribution of 1 CT & N D2D pairs within the cell
   c) Distance vectors/matrix $\leftarrow R_{D_j}$, R_{CD_j}, $R_{D2O_{lj}}$, $\left(\forall j/l \in \mathcal{DT}\right)$
2: Compute initial cell spectral efficiency $\leftarrow \eta_0$
3: **while** $\eta_{\mathcal{X}} > \eta_{\mathcal{X}-1}$ **do**
4: **for** $\mathcal{X} = 1 : N$ **do**
5: Compute limits (eq. 4.16/4.24) $\leftarrow R_{D\mathcal{X}}^{FST/CL}$, $R_{CD\mathcal{X}}^{FST/CL}$, $R_{D2O\mathcal{X}}^{FST/CL}$
6: **if** $\mathcal{X} = 1$ **then**
7: Select first best D2D pair with $max.\left(w_1 R_{D_j} + w_2 R_{CD_j}\right)$ & $R_{D_j} > R_{D\mathcal{X}}^{FST/CL}$ & $R_{CD_j} > R_{CD\mathcal{X}}^{FST/CL}$
8: **else**
9: Select subsequent best D2D pair with $max.\left(w_1 R_{D_j} + w_2 R_{CD_j} + w_3 \sum_{l=1, l\neq j}^{\mathcal{X}-1} R_{D2O_{lj}}\right)$ & $R_{D_j} > R_{D\mathcal{X}}^{FST/CL}$ & $R_{CD_j} > R_{CD\mathcal{X}}^{FST/CL}$ & $R_{D2O_{lj}} > R_{D2O\mathcal{X}}^{FST/CL}$
10: **end if**
11: Allocate all users' transmit power using FST/CL schemes (eq. 4.15/4.28)
12: Compute all users' SINRs (eq. 4.3) $\leftarrow \Gamma_C$, Γ_{D_j}
13: Compute new cell spectral efficiency (eq. 4.1) $\leftarrow \eta_{\mathcal{X}}$
14: **end for**
15: **end while**
16: **return** Γ_C, Γ_{D_j}, $\mathcal{X}^{max} \leftarrow \mathcal{X}$ and final spectral efficiency $\leftarrow \eta_{\mathcal{X}}$

Accordingly, the selection only considers two distance terms: 1) DT_{Tx}-BS distance, R_{D_j} and 2) CT-DT_{Rx} distance, R_{CD_j} (**line 7**). For subsequent selection of D2D pairs sharing a RB (i.e. $\mathcal{X} > 1$ - **line 8**), the BS and DT_{Rx} get interference from multiple users and thus a third distance term: DT_{Tx}-DT_{Rx}, $R_{D2O_{lj}}$, is also taken into account (**line 9**).

The AOS algorithm uses a nested loop (**line 3 and 4**) to sequentially select new D2D pairs that share the RB for as long as the achieved new spectral efficiency is better than the previous one. The algorithm exits the loop if there is no increase in the cell spectral efficiency during the selection process. Finally, the algorithm returns the users' SINRs (Γ_C and Γ_{D_j}), the final maximum number, $\mathcal{X}^{max}$, of assigned D2D pairs and the respective total cell spectral efficiency, $\eta_{\mathcal{X}}$.

4.5.2 Partial Random Selection (PRS)

The PRS algorithm is a psuedo-random D2D pair selection algorithm that provides for fairness while choosing candidate D2D pairs to share the RB. The fairness is provided by the fact that any D2D pair whose resultant interference is tolerable by other users sharing the RB is a candidate for resource sharing and can be randomly selected to reuse the RB. A given D2D pair is a candidate for resource sharing after fulfiling the reuse distance requirements in section 4.4. Therefore, all candidate D2D pairs that do not violate the ILA regions (i.e. causing tolerable interference) have equal selection probability to share a RB. The PRS algorithm basic idea is similar to that applied by AOS with the difference that selection of the best D2D pairs is not required. However,

the selected D2D pairs using PRS may not necessarily result in maximum cell spectral efficiency as is the case for the AOS algorithm.

In this case, algorithm 4.2 shows that any D2D user is randomly selected only after fulfilling the reuse distances in equations 4.16 and 4.24 (**line 7 and 9**). It is the fulfillment of these requirements before D2D pair selection that makes this algorithm partially random. With the exception of this difference in D2D pairs selection, the flow of the PRS algorithm is similar to the AOS algorithm in section 4.5.1. The next section analyses the performance of these algorithms.

Algorithm 4.2: PRS algorithm for D2D pairs sharing a scheduled CT RB

1: Given: a) parameters $\leftarrow \Gamma_D^{target}$, Γ_D^{th}, Γ_C^{target}, Γ_C^{th}, $\mathcal{P}_C^{max}$, $\mathcal{P}_D^{target}$, α
   b) Distribution of 1 CT & N D2D pairs within the cell
   c) Distance vectors/matrix $\leftarrow R_{D_j}$, R_{CD_j}, $R_{D2O_{lj}}$, $\left(\forall j/l \in \mathcal{DT}\right)$
2: Compute initial cell spectral efficiency $\leftarrow \eta_0$
3: **while** $\eta_{\mathcal{X}} > \eta_{\mathcal{X}-1}$ **do**
4: **for** $\mathcal{X} = 1 : N$ **do**
5: Compute limits (eq. 4.16/4.24) $\leftarrow R_{D\mathcal{X}}^{FST/CL}$, $R_{CD\mathcal{X}}^{FST/CL}$, $R_{D2O\mathcal{X}}^{FST/CL}$
6: **if** $\mathcal{X} = 1$ **then**
7: Randomly select any first D2D pair with $R_{D_j} > R_{D\mathcal{X}}^{FST/CL}$ & $R_{CD_j} > R_{CD\mathcal{X}}^{FST/CL}$
8: **else**
9: Randomly select any subsequent D2D pair with $R_{D_j} > R_{D\mathcal{X}}^{FST/CL}$ & $R_{CD_j} > R_{CD\mathcal{X}}^{FST/CL}$ & $R_{D2O_{lj}} > R_{D2O\mathcal{X}}^{FST/CL}$
10: **end if**
11: Allocate users' transmit power using FST/CL schemes (eq. 4.15/4.28)
12: Compute all users' SINRs (eq. 4.3) $\leftarrow \Gamma_C$, Γ_{D_j}
13: Compute new cell spectral efficiency (eq. 4.1) $\leftarrow \eta_{\mathcal{X}}$
14: **end for**
15: **end while**
16: **return** Γ_C, Γ_{D_j}, $\mathcal{X}^{max} \leftarrow \mathcal{X}$ and final spectral efficiency $\leftarrow \eta_{\mathcal{X}}$

4.5.3 Simulation Results and Discussion

The total cell spectral efficiency is the main performance metric used to assess the performance of the AOS and PRS algorithms. Further, other performance evaluations of the two algorithms based on number of assigned D2D pairs, their allocated transmit power and CT/$\text{DT}_{\text{Rx}s}$ achieved SINRs are also presented. Table 4.4 gives the applied simulation parameters together with others in section 3.3 for this performance evaluation. The FST and CL power control strategies discussed in section 4.4 are employed after the D2D pairs selection in each simulation run for both algorithms.

In this analysis, the AOS and PRS algorithms' performance is compared with the UIP scheme presented section 4.3. The UIP scheme increases the CT transmit power to provide an interference margin that guarantees the CT's SINR during RB reuse. All D2D pairs within the cell equally share this interference margin to set their transmit powers without any selection criteria. For a fair performance comparison in each simulation run, the same number, $\mathcal{X}^{max}$ of D2D pairs selected to share the RB from AOS/PRS

Table 4.4: AOS and PRS simulation parameters

Parameter	Symbol	Default value
Number of CTs	M	1
Number of D2D pairs	N	50
Target D2D transmit power	$\mathcal{P}_D^{target}$	10 dBm
max. D2D pair separation	R_{D2D}	20 m

algorithms is used in the UIP scheme. This number is randomly selected from all the distributed D2D pairs within the cell because the UIP scheme applys no selection criteria.

Cell Spectral Efficiency Performance

Figure 4.11 presents simulation results of the single-cell spectral efficiency performance for the AOS, PRS and UIP algorithms. Figure 4.11(a) shows the average total cell spectral efficiency (from all simulation runs) as a function of the number of assigned D2D pairs sharing the RB for the AOS and PRS algorithms when applying FST and CL power control strategies and UIP algorithm. The results show comparable performance for all schemes when fewer number of assigned D2D pairs share the RB, with the UIP scheme posting marginally better spectral efficiency. However, with higher numbers of assigned D2D pairs sharing the RB, the AOS and PRS algorithms increasingly outperform the UIP scheme with the AOS algorithm being the best. This inferior performance of the UIP scheme is due to its higher mutual interference between the assigned D2D pairs reusing the CT's RB. This arises from the UIP scheme's fully random nature of selecting D2D pairs sharing the RB without consideration of user ILAs.

Additionally, for each of the power control strategies (i.e. FST and CL), the AOS algorithm performs better than the PRS algorithm owing to its greedy approach in the selection of D2D pairs to share the RB. The AOS and PRS algorithms show that up to 12 - 13 D2D pairs can be assigned to share resources beyond which the spectral efficiency is adversely affected due to increased mutual interference. This result is close to that in the analytical scenario where a maximum of 16 D2D pairs were estimated to share the

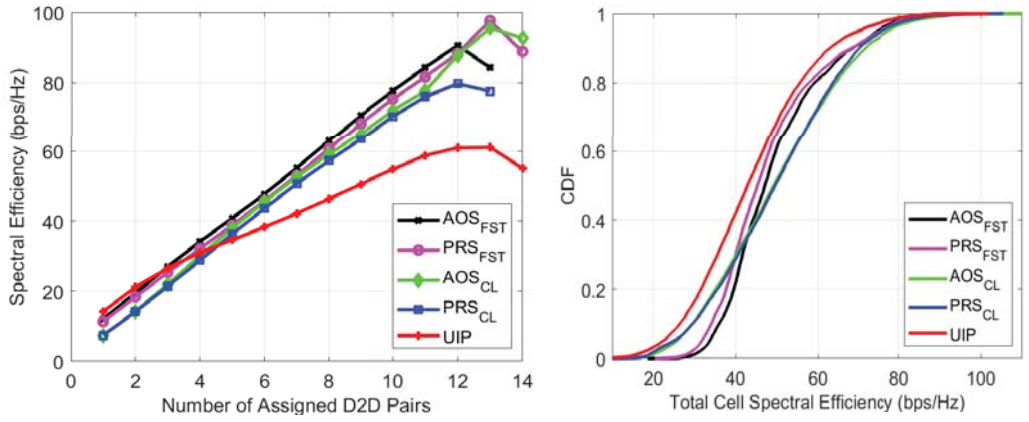

(a) Spectral efficiency versus number of assigned D2D pairs (b) Total cell spectral efficiency CDF

Figure 4.11: Cell spectral efficiency performance.

RB. This marginal difference is attributed to the shadow fading effects that are included in simulations for AOS and PRS algorithms.

Furthermore, the maximum spectral efficiency performance of both AOS and PRS algorithms is up to 67% better than the performance of the UIP scheme. Similarly, the performance of both proposed algorithms compared to the analytical results (discussed in section 4.2) increases by about 10%. This is attributed to the criteria of both algorithms that maintains sufficient distance between users sharing the RB and hence minimizing their mutual interference. The selected D2D pairs are thus able to achieve higher SINRs (as discussed below) and contribute towards better total cell spectral efficiency performance.

Figure 4.11(b) shows the total cell spectral efficiency CDF across all simulation runs where, for similar reasons discussed above, the AOS and PRS algorithms perform better than the UIP scheme. On average, both AOS and PRS algorithms applying the CL power control strategy post the best results of approximately 52 bps/Hz each, followed by the algorithms applying the FST power control strategy with averages of approximately 50 and 48 bps/Hz, respectively. The UIP scheme achieves the least average total cell spectral efficiency of about 44 bps/Hz.

Number of Assigned D2D pairs and Transmit Power Comparison

Figure 4.12 presents the CDF comparison of total number, $\mathcal{X}^{max}$ of assigned D2D pairs and their allocated transmit power for the three algorithms across all simulation runs. Figure 4.12(a) shows the total number of assigned D2D pairs performance in which a marginal difference between AOS and PRS is observed. As discussed in section 4.2.1, depending on R_C in the different simulation runs, $\mathcal{X}^{max}$ is within the range 2 - 13 for the two proposed algorithms, with an average of 6 assigned D2D pairs. This observed small difference in $\mathcal{X}^{max}$ between the two algorithms accounts for the marginal spectral efficiency superiority of AOS algorithm over PRS.

Figure 4.12(b) presents the CDF of the allocated transmit power to $\mathrm{DT}_{\mathrm{Tx}s}$ selected to share the RB. The results show similar transmit power allocation for the selected D2D pairs irrespective of whether FST or CL power control strategy is applied. Despite

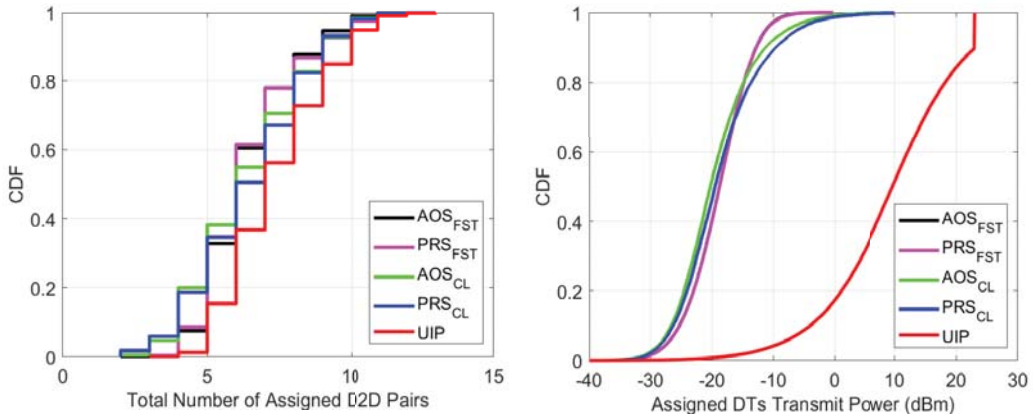

(a) Number of assigned D2D pairs (b) $\mathrm{DT}_{\mathrm{Tx}}$ allocated power

FIGURE 4.12: Number of Assigned D2D pairs and their allocated transmit power.

the fact that the CL strategy is expected to allocate lower and sufficient DT_{Tx} power to achieve Γ_D^{th}, higher numbers of D2D pairs sharing the RB require increasing P_{D_j} to similar levels as the FST strategy. However, the UIP scheme displays the highest transmit power allocation to the DT_{Txs}. This arises from its power allocation strategy where selected D2D pairs equally share the interference margin provided by the CT and also considers the DT_{Tx}-BS channel gain, G_{D_jB}. Therefore, with UIP scheme, the allocated P_{D_j} will be high for smaller number of D2D pairs sharing the RB and low G_{D_jB} (i.e. when the D2D pairs are near the cell edge).

Users SINR Comparison

Figure 4.13 presents the comparison of the final achieved users' (i.e. CT and DTs) SINRs for the three algorithms across all simulation runs. Figure 4.13(a) shows the CDF of the CT's SINR where it is observed that the AOS algorithm using the FST power control strategy gives the best results of nearly zero CT outage probability. This is because the FST strategy allocates the CT higher transmit power than necessary to achieve Γ_C^{th}. Consequently, the CT is more resilient to the interference during RB reuse. The UIP scheme gives a constant CT SINR, i.e. Γ_C^{th}, as per its design in which the CT threshold SINR is always preserved. Furthermore, with the CL power control strategy, both AOS and PRS algorithms result in the CT's SINR mostly around Γ_C^{th} with approximately 20% outage probability. This is because the CL power control strategy allocates the CT's transmit power in such a way that the CT just achieves Γ_C^{th}. This, compared to the FST strategy, results in the CT's limited resilience to interference arising from resource reuse and so any variations in the radio channel conditions lead to the CT's outage.

Figure 4.13(b) shows the CDF of the DT_{Rxs} SINRs and demonstrates that both AOS and PRS algorithms using the two power control strategies give significantly lower DT_{Rx} outage probability (below 10%) in comparison to that of the UIP scheme (approximately 43%). This is attributed to the applied selection criteria that ensures minimal or no mutual interference between the chosen D2D pairs sharing the RB. The poor performance of the UIP is due to the lack of selection criteria and high allocated DT_{Tx} transmit

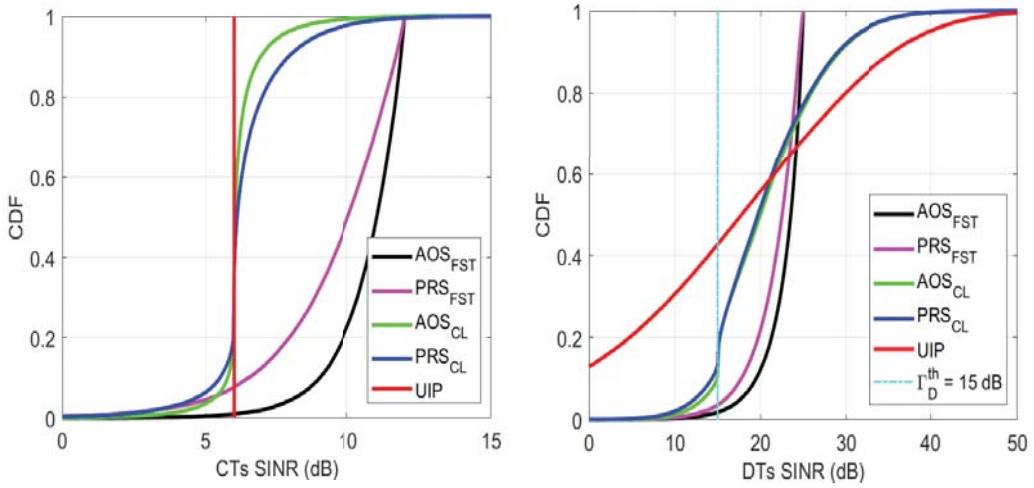

(a) CT SINR performance (b) DT_{Rxs} SINR performance

FIGURE 4.13: Users' SINR performance.

power resulting in increased mutual interference between D2D pairs sharing the RB. Additionally, some selected D2D pairs achieve very high SINRs (above 30 dB) for both algorithms using CL strategy and UIP scheme due to their high transmit power allocataions (illustrated in figure 4.12(b)). As earlier observed, again the AOS algorithm is the most superior compared with the PRS algorithm for both power control strategies since it offers higher guarantees of achieving all users' threshold SINRs for the selected number, $\mathcal{X}^{max}$, of D2D pairs sharing the RB. Similar to the CT's SINR performance, the FST power control strategy grants the selected D2D pairs higher resilience to interference experienced during resource reuse.

4.6 Summary

This chapter presented the feasibiliy of assigning multiple D2D pairs to share cellular resources (RBs) already scheduled for a single CT while ensuring that all users achieve their threshold SINR requirements. Initially, the factors affecting the reuse of a given RB by multiple D2D pairs are reviewed. The discussion focused on how users' transmit power, users distribution within the cell with respect to the BS and the D2D separation impacts the number of D2D pairs that can share resources and by extension, the achieved total cell spectral efficiency. The analysis demonstrated better spectral efficiency results when resources of a CT close to the BS and having high transmit power are shared with cell edge D2D pairs whose DTs are in closer proximity (not exceeding 10% of the cell radius) of each other.

With learnings from the analytical study, a UIP scheme where the BS controls all users' transmit power to guarantee the CT's threshold SINR was proposed. The BS assigned higher transmit power to the CT, creating an interference margin that allowed multiple D2D pairs to share its radio resources. Here, control of the D2D pairs' transmit power is such that each $\mathrm{DT_{Tx}}$ contributed similar interference power at the BS. This is critical given that total interference at the BS should be within the interference margin set by the CT transmit power, P_C. The simulation results for this scheme registered significant enhancement of the cell spectral efficiency by up to 20 times when compared with the conventional cellular communication mode where no resource reuse within the cell is allowed. However, despite the scheme's demonstrated promise of achieving the CT's threshold SINR, a significant percentage of D2D pairs using the allocated transmit power failed to attain their threshold SINRs. It was observed that further performance improvements could be achieved if selection criteria for D2D pairs sharing resources are available. These selection criteria required an explicit framework of resource reuse within the cell's coverage area.

Finally, the spatial resource reuse framework for multiple D2D pairs within a single cell was developed. Starting with the formulation of ILA sizes with respect to the degree of resource reuse while using known LTE power control strategies (i.e. FST and CL), the regions for RB 'no-reuse' within the cell were identified. The chapter then discussed the application of this framework in the development of two selection algorithms: AOS and PRS. The algorithms' performance was evaluated in a single-cell environment where one CT and several D2D pairs are uniformly distributed within the cell. The BS then utilized the algorithms to select the D2D pairs that are sufficiently separated from each other to share radio resources scheduled for the CT and allocate all users' transmit power. Higher cell spectral efficiency performance compared with analytical results was observed while

simultaneously achieving the threshold SINRs of both the CT and D2D pairs sharing resources. In particular, the AOS algorithm, especially when applying the FST power control strategy, exhibited higher guarantees for all users to achieve their threshold SINRs during resource sharing while achieving good total cell spectral efficiency performance.

However, a limitation of this study is the fact that a single-cell scenario is considered, thus ignoring inter-cell interference. In realistic network scenarios, this additional interference from neighbouring cells negatively impacts the CT/D2D pairs' SINRs and reduces the total spectral efficiency. This is explored in the next chapter.

CHAPTER 5

Multiple Resources Assignment Problem

Contents

Chapter 4 presented algorithms that select appropriate D2D pairs that should be allowed to share the spectrum resources scheduled for a single CT with the objective of maximizing total spectral efficiency as well as fulfilling all users (CT and DTs) threshold SINRs. This simplified model acted as a proof of concept for several D2D pairs sharing resources utilized by a given CT in a single-cell scenario. However, in a real network, each cell has multiple CTs utilizing the spectrum resources scheduled by the BS. In LTE for example,

the network is comprised of several cells with a number of CTs distributed throughout the coverage area. The available spectrum is divided into multiple smaller bandwidth radio resources in form of RBs that are scheduled for CTs during their conventional communication through the BS. In such cases where multiple RBs are allocated to different CTs, the D2D pairs can potentially share any CT's RBs with the objective of maximizing the total network spectral efficiency. These multiple RBs provide an opportunity to increase the number of D2D pairs that share resources within the network. However, new algorithms that assign D2D pairs to multiple RBs are required in order to maximize the total network spectral efficiency.

This chapter examines the assignment problem of D2D pairs to different resources scheduled for multiple CTs. Here, the multiple resources context refers to the RBs scheduled for different CTs that are distributed within the network's coverage area. Specifically, the task is formulated as a Generalized Assignment Problem (GAP) and the assignment objectives are given in section 5.1. Thereafter, section 5.2 discusses two algorithms that assess the various sharing options introduced by multiple CTs and how the algorithms select appropriate D2D pairs to share the different CTs' RBs. Sections 5.3 and 5.4 then present the perforomance evaluation of the two algorithms in single-cell and multi-cell scenarios. Further, enhancements of the algorithms to meet all users' threshold SINRs performance within the multi-cell scenario are considered in section 5.5 before concluding the chapter in section 5.6.

5.1 D2D Pairs Assignment Problem Formulation

The availability of multiple RBs scheduled for CTs in cellular networks presents an opportunity for increased number of D2D pairs that share these resources. Figure 5.1 shows the scenario of several D2D pairs sharing multiple UL resources. The scenario considers a single cell in which M CTs and N D2D pairs (where $N \gg M$) are uniformly distributed around the BS, as shown in figure 5.1(a). All the available RBs are already

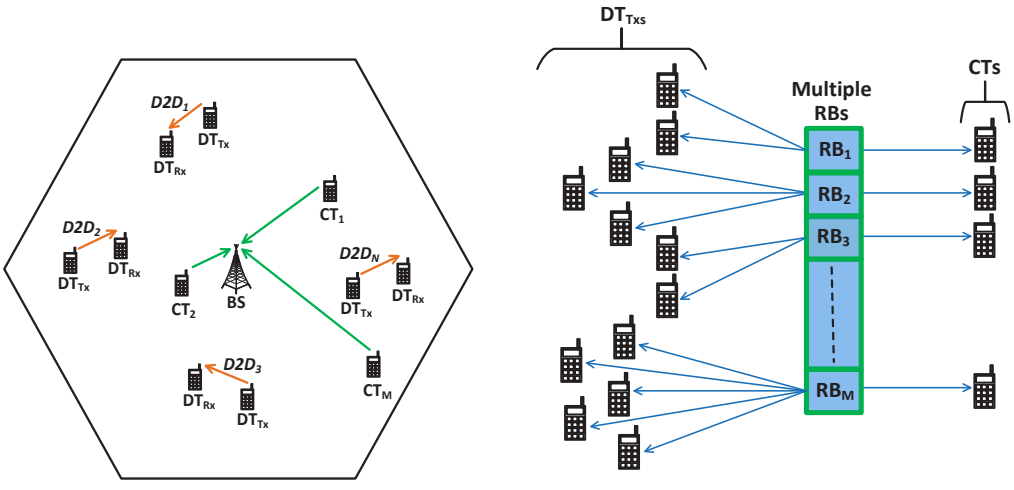

(a) CTs and D2D pairs distribution within a cell

(b) $DT_{Tx}s$ sharing multiple RBs assigned to CTs

FIGURE 5.1: Multiple uplink resource sharing with several D2D pairs.

scheduled for use by the CTs and thus D2D pairs have to share these resources as ilustrated in figure 5.1(b). However, in order to achieve the objective of maximizing the cell spectral efficiency, this presents a new problem, namely: How to select suitable D2D pairs allowed to share the RBs scheduled for each specific CT while ensuring that all UTs' threshold SINRs are met? This problem is modelled as a GAP, where a given CT's RB also needs to be assigned to other D2D users [64] [65] [66].

In this model, a given D2D pair is allowed to share the RB of only a single CT, but also provides for a given CT's RB to be shared with several other D2D pairs. The assignment should still ensure that all UTs achieve their threshold SINRs while sharing the CTs' RBs. Numerically, the task of selecting the D2D pairs assigned to the different CTs' RBs is formulated in equation 5.1 as:

$$\max_{x_{ji}} \quad \sum_{i=1}^{M}\sum_{j=1}^{N}\Big[log_2\big(1+\Gamma_{C_i}\big)+log_2\big(1+x_{ji}\Gamma_{D_j}\big)\Big] \tag{5.1a}$$

s.t.

$$x_{ji}\in\big\{0,1\big\};\quad \forall i\in\mathcal{CT}\ and\ \ \forall j\in\mathcal{DT}, \tag{5.1b}$$

$$\sum_{i=1}^{M} x_{ji}\in\big\{0,1\big\}, \tag{5.1c}$$

$$\sum_{j=1}^{N} I_{D_{ji}}x_{ji}\leq\mathcal{I}_{C_i}^{max}, \tag{5.1d}$$

$$\Gamma_{C_i}=\frac{P_{C_i}G_{C_i}}{\sum\limits_{j=1}^{N}x_{ji}P_{D_j}G_{D_jB}+\mathcal{N}}\geq\Gamma_C^{th}, \tag{5.1e}$$

$$\Gamma_{D_j}=\frac{x_{ji}P_{D_j}G_{D2D_j}}{P_{C_i}G_{C_iD_j}+\sum\limits_{l=1,l\neq j}^{N}x_{li}P_{D_l}G_{D2O_{lj}}+\mathcal{N}}\geq\Gamma_D^{th}, \tag{5.1f}$$

$$P_{C_i}\leq\mathcal{P}_C^{max}, \tag{5.1g}$$

$$P_{D_j}\leq\mathcal{P}_D^{max}. \tag{5.1h}$$

Equation 5.1 is the objective function seeking to maximize total cell spectral efficiency given as the summation of spectral efficiencies of individual UTs using the Shannon's capacity formula. Therein, x_{ji} is a binary variable equal to 1 when the j^{th} $\mathrm{DT_{Tx}}$ shares the RB scheduled for the i^{th} CT and 0 otherwise; $I_{D_{ji}}$ is the contribution of the j^{th} $\mathrm{DT_{Tx}}$ to the interference at the BS when $x_{ji}=1$; and $\mathcal{I}_{C_i}^{max}$ is the interference margin (maximum tolerable cumulative interference) at the BS within the RB scheduled for the i^{th} CT. The rest of the parameters are as defined in section 3.3.

The constraint 5.1c ensures that a given D2D pair shares the RB scheduled for a single CT and 5.1d allows several other D2D pairs to share the RB of a single CT as long as their accumulated interference at the BS does not exceed that CT's maximum allowed interference margin at the BS. Constraints 5.1e and 5.1f guarantee that the CTs and DTs achieve their threshold SINRs while 5.1g and 5.1h ensure that the CTs and DTs do not exceed their maximum transmit powers.

The problem in equation 5.1 is known to be NP-hard for which the optimal solution is obtained through an exhaustive search of all possible combinations of x_{ji}. However, as

highlighted in section 4.4, not all D2D pairs are potential candidates for sharing the CTs' RBs. This curtails the exhaustive search burden through consideration of only potential D2D pairs contributing to the performance objectives.

The selection of potential D2D pairs to share a given CT's RB is based on their location with respect to the reuse regions. These reuse regions for a given CT are defined in terms of reuse distances that are dependent on the CT's location within the cell (refer to section 4.4). The FST power control strategy is adopted for both CTs and D2D pairs in the multiple RBs sharing scenario due to it's superior spectral efficiency performance exhibited in section 4.5.3. The updated reuse distances, based on the different locations of the various CTs within the cell, for the FST power control strategy are provided in equations 5.2. These updated distances are used by the selection algorithms to identify appropriate D2D pairs assigned to given CT's RB within the cell.

$$R_{D_j}^{reuse} \geq \left(\mathcal{X}_i \frac{1}{\mathcal{I}_{C_i}^{max}}\right)^{\frac{1}{\alpha}} R_{D2D} \equiv R_{D\mathcal{X}_i}^{FST} \tag{5.2a}$$

$$R_{C_iD_j}^{reuse} \geq \left(\mathcal{X}_i \frac{\Gamma_C^{target}}{\Gamma_D^{target}} \frac{1}{\mathcal{I}_{D_j}^{max}}\right)^{\frac{1}{\alpha}} R_{C_i} \equiv R_{C_iD\mathcal{X}_i}^{FST} \tag{5.2b}$$

$$R_{D2O_{lj}}^{reuse} \geq \left(\mathcal{X}_i \frac{1}{\mathcal{I}_{D_j}^{max}}\right)^{\frac{1}{\alpha}} R_{D2D} \equiv R_{D2O\mathcal{X}_i}^{FST} \tag{5.2c}$$

where $\mathcal{X}_i = \sum_{j=1}^{N} x_{ji}$ is the number of D2D pairs that share the i^{th} CT's RB.

5.2 Algorithms for Multiple Resource Assignment

To optimally assign D2D pairs to RBs already scheduled for the different CTs within the cell, it is necessary to develop appropriate algorithms that concurrently maximize the total cell spectral efficiency and achieve all UTs' threshold SINRs. In this regard, two algorithms, i.e. Multi-User Opportunistic (MU-O) and Multi-User Random (MU-R) are proposed to select suitable D2D pairs sharing the RBs scheduled for the different CTs [20]. The following sections describe these algorithms in details.

5.2.1 Multi-User Opportunistic (MU-O)

The MU-O algorithm is a sub-optimal algorithm that tries to assign the best D2D pairs to the different CT's RB resulting in maximum spectral efficiency. The best D2D pairs for a given CT's RB are those that cause least interference to the BS and other D2D pairs sharing the CT's RB. Additionally, the most suitable CT sharing its RB with given D2D pairs, is the one for which the selected D2D pairs maximize their individual spectral efficiencies under threshold SINR constraints. In this work, the separation among UTs (i.e. from the BS, other D2D pairs and the CTs with which the RB is shared) is considered as the proxy measure of interference to select the best D2D pairs and most suitable CT's RB to be shared. This approximation ignores shadow fading effects, which leads to errors in instantaneous SINR measurements at the BS and $\mathrm{DT_{Rx}}s$. However, such SINR measurement errors can be ignored in the network's long-term average spectral efficiency performance.

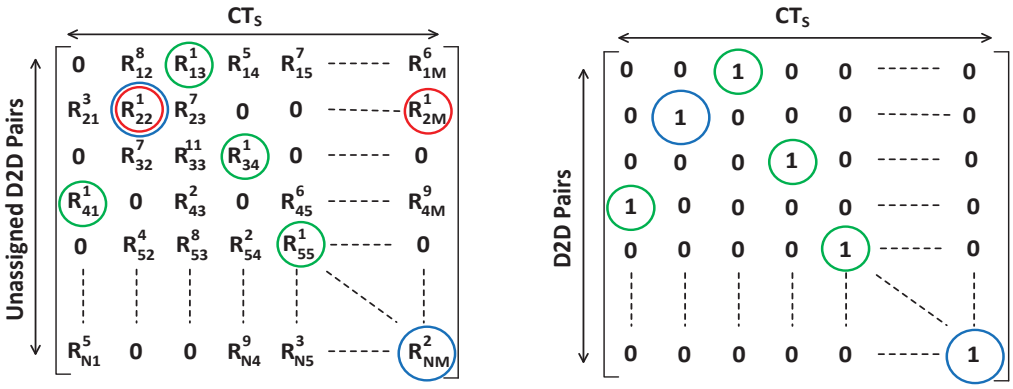

(a) Selection matrix of unassigned D2D pairs

(b) Update of RB assignment matrix, x_{ji}

FIGURE 5.2: MU-O assignment procedure of CTs' RBs to D2D pairs.

Figure 5.2 illustrates the MU-O algorithm basic idea, which is to select the farthest D2D pairs from other UTs already sharing a given CT's RB. The algorithm computes a selection matrix to identify all potential D2D pairs that can share the CTs' RBs as shown in figure 5.2(a). The entries, R_{ji} in this selection matrix are the distance computations of either $\left(R_{D_j} + R_{C_iD_j}\right)$ for the first D2D pair or $\left(R_{D_j} + R_{C_iD_j} + \sum_{l=1,l\neq j}^{\mathcal{X}_i-1} R_{D2O_{lj}}\right)$ for subsequent D2D pairs being considered to share a given CT's RB after fulfillment of reuse distances in equation 5.2. A zero entry in this matrix indicates that the j^{th} D2D pair does not fulfil the reuse distances in equation 5.2 (i.e., it voilates the ILA regions) for the i^{th} CT's RB.

The non-zero column entries in the selection matrix are then ranked in descending order as indicated by the superscripts. The first-ranked D2D pair in each column (indicated by green circles in figure 5.2(a)) is selected as the best D2D pair to share the given CT's RB. Accordingly, the RB assignment matrix, x_{ji} is updated with an entry of 1 for the j^{th} D2D pair selected to share the i^{th} CT's RB as shown in figure 5.2(b). However, if a given D2D pair is ranked as the first for multiple CTs' RBs (as indicated by red circles in figure 5.2(a)), a tie-break is required to meet constraint 5.1c. In this case the D2D pair is assigned to the CT's RB with the higher (highest) entry in the selection matrix. The second-ranked D2D pairs are then assigned to other CTs' RBs (as shown by the blue circles in figure 5.2(b)). The MU-O algorithm repeats the selection process by always recomputing a new selection matrix using unassigned D2D pairs until either none of the unassigned D2D pairs meet the updated reuse distance requirements or when further sharing of all the CTs' RBs negatively impacts each of their spectral efficiencies. Upon completion of RBs assignment to suitable D2D pairs, the cell spectral efficiency and UTs' SINRs are computed.

Algorithm 5.1 shows the proposed MU-O D2D pairs selection scheme. As input, the algorithm takes network parameters, CTs and D2D users distribution within the cell, and their respective distance vectors and matrices. Then on execution, the algorithm is initialized with two categories of variables, i.e.:

1. Internal input variables

(a) Vector $\mathcal{F}$: flags set to 0 when a RB scheduled for i^{th} CT can be shared with other D2D pairs and set to 1 otherwise.

(b) Matrix $\mathcal{B}$: selection matrix from which the best D2D pair to share i^{th} CT RB is chosen.

(c) Vector $\mathcal{R}$: counter for number of times j^{th} D2D pair is selected as best to share multiple CT RBs.

(d) matrix x_{ji}: assignment matrix indicating whether the j^{th} D2D pair is assigned to the i^{th} CT's RB or not.

(e) Vector $\mathcal{X}$: counter for the number of D2D pairs assigned to each RB scheduled for i^{th} CT in the cell.

2. Output variables

(a) Y: counter for the number of D2D pairs assigned to all scheduled RBs in the cell.

(b) Sets $\mathcal{S}_i$: set of D2D pairs Identifier (ID) that share i^{th} CT RB.

(c) η_{cell}: total spectral efficiency for all UTs assigned RBs in the cell.

The algorithm selects the instantaneous best D2D pair, $\mathcal{B}_i$ to share the i^{th} CT's RB as the one having maximum summed distance from all other interfering UTs after satisfying the reuse distance requirements in equations 5.2 (**lines 11 and 13**). Selection of the first instantaneous best D2D pair sharing any given CT's RB (i.e. $\mathcal{X}_i = 1$ - **line 10**) considers only two distance parameters, i.e.: 1) $R_{C_iD_j}$ and 2) R_{D_j} (**line 11**). This is because the BS and DT_{Rx} observe interference from a single UT within the cell. Selection of subsequent instantaneous best D2D pairs sharing the CT's RB (i.e. $\mathcal{X}_i > 1$ - **line 12**) additionally considers a third distance parameter: $R_{D2O_{lj}}$. This third parameter accounts for the mutual interference between multiple D2D pairs sharing a given CT's RB (**line 13**).

The counter $\mathcal{R}_j$ is increased by 1 whenever the j^{th} D2D pair is selected as the instantaneous best to share a given CT's RB (**line 16**). In case $\mathcal{R}_j > 1$, the j^{th} D2D pair is the instantaneous best candidate to share RBs scheduled to more than one CT. A tie-break is required for such scenarios since any given D2D pair should share the RB of only a single CT as per constraint 5.1c. The tie-break is achieved by assigning the CT's RB to the D2D Pair with the highest $R_{C_iD_j}$ (**line 20**).

Once all D2D pair candidates for sharing scheduled RBs are identified in $\mathcal{B}_i$, transmit power allocations are done followed by UTs SINR and individual RB spectral efficiency computations (**lines 24 - 26**). The algorithm continues sharing a given CT's RB with multiple other D2D pairs as long as the new spectral efficiency, $\eta_{i\mathcal{X}_i}$ is better than the previous one $\eta_{i(\mathcal{X}_i-1)}$. In such cases, $\mathcal{B}_i$ is added to the respective sets $\mathcal{S}_i$ and counter Y is increased by 1. When $\eta_{i\mathcal{X}_i} < \eta_{i(\mathcal{X}_i-1)}$, the i^{th} CT RB is then flagged as full (**line 31**) and no further sharing of the i^{th} CT RB is allowed. Finally, η_{cell} is computed and returned together with all assigned UTs' SINRs and total number, Y of D2D pairs that are assigned resources in the cell.

Algorithm 5.1: MU-O scheme for DTs sharing multiple RBs

Given: a) parameters $\leftarrow \Gamma_D^{target}$, Γ_D^{th}, Γ_C^{target}, Γ_C^{th}, R_{D2D}, R_{cell} & α
b) Distribution of 'M' CTs & 'N' D2D users within the cell
c) Distance vectors/matrices $\leftarrow R_{C_i}$, R_{D_j}, $R_{C_iD_j}$ & $R_{D2O_{lj}}$ $\left(\forall i \in \mathcal{CT},\ \forall j/l \in \mathcal{DT}\right)$
d) Initialize Y, vectors $\mathcal{F}$ & $\mathcal{X}$ of length $M \leftarrow 0$ & empty sets $\mathcal{S}_i$ $\left(\forall i \in \mathcal{CT}\right)$
Compute initial spectral efficiency vector for all CTs$\leftarrow \eta_{i0}$
while $Y < N$ **do**
  Initialize η_{cell} , matrix $\mathcal{B}$ & vector $\mathcal{R}$ of length $N \leftarrow 0$
  for i=1:M **do**
    if $\mathcal{F}_i = 0$ **then**
      $\mathcal{X}_i \leftarrow \mathcal{X}_i + 1$
      Compute reuse distance limits (eq. 5.2) $\leftarrow R_{D_{\mathcal{X}_i}}^{FST}$, $R_{C_iD_{\mathcal{X}_i}}^{FST}$, $R_{D2O_{\mathcal{X}_i}}^{FST}$
      for j=1:N **do**
        if $\mathcal{X}_i = 1$ **then**
          Compute $\mathcal{B}$ and select best D2D user, $\mathcal{B}_i$
          $\leftarrow max.\left(R_{D_j} + R_{C_iD_j}\right)$ & $R_{D_j} > R_{D_{\mathcal{X}_i}}^{FST}$ & $R_{C_iD_j} > R_{C_iD_{\mathcal{X}_i}}^{FST}$
        else
          Compute $\mathcal{B}$ and select best D2D user, $\mathcal{B}_i$
          $\leftarrow max.\left(R_{D_j} + R_{C_iD_j} + \sum_{l=1,l\neq j}^{\mathcal{X}_i - 1} R_{D2O_{lj}}\right)$ & $R_{D_j} > R_{D_{\mathcal{X}_i}}^{FST}$ & $R_{C_iD_j} > R_{C_iD_{\mathcal{X}_i}}^{FST}$ & $R_{D2O_{lj}} > R_{D2O_{\mathcal{X}_i}}^{FST}$
        end if
      end for
      When best D2D user is repeatedly selected by other CTs $\mathcal{R}_j \leftarrow \mathcal{R}_j + 1$
    end if
  end for
  if $R_j > 1$ **then**
    Tie-break: Assign best D2D user to RB scheduled for CT with highest $R_{C_iD_j}$
  end if
  for i=1:M **do**
    if $\mathcal{B}_i \neq 0$ **then**
      Allocate users' transmit power using FST strategy
      Compute users' SINRs $\leftarrow \Gamma_{C_i}$, Γ_{D_j}
      Compute new spectral efficiency $\leftarrow \eta_{i\mathcal{X}_i}$
      if $\eta_{i\mathcal{X}_i} > \eta_{i(\mathcal{X}_i - 1)}$ **then**
        Add $\mathcal{B}_i$ to set $\mathcal{S}_i$
        Number of assigned D2D users, $Y \leftarrow Y + 1$
      else
        Mark i^{th} CT RB as full: $\mathcal{F}_i = 1$
      end if
    end if
    Compute total cell spectral efficiency, $\eta_{cell} \leftarrow \eta_{cell} + \eta_{i\mathcal{X}_i}$
  end for
end while
return Γ_{C_i}, Γ_{D_j}, Y, η_{cell}

5.2.2 Multi-User Random (MU-R)

The MU-R algorithm presents a different strategy of selecting candidate D2D pairs that share RBs scheduled for multiple CTs within the cell. MU-R selects candidate D2D pairs randomly as long as their resultant interference is tolerable by other UTs sharing the RB. The D2D pairs causing tolerable interference to other UTs are those that do not violate the ILA regions of the shared RBs as specified by equation 5.2. This selection strategy provides a higher probability for any D2D pair causing tolerable interference to be assigned a shared CT's RB, hence making it a fairer strategy of selecting candidate D2D pairs. However, this may not necessarily result in better spectral efficiency performance compared with MU-O algorithm.

Figure 5.3 shows the basic idea of the MU-R algorithm, where any D2D pair fulfilling the reuse distances in equation 5.2 is selected to share a given CT's RB. The MU-R algorithm computes the selection matrix in a similar manner as described for MU-O in section 5.2.1. However, different from the MU-O algorithm, ranking of the non-zero column entries in the selection matrix is not required in MU-R algorithm. Therefore, as shown by green circles in figure 5.3(a), any D2D pair is randomly selected to share the i^{th} CT's RB while considering the constraint in equation 5.1c. The RB assignment matrix, x_{ji} is subsequently updated with an entry of 1 for the j^{th} D2D pair selected to share the i^{th} CT's RB as shown in figure 5.3(b). The MU-R algorithm repeats the selection process by always recomputing a new selection matrix using unassigned D2D pairs until either none of the unassigned D2D pairs meet the updated reuse distance requirements or when further sharing of all the CTs' RBs negatively impacts each of their spectral efficiencies. Finally, the cell spectral efficiency and UTs' SINRs are computed upon completion of RBs assignment to suitable D2D pairs.

Algorithm 5.2 gives the proposed MU-R D2D pairs selection strategy. This algorithm has similar inputs and initializations as algorithm 5.1. However, the selection matrix $\mathcal{B}$ is replaced with matrix $\mathcal{A}$ comprising of any D2D pairs that can be selected to share the i^{th} CT RB. Additionally, vector $\mathcal{R}$ is also not necessary since candidate D2D pairs are randomly selected after fulfilling the reuse distances in equations 5.2 (**line 10 and 12**). The random selection is in accordance with the constraint in equation 5.1c. The requirement that candidate D2D pairs must first fulfill the reuse distances before their

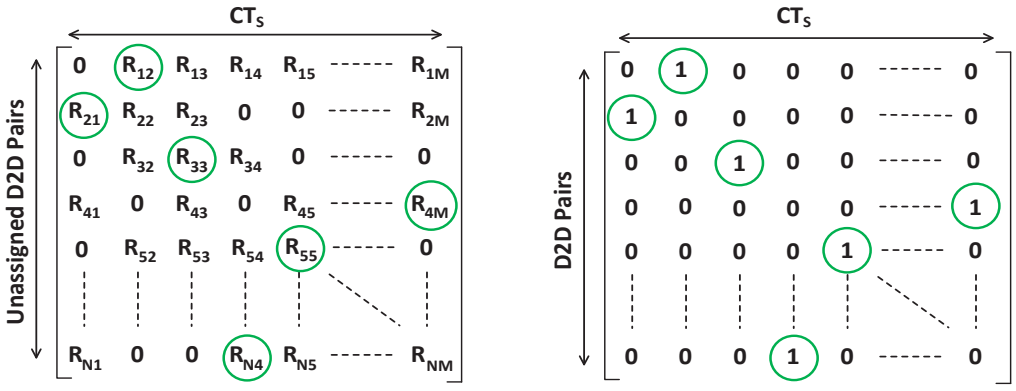

(a) Selection matrix of unassigned D2D pairs

(b) Update of RB assignment matrix, x_{ji}

FIGURE 5.3: MU-R assignment procedure of CTs' RBs to D2D pairs.

Algorithm 5.2: MU-R scheme for DTs sharing multiple RBs

Given: a) parameters $\leftarrow \Gamma_D^{target}$, Γ_D^{th}, Γ_C^{target}, Γ_C^{th}, R_{D2D}, R_{cell} & α
b) Distribution of 'M' CTs & 'N' D2D pairs within the cell
c) Distance vectors/matrices $\leftarrow R_{C_i}$, R_{D_j}, $R_{C_iD_j}$ & $R_{D2O_{lj}}$ $\left(\forall i \in \mathcal{CT},\ \forall j/l \in \mathcal{DT}\right)$
d) Initialize Y, vectors $\mathcal{F}$ & $\mathcal{X}$ of length $M \leftarrow 0$ & empty sets $\mathcal{S}_i$ $\left(\forall i \in \mathcal{CT}\right)$
Compute initial spectral efficiency vector for all CTs$\leftarrow \eta_{i0}$
for i=1:M **do**
  Initialize η_{cell} and matrix $\mathcal{A} \leftarrow 0$
  for j=1:N **do**
    if $\mathcal{F}_i = 0$ **then**
      $\mathcal{X}_i \leftarrow \mathcal{X}_i + 1$
      Compute reuse distance limits (eq. 5.2) $\leftarrow R_{D_{\mathcal{X}_i}}^{FST}$, $R_{C_iD_{\mathcal{X}_i}}^{FST}$, $R_{D2O_{\mathcal{X}_i}}^{FST}$
      if $\mathcal{X}_i = 1$ **then**
        Compute $\mathcal{A}$ and randomly select any D2D pair, $\mathcal{A}_i$ with $R_{D_j} > R_{D_{\mathcal{X}_i}}^{FST}$ & $R_{C_iD_j} > R_{C_iD_{\mathcal{X}_i}}^{FST}$
      else
        Compute $\mathcal{A}$ and randomly select any D2D pair, $\mathcal{A}_i$ with $R_{D_j} > R_{D_{\mathcal{X}_i}}^{FST}$ & $R_{C_iD_j} > R_{C_iD_{\mathcal{X}_i}}^{FST}$ & $R_{D2O_{lj}} > R_{D2O_{\mathcal{X}_i}}^{FST}$
      end if
      if $\mathcal{A}_i \neq 0$ **then**
        Allocate users' transmit power using FST strategy
        Compute users' SINRs $\leftarrow \Gamma_{C_i}$, Γ_{D_j}
        Compute new spectral efficiency $\leftarrow \eta_{i\mathcal{X}_i}$
        if $\eta_{i\mathcal{X}_i} > \eta_{i(\mathcal{X}_i-1)}$ **then**
          Add $\mathcal{A}_i$ to set $\mathcal{S}_i$
          Number of assigned D2D users, $Y \leftarrow Y + 1$
        else
          Mark i^{th} CT RB as full: $\mathcal{F}_i = 1$
        end if
      end if
    end if
    Compute total cell spectral efficiency, $\eta_{cell} \leftarrow \eta_{cell} + \eta_{i\mathcal{X}_i}$
  end for
end for
return Γ_{C_i}, Γ_{D_j}, Y, η_{cell}

random selection makes this a partially-random strategy. The MU-R algorithm flow after random selection of candidate D2D users is similar to the MU-O algorithm described in section 5.2.1.

5.3 Single-Cell Simulation Results and Discussion

The performance evaluation of MU-O and MU-R algorithms considers three metrics: 1) total cell spectral efficiency, which is a summation of all individual UTs' spectral efficiencies when sharing the CTs' RBs; 2) total number of assigned D2D pairs, which is an aggregated number of D2D pairs sharing the different CTs' RBs; and 3) all UTs (i.e. CTs and D2D pairs) achieved SINRs. Table 5.1 gives the simulation parameters

used in this single-cell performance evaluation together with others given in section 3.3. Additionally, the FST power control strategy discussd in section 4.4 is employed for all UTs in the simulation runs.

TABLE 5.1: MU-O and MU-R single-cell simulation parameters

Parameter	**Symbol**	**Default value**
Number of CTs	M	10
Number of D2D pairs	N	500
max. D2D pair separation	R_{D2D}	20 m

For a comparative evaluation of MU-O and MU-R algorithms, results of a state of the art scheme, DPS [55] (discussed in section 2.3.5) implemented in a single cell environment are also included. In the DPS scheme, the BS uses an established CT interference margin to share RBs with multiple D2D pairs. The CT's interference margin on any given RB is similar to that provided by the FST power control strategy. The scheme uses a Stackelberg game approach where the BS, as a leader, first measures the CT's interference margin and sets different interference prices for each D2D pair wishing to share the CT's RB. The goal of the BS in setting different prices is to maximize its revenue charged from the D2D pairs within its interference margin. The BS charges each D2D pair a price corresponding to its caused intereference at the BS. The D2D pairs, as followers, then distributively and competitively adapt their individual transmit powers to maximize their throughput according to prices provided by the BS. Through this game, some D2D pairs decide not to transmit on a given RB (i.e. D2D pairs are not assigned to share that RB) while others adopt transmit powers that maximize their individual throughputs (i.e. D2D pairs are assigned to share that RB). After the DPS scheme's assignment of D2D pairs to share the CTs' RBs, the FST transmit power allocation strategy (as used by MU-O and MU-R algorithms) is applied so as to compare the effectiveness of D2D pairs selection by all three algorithms.

5.3.1 Total Cell Spectral Efficiency

Figure 5.4 shows simulation results of the single-cell spectral efficiency performance for MU-O, MU-R and DPS algorithms. Figure 5.4(a) presents the average performance, over all simulation runs, of the total cell spectral efficiency with increasing number of assigned D2D pairs for all algorithms. Comparing the average cell spectral efficiency, η_{cell} of all schemes, similar performance is observed with low number of assigned D2D pairs. However, significant performance differences especially with the DPS scheme are seen as the number of assigned D2D pairs increases. These performance differences arise from the increased mutual interferences among the many users sharing RBs. In particular, the competitiveness in D2D pairs selection by the DPS scheme ignores the mutual interference between them while sharing RBs. This results in higher mutual interference, between selected D2D pairs, for this scheme and subsequently in its magnified poor performance.

Additionally, the MU-O algorithm is also observed to perform marginally better than MU-R for a given number of assigned D2D pairs. This is attributed to selection of the least interfering (i.e. farthest) D2D pairs to share RBs resulting in lower mutual interference among assigned D2D pairs and hence better η_{cell} performance. Comparing this average cell spectral efficiency preformance with that of a single shared RB in

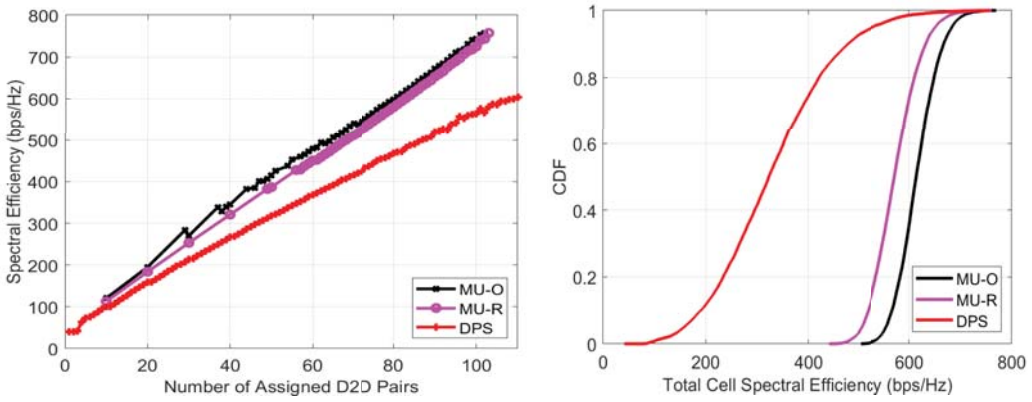

(a) Spectral efficiency versus number of assigned D2D pairs (b) Total cell spectral efficiency CDF

FIGURE 5.4: Single-cell spectral efficiency performance.

section 4.5.3 clearly demonstrates that the achieved cell spectral efficiency is linearly proportional to the number of shared RBs. The higher cell spectral efficiency performance arises from the increased number of assigned D2D pairs sharing the RBs.

Figure 5.4(b) shows the total cell spectral efficiency CDF across all simulation runs where the MU-O and MU-R algorithms perform in a closely similar manner, ranging from 500 - 750 bps/Hz with an average of approximately 615 and 575 bps/Hz respectively. However, for similar reasons discussed above, MU-O posts better results than MU-R. The DPS scheme's cell spectral efficiency performance (averaging about 320 bps/Hz) is distinctively the least owing to it's higher mutual interference among selected D2D pairs sharing RBs and low D2D pair assignment capability (discussed in section 5.3.2 below).

The results in figure 5.4 show that increasing the number of candidate CTs whose RBs are shared creates a multiplexing gain in the achieved average spectral efficiency performance. In particular, for every CT's RB shared by multiple D2D pairs in the scenario where multiple CTs are available, there is a significant multiplexing gain when compared to the case of only 1 CT available (results in figure 4.11 in section 4.5.3). This multiplexing gain arises from the possibility of D2D pairs within the cell sharing any of the given multiple CTs' RBs as long as the constraints in equation 5.1 are fulfilled. Table 5.2 shows the multiplexing gain of the MU-O and MU-R algorithms over the AOS and PRS algorithms discussed in section 4.5. A ten-fold increase in the number of CTs whose RBs are shared by the D2D pairs within the cell resulted in 23% and 20% gain in the achieved average total cell spectral efficiency for the MU-O and MU-R algorithms, respectively.

TABLE 5.2: Multiplexing gain of MU-O and MU-R algorithms

	1 CT:50 D2D pairs (Section 4.5.3 scenario)		10 CTs:500 D2D pairs (Section 5.3 scenario)		% Gain (per CT's RB)	
Measure	**AOS$_{FST}$**	**PRS$_{FST}$**	**MU-O**	**MU-R**	**MU-O: AOS$_{FST}$**	**MU-R: PRS$_{FST}$**
Average η_{cell} (bps/Hz)	50	48	615	575	23%	20%

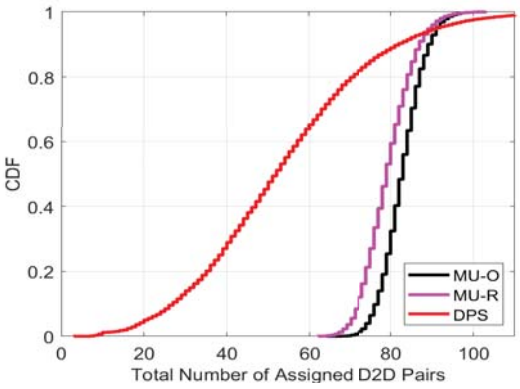

FIGURE 5.5: Number of assigned D2D pairs CDF performance

5.3.2 Number of Assigned D2D Pairs

Figure 5.5 presents the CDF comparisons of number of assigned D2D pairs for all the algorithms across all simulation runs. The MU-O and MU-R algorithms are observed to have nearly similar number of assigned D2D pairs, ranging from 60 to 100 and averaging around 80 D2D pairs. The DPS scheme has the least number of assigned D2D users with a wider range (5 to 110) and averaging about 50 D2D pairs sharing the scheduled RBs in the cell. The DPS scheme's small number of assigned D2D pairs is attributed to the higher mutual interference between the selected D2D pairs. With such strong mutual interference, only a smaller number of D2D pairs can be selected to avoid the deterioration of the total cell spectral efficiency.

5.3.3 CTs and D2D Pairs' SINR

Figure 5.6 shows the CDF comparison of the achieved CTs' and DTs' SINRs for all algorithms across all simulation runs. The CTs' SINR is presented in figure 5.6(a) where the MU-O algorithm gives the best results with the least outage probability and highest

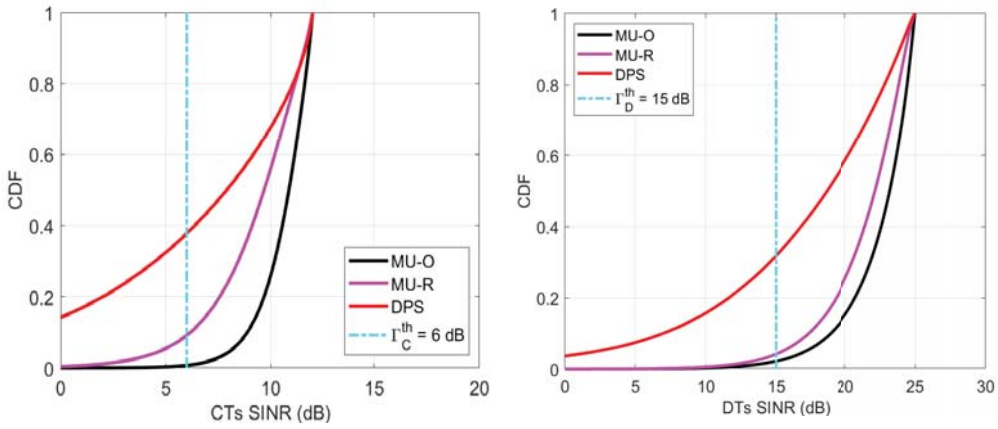

(a) CTs SINR performance

(b) DTs SINR performance

FIGURE 5.6: Users' SINR performance.

achieved SINRs. This is mainly due to two reasons: 1) slightly higher CTs transmit power allocations creating an interference margin during RBs sharing and 2) the algorithms ability to ensure selected D2D pairs sharing RBs are the farthest from the BS hence causing the least interference.

The worst CTs outage probabiliy is observed with the DPS scheme, which is about 40%, despite the fact that this scheme prioritized the CTs' communication with an interference margin constraint at the BS. This poor performance is attributed to the use of FST transmit power allocation strategy to compare the effectiveness of D2D pairs selection. The assigned D2D pairs thus cause higher interference to the CTs, exceeding their interference margins. This transmit power allocation strategy is different from that of the original DPS scheme, which ensures that the CTs achieve their threshold SINRs.

Figure 5.6(b) shows the DTs SINR performance for the assigned D2D pairs in which the MU-O and MU-R algorithms demonstrate superior SINR results. Both MU-O and MU-R algorithms have signficantly low D2D pairs outage probability (below 5%) compared with the 30% probability of outage for the DPS scheme. The inferior DPS performance in this regard is due to the fact that mutual interference among assigned D2D pairs is not taken into consideration during the CT's RB sharing.

5.4 Multi-Cell Simulation Results and Discussion

The MU-O and MU-R performance is also evaluated in a multi-cell environment to assess the impact of ICI when D2D pairs share the CTs' RBs. Owing to the low D2D pairs transmit power, only first-tier cell neighbours are considered in the simulations. Therefore, a seven-cells environment (presented in chapter 3) is used with each cell independently running both algorithms to share the CTs' RBs with D2D pairs. Table 5.3 gives the simulation parameters used in this multi-cell performance evaluation together with others given in section 3.3. Similar to the single-cell scenario, the FST power control strategy is employed for all UTs in the simulation runs.

In order to accurately assess the worst case ICI impact onto a given cell of interest, both algorithms are first run in all neighbouring cells to complete the assignment of suitable D2D pairs to the shared RBs. Thereafter, the algorithms are applied in the cell of interest and its performance evaluations include ICI from known locations of assigned D2D pairs in all neighbour cells. The simulated MU-O and MU-R performance results for a single-cell (i.e. isolated cell) environment in which the impact of ICI is not considered are also included for a comparative assessment.

Table 5.3: MU-O and MU-R multi-cell simulation parameters

Parameter	**Symbol**	**Default value**
Number of cells		7
Number of CTs per cell	M	10
Number of D2D pairs per cell	N	500
max. D2D pair separation	R_{D2D}	20 m

5.4.1 Total Cell Spectral Efficiency

Figure 5.7 presents cell spectral efficiency results for MU-O and MU-R algorithms in single-cell and multi-cell scenarios. As shown in figure 5.7(a), the average of the total cell spectral efficiency over all simulation runs increases with the number of assigned D2D pairs in both scenarios. However, there are spectral efficiency performance differences between the two scenarios, which become more distinct with higher number of assigned D2D pairs. As expected, better performance is realized for the single-cell scenario compared to the multi-cell scenario. Such performance difference is a direct consequence of ICI from neighbouring cells, which is compounded with increasing intra-cell interference as more D2D pairs share RBs in the multi-cell scenario. In effect, the ICI further deteriorates the individual assigned D2D pairs' spectral efficiencies and hence the poor total cell spectral efficiency performance in the multi-cell scenario.

Interestingly, the MU-R algorithm marginally performs better than MU-O in the multi-cell scenario. However, the reverse spectral efficiency performance for the two algorithms is observed in the single-cell scenario. This is due to the fact that MU-O considers the farthest D2D pairs that are close to the cell edge as the most suitable D2D pairs to share RBs. These D2D pairs are the most affected by ICI especially when there is no coordination among cells during sharing of RBs. This results in lower individual spectral efficiencies for the D2D pairs assigned using the MU-O algorithm.

Figure 5.7(b) shows the total cell spectral efficiency CDF for the two sceanrios across all simulation runs. The total cell spectral efficiency is observed to drop by 25% - 35% for all algorithms in a multi-cell scenario compared with the single-cell scenario. The performance difference between the two algorithms is bigger in the single-cell scenario with MU-O achieving better results. However, the multi-cell scenario exhibits marginal performance differences for both algorithms with MU-R being better than MU-O as explained above.

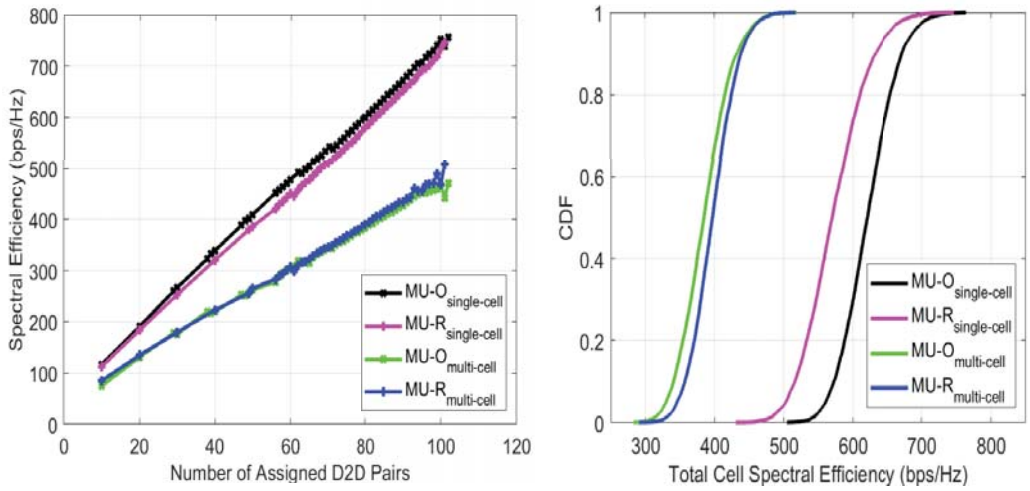

(a) spectral efficiency versus number of assigned D2D pairs (b) Cell spectral efficiency CDF

FIGURE 5.7: Single-cell versus multi-cell spectral efficiency performance.

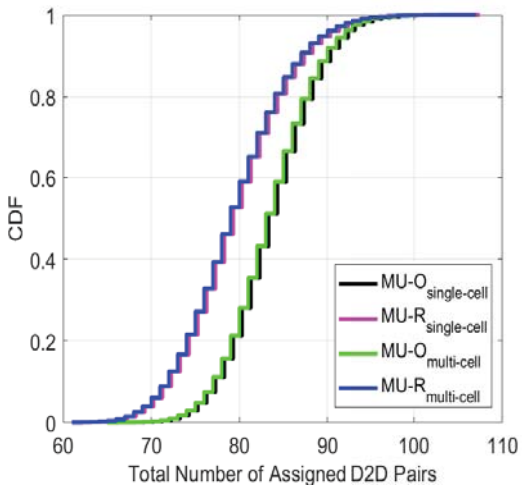

FIGURE 5.8: Number of assigned D2D pairs CDF performance

5.4.2 Number of Assigned D2D Pairs

Figure 5.8 presents the algorithms' CDF comparisons of number of assigned D2D pairs in the two scenarios across all simulation runs. Each algorithm is observed to have similar number of assigned D2D pairs in the two scenarios, where MU-O algorithm assigns higher number of D2D pairs averaging 83 compared with 79 for MU-R algorithm. Despite the similar number of assigned D2D pairs in both single-cell and multi-cell scenarios, ICI deteriorates the individual spectral efficiencies of the assigned D2D pairs in the multi-cell scenario leading to this scenario's poor total cell spectral effficiency performance as explained in section 5.4.1.

5.4.3 CTs and D2D Pairs' SINR

Figure 5.9 compares CDFs for UTs' achieved SINRs while sharing RBs across all simulation runs. Figure 5.9(a) shows that the CTs' SINRs, in both single-cell and multi-cell scenarios, are marginally impacted when MU-O and MU-R algorithms are employed. This observation is due to the low transmit power utilized by D2D pairs and their poor channel gains from neighbouring cells towards a distant BS. The CTs outage probability in this case remains close to zero for MU-O algorithm and approximately 10% for MU-R algorithm.

Figure 5.9(b) presents the assigned D2D pairs' SINR results where increased outage probability (of approximately 0.5) is observed in the multi-cell scenario for the two algorithms. This arises from the ICI experienced by the assigned D2D pairs sharing RBs. MU-O algorithm in the multi-cell scenario displays the worst DTs SINR performance owing to its strategy of selecting cell-edge D2D pairs to share RBs. These cell-edge D2D pairs are the most impacted by ICI during RB sharing.

Despite spectral efficiency gains from MU-O and MU-R algorithms in the realistic multi-cell scenario, their failure to guarantee both CTs and assigned D2D pairs threshold SINRs justifies the need for further enhancements in these algorithms. The goal of these enhancements is to minimize UTs' outage probability (i.e. guarantee UTs' threshold

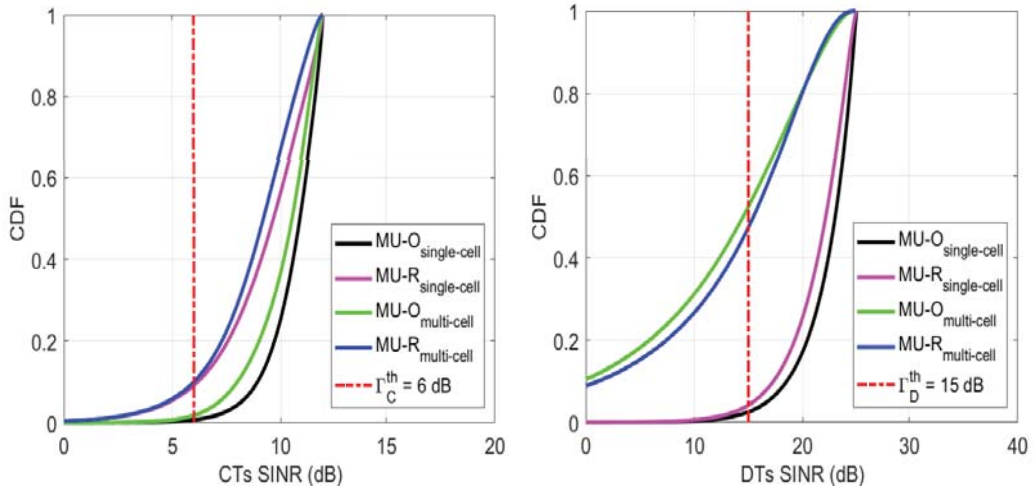

(a) CTs SINR performance (b) DTs SINR performance

FIGURE 5.9: Single-cell vs multi-cell Users' SINR performance.

SINRs) through managing the impact of ICI. The following section proposes some enhancements to improve the algorithms' performance.

5.5 Multi-Cell Resource Assignment Enhancements

The resource assignment algorithms discussed so far employ a distance-based selection criteria. The algorithms' input reuse distance limits for given network/performance parameters depend on $\mathcal{X}_i$ within the cell where RBs are shared. However, as observed in realistic network scenarios comprising of multiple cells, ICI degrades the algorithms' SINR performance. This justifys the need to also consider the number, $\mathcal{X}_i^{neighbours}$ of the assigned neighbouring cells D2D pairs in the selection criteria for D2D pairs sharing similar RBs in a given cell. Such a consideration requires coordination among BSs during resource assignment (e.g. over the X2 interface between eNBs in LTE networks) while simultaneously running the algorithms in the different cells.

5.5.1 Inter-cell D2D Interference Coordination

The coordination between BSs introduces additional signalling overhead and delay in resource assignment to D2D pairs since the number of assigned D2D pairs changes rapidly in different intervals. A proposed approach to mitigate the negative impacts of coordination among BSs is to define a reuse coefficient, β within each cell that accounts for RB sharing in neighbouring cells. Using β, equation 5.3 provides the amended number of D2D pairs, $\mathcal{X}_i^{\beta}$ sharing a given CT's RB. Thereafter, computations of more stringent reuse distance limits then follow. These stringent reuse distance limits imply that the selected D2D pairs sharing given RBs have higher separation from each other. The selected D2D pairs are consequently more resilient to ICI in addition to the intra-cell

interference arising from RB reuse.

$$\mathcal{X}_i^{\beta} = \beta \cdot \mathcal{X}_i \,; \quad (where \;\; \beta \geq 1) \tag{5.3}$$

Setting $\beta = 1$ means that the sharing of RBs within the neighbouring cells is not considered.

Using $\mathcal{X}_i^{\beta}$, the reuse distances defining a given RB's reuse (ILA) regions in the cell are accordingly updated for the FST power control strategy in equation 5.4. These updated reuse distances are used by the selection algorithms to identify appropriate D2D pairs allowed to share the CTs' RBs.

$$R_{D_j}^{reuse} \geq \left(\mathcal{X}_i^{\beta} \frac{1}{\mathcal{I}_{C_i}^{max}} \right)^{\frac{1}{\alpha}} d_{D_{max}} \equiv R_{D_{\mathcal{X}_i^{\beta}}}^{FST}, \tag{5.4a}$$

$$R_{C_iD_j}^{reuse} \geq \left(\mathcal{X}_i^{\beta} \frac{\Gamma_C^{target}}{\Gamma_D^{target}} \frac{1}{\mathcal{I}_{D_j}^{max}} \right)^{\frac{1}{\alpha}} R_{C_i} \equiv R_{C_iD_{\mathcal{X}_i^{\beta}}}^{FST}, \tag{5.4b}$$

$$R_{D2O_{lj}}^{reuse} \geq \left(\mathcal{X}_i^{\beta} \frac{1}{\mathcal{I}_{D_j}^{max}} \right)^{\frac{1}{\alpha}} R_{D2D} \equiv R_{D2O_{\mathcal{X}_i^{\beta}}}^{FST}. \tag{5.4c}$$

Using the conditions in equation 5.4, it is possible that some of the selected D2D pairs in each cell are found very close to the cell edge. Such cell-edge D2D pairs sharing RBs experience the strongest ICI resulting in their poor SINR performance. To circumvent such a situation, it is important that the selection process in all cells maintains the separation, $R_{D2O_{\mathcal{X}_i^{\beta}}}^{FST}$ in equation 5.4c, between selected D2D Pairs across all cell edges. To achieve the $R_{D2O_{\mathcal{X}_i^{\beta}}}^{FST}$ separation between D2D pairs across cell boundaries, R_{D_j} of the selected D2D pairs in their respective cells must satisfy another condition defined in equation 5.5.

$$R_{D_j} < \left(R_{cell} - 0.5 \cdot R_{D2O_{\mathcal{X}_i^{\beta}}}^{FST} \right) \tag{5.5}$$

The above enhancements (equation 5.4) and additional condition (equation 5.5) to the selection criteria serve as inputs to new enhanced algorithms, i.e. enhanced MU-O (eMU-O) and enhanced MU-R (eMU-R), as presented in section 5.5.2.

5.5.2 Enhanced eMU-O and eMU-R Algorithms

The eMU-O and eMU-R algorithms employing the more stringent criteria discussed in section 5.5.1 above are shown in algorithms 5.3 and 5.4, respectively. The main idea of these enhanced algorithms is to incorporate the increased ILA regions (equation 5.4) due to RB reuse in neighbouring cells and also avoid selecting cell-edge D2D pairs (equation 5.5) to minimize the ICI impact on the assigned D2D pairs. The flow of both enhanced algorithms is similar to that described for algorithms 5.1 and 5.2. However, in the eMU-O algorithm, the new criteria are reflected in **lines** 8**,** 11 **and** 13 of the algorithm. Similarly, the changes in the eMU-R algorithm are on **lines** 8**,** 10 **and** 12.

Algorithm 5.3: eMU-O scheme for DTs sharing multiple RBs

Given: a) parameters $\leftarrow \Gamma_D^{target}$, Γ_D^{th}, Γ_C^{target}, Γ_C^{th}, R_{D2D}, R_{cell}, α & β
b) Distribution of 'M' CTs & 'N' D2D pairs within the cell
c) Distance vectors/matrices $\leftarrow R_{C_i}$, R_{D_j}, $R_{C_iD_j}$ & $R_{D2O_{lj}}$ $\left(\forall i \in \mathcal{CT},\ \forall j/l \in \mathcal{DT}\right)$
d) Initialize Y, vectors $\mathcal{F}$ & $\mathcal{X}$ of length $M \leftarrow 0$ & empty sets $\mathcal{S}_i$ $\left(\forall i \in \mathcal{CT}\right)$
Compute initial spectral efficiency vector for all CTs$\leftarrow \eta_{i0}$
while $\mathcal{Y} < N$ **do**
  Initialize η_{cell} and vectors $\mathcal{B}$ of length M & $\mathcal{R}$ of length $N \leftarrow 0$
  for i=1:M **do**
    if $\mathcal{F}_i = 0$ **then**
      $\mathcal{X}_i \leftarrow \mathcal{X}_i + 1$
      Compute reuse distance limits (eq. 5.4) $\leftarrow R^{FST}_{D_{\mathcal{X}_i^\beta}}$, $R^{FST}_{C_iD_{\mathcal{X}_i^\beta}}$, $R^{FST}_{D2O_{\mathcal{X}_i^\beta}}$
      for j=1:N **do**
        if $\mathcal{X}_i = 1$ **then**
          Select best D2D pair, $\mathcal{B}_i \leftarrow max.\left(R_{D_j} + R_{C_iD_j}\right)$ & $R_{D_j} > R^{FST}_{D_{\mathcal{X}_i^\beta}}$ & $R_{C_iD_j} > R^{FST}_{C_iD_{\mathcal{X}_i^\beta}}$ & $R_{D_j} < \left(R_{cell} - 0.5 \cdot R^{FST}_{D2O_{\mathcal{X}_i^\beta}}\right)$
        else
          Select best D2D pair, $\mathcal{B}_i$ $\leftarrow max.\left(R_{D_j} + R_{C_iD_j} + \sum_{l=1,l\neq j}^{\mathcal{X}_i - 1} R_{D_{lj}}\right)$ & $R_{D_j} > R^{FST}_{D_{\mathcal{X}_i^\beta}}$ & $R_{C_iD_j} > R^{FST}_{C_iD_{\mathcal{X}_i^\beta}}$ & $R_{D2O_{lj}} > R^{FST}_{D2O_{\mathcal{X}_i^\beta}}$ & $R_{D_j} < \left(R_{cell} - 0.5 \cdot R^{FST}_{D2O_{\mathcal{X}_i^\beta}}\right)$
        end if
      end for
      When best D2D pair is repeatedly selected by other CTs $\mathcal{R}_j \leftarrow \mathcal{R}_j + 1$
    end if
  end for
  if $R_j > 1$ **then**
    Tie-break: Assign best D2D pair to RB scheduled for CT with highest $R_{C_iD_j}$
  end if
  for i=1:M **do**
    if $\mathcal{B}_i \neq 0$ **then**
      Allocate UTs' transmit power using FST scheme
      Compute UTs' SINRs $\leftarrow \Gamma_{C_i}$, Γ_{D_j}
      Compute new spectral efficiency $\leftarrow \eta_{i\mathcal{X}_i}$
      if $\eta_{i\mathcal{X}_i} > \eta_{i(\mathcal{X}_i - 1)}$ **then**
        Add $\mathcal{B}_i$ to set $\mathcal{S}_i$
        Number of assigned D2D pairs, $\mathcal{Y} \leftarrow \mathcal{Y} + 1$
      else
        Mark i^{th} CT RB as full: $\mathcal{F}_i = 1$
      end if
    end if
    Compute total cell spectral efficiency, $\eta_{cell} \leftarrow \eta_{cell} + \eta_{i\mathcal{X}_i}$
  end for
end while
return Γ_{C_i}, Γ_{D_j}, $\mathcal{Y}$, η_{cell}

Algorithm 5.4: eMU-R scheme for DTs sharing multiple RBs

Given: a) parameters $\leftarrow \Gamma_D^{target}$, Γ_D^{th}, Γ_C^{target}, Γ_C^{th}, R_{D2D}, R_{cell}, α & β
b) Distribution of 'M' CTs & 'N' D2D pairs within the cell
c) Distance vectors/matrices $\leftarrow R_{C_i}$, R_{D_j}, $R_{C_iD_j}$ & $R_{D_{lj}}$ $\left(\forall i \in \mathcal{CT},\ \forall j/l \in \mathcal{DT}\right)$
d) Initialize $\mathcal{Y}$, vectors $\mathcal{F}$ & $\mathcal{X}$ of length $M \leftarrow 0$ & empty sets $\mathcal{S}_i$ $\left(\forall i \in \mathcal{CT}\right)$
Compute initial spectral efficiency vector for all CTs$\leftarrow \eta_{i0}$
for i=1:M **do**
  Initialize η_{cell} and vector $\mathcal{A}$ of length $M \leftarrow 0$
  for j=1:N **do**
    if $\mathcal{F}_i = 0$ **then**
      $\mathcal{X}_i \leftarrow \mathcal{X}_i + 1$
      Compute reuse distance limits (eq. 5.4) $\leftarrow R^{FST}_{D_{\mathcal{X}_i^\beta}}$, $R^{FST}_{C_iD_{\mathcal{X}_i^\beta}}$, $R^{FST}_{D2O_{\mathcal{X}_i^\beta}}$
      if $\mathcal{X}_i = 1$ **then**
        Randomly select any D2D pair, $\mathcal{A}_i$ with $R_{D_j} > R^{FST}_{D_{\mathcal{X}_i^\beta}}$ & $R_{C_iD_j} > R^{FST}_{C_iD_{\mathcal{X}_i^\beta}}$ & $R_{D_j} < \left(R_{cell} - 0.5 \cdot R^{FST}_{D2O_{\mathcal{X}_i^\beta}}\right)$
      else
        Randomly select any D2D pair, $\mathcal{A}_i$ with $R_{D_j} > R^{FST}_{D_{\mathcal{X}_i^\beta}}$ & $R_{C_iD_j} > R^{FST}_{C_iD_{\mathcal{X}_i^\beta}}$ & $R_{D2O_{lj}} > R^{FST}_{D2O_{\mathcal{X}_i^\beta}}$ & $R_{D_j} < \left(R_{cell} - 0.5 \cdot R^{FST}_{D2O_{\mathcal{X}_i^\beta}}\right)$
      end if
      if $\mathcal{A}_i \neq 0$ **then**
        Allocate UTs' transmit power using FST scheme
        Compute UTs' SINRs $\leftarrow \Gamma_{C_i}$, Γ_{D_j}
        Compute new spectral efficiency $\leftarrow \eta_{i\mathcal{X}_i}$
        if $\eta_{i\mathcal{X}_i} > \eta_{i(\mathcal{X}_i-1)}$ **then**
          Add $\mathcal{A}_i$ to set $\mathcal{S}_i$
          Number of assigned D2D pairs, $\mathcal{Y} \leftarrow \mathcal{Y} + 1$
        else
          Mark i^{th} CT RB as full: $\mathcal{F}_i = 1$
        end if
      end if
    end if
    Compute total cell spectral efficiency, $\eta_{cell} \leftarrow \eta_{cell} + \eta_{i\mathcal{X}_i}$
  end for
end for
return Γ_{C_i}, Γ_{D_j}, $\mathcal{Y}$, η_{cell}

5.5.3 Simulation Results and Discussion

Similar to the preceding simulation studies in section 5.4, this study reuses the seven-cells scenario and metrics, i.e., 1) total cell spectral efficiency, 2) total number of assigned D2D users and 3) achieved users SINRs to assess the enhanced algorithms performance. Table 5.4 gives the simulation parameters used for the enhanced algorithms performance evaluation together with others given in section 3.3. In these simulations, a uniform reuse coefficient of 2 (i.e. $\beta = 2$) is applied with the presumption that the extent of RB reuse in all neighbouring cells is viewed as equal to that in a given cell. This uniform β setting may definitely not be the best strategy to optimize spectral efficiency under the users' threshold SINR constraints. A better strategy of using different β settings per RB in each cell would result in improved performance since the various CTs' RBs are expected to experience different interference. However, the determination of the optimal differentiated β settings requires a detailed study of how resource assignments from all cells affect each other. Such a study could not be contained within this thesis' schedule and thus is left for future research.

Table 5.4: eMU-O and eMU-R multi-cell simulation parameters

Parameter	**Symbol**	**Default value**
Number of cells		7
Number of CTs per cell	M	10
Number of D2D pairs per cell	N	500
Reuse coefficient	β	2
max. D2D pair separation	R_{D2D}	20 m

Meanwhile, with the setting of β, each cell independently runs the enhanced algorithms to select appropriate D2D pairs to share the CTs' RBs within that cell. Thereafter, performance of the enhanced algorithms is evaluated on a cell level as described below.

Total Cell Spectral Efficiency

Figure 5.10 presents the cell spectral efficiency simulation results for the eMU-O and eMU-R algorithms in a multi-cell scenario. Figure 5.10(a) shows that both algorithms achieve higher average spectral efficiency with increasing number of assigned D2D pairs. The eMU-O algorithm presents better spectral efficiency performance than eMU-R algorithm. This is because the enhancements that provided for increased spacing between selected D2D pairs especially at the cell edges resulted in control of ICI which negatively impacted MU-O performance more than MU-R. Therefore, the eMU-O algorithm that selects the farthest D2D pairs causing least mutual interference to others sharing resources presented better spectral efficiency than eMU-R.

Figure 5.10(b) shows the CDF of the achieved cell spectral efficiency for both eMU-O and eMU-R across all simulation runs. As observed above, eMU-O algorithm provides a higher spectral efficiency performance compared to eMU-R. On average, eMU-O and eMU-R achieve 240 and 220 bps/Hz cell spectral efficiency respectively. Table 5.5 compares this performance with the multi-cell scenario before algorithm enhancements. Both algorithms show a decrease of 38 - 45% in their cell spectral efficiency. This is attributed to the lower number of selected D2D pairs while using more stringent selection

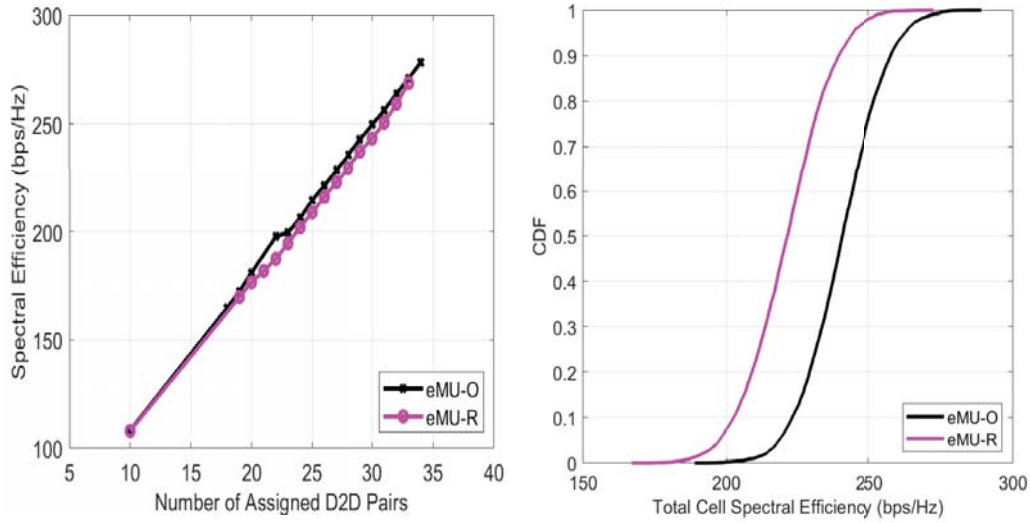

(a) Spectral efficiency versus number of assigned D2D pairs

(b) Cell spectral efficiency CDF

FIGURE 5.10: Multi-cell spectral efficiency performance.

TABLE 5.5: Multi-cell spectral efficiency performance comparison

Algorithm	Average Total Cell Spectral Efficiency (bps/Hz)		% change
	Before Enhancement	**After Enhancement**	
MU-O	390	240	-38
MU-R	400	220	-45

criteria. The more stringent selection criteria in the enhanced algorithms results in higher separation between the selected D2D pairs sharing the CTs' RBs.

Number of Assigned D2D Pairs

Figure 5.11 shows the total number of assigned D2D pairs within a cell using the enhanced algorithms. There is a marginal difference in the number of assigned D2D pairs between the two algorithms with eMU-O having a higher number of assigned D2D pairs, averaging 29, compared to eMU-R that averagely assigned 27 D2D pairs. Table 5.6 compares the number of assigned D2D pairs before and after the algorithms' enhancements. As discussed above, all enhanced algorithms register a decline of approximately 65% in the number of assigned D2D pairs after enhancements due to their increased stringent selection criteria.

TABLE 5.6: Number of assigned D2D pairs performance comparison

Algorithm	Average Number of Assigned D2D Pairs		% change
	Before Enhancement	**After Enhancement**	
MU-O	83	29	-65
MU-R	79	27	-66

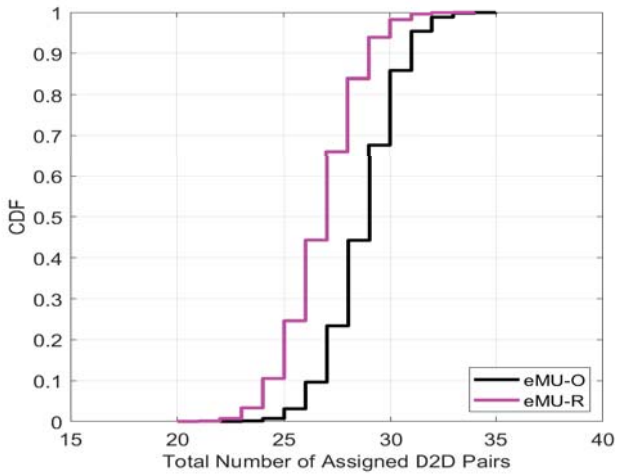

FIGURE 5.11: Total number of assigned D2D pairs performance

CTs and D2D Pairs' SINR Performance

Figure 5.12 presents the UTs SINR performance across all simulation runs during RB reuse within a given cell. The CTs' SINR performance for the enhanced algorithms is shown in figure 5.12(a). Here, it is observed that eMU-O still performs better than eMU-R as was the case before the algorithms' enhancements.

Figure 5.12(b) shows the assigned D2D pairs SINR performance of the enhanced algorithms. Similar to the CTs' SINR performance, eMU-O performs better than eMU-R but with a marginal difference in the outage probability of the assigned D2D pairs. Additionally, table 5.7 shows that the assigned D2D pairs outage probability is significantly improved with both enhanced algorithms when compared to before applying the enhancements. This is attributed to the increased separation between assigned D2D pairs and avoidance of cell-edge pairs in the selection criteria. Therefore, the assigned

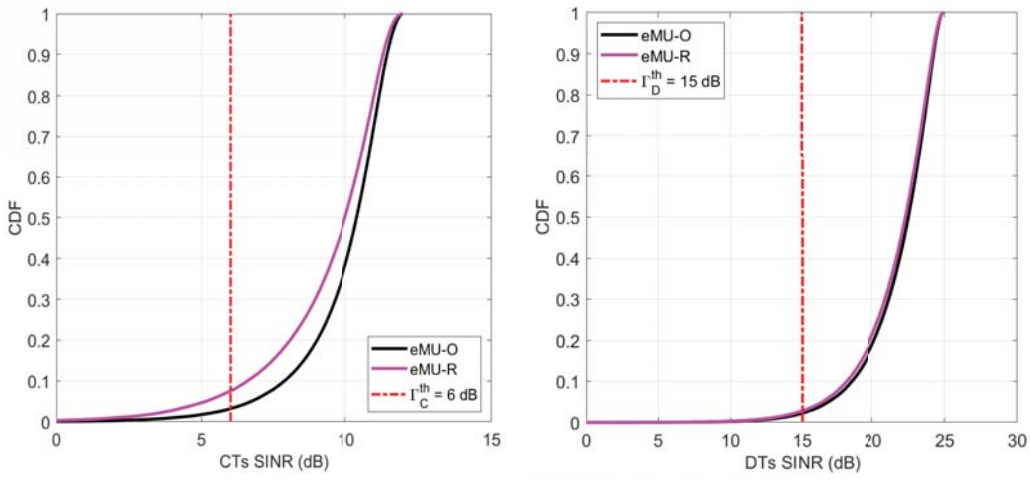

(a) CTs SINR performance (b) DTs SINR performance

FIGURE 5.12: UTs' SINR performance.

Table 5.7: UTs outage probability performance comparison

UTs	Algorithm	UTs Outage Probability (%)		% change
		Before Enhancement	**After Enhancement**	
CTs	MU-O	2	2	0
	MU-R	8	8	0
DTs	MU-O	53	3	-50
	MU-R	48	3	-45

D2D pairs experience less intra-cell interference and ICI enabling them to achieve their threshold SINRs. Table 5.7 shows the UTs outage probability performance before and after the algorithms' enhancements. The applied enhancements had no impact on the CTs' outage probability.

The result shows a clear trade-off between increasing cell spectral efficiency through assignment of more D2D pairs and minimizing the assigned D2D pairs outage probability (i.e. ensuring that they achieve their threshold SINRs) in a multi-cell scenario. The MU-O and MU-R algorithms achieved better spectral efficiency performance than eMU-O and eMU-R at the expense of higher outage probability (poor SINR performance) for the assigned D2D pairs. On the oher hand, eMU-O and eMU-R minimized the outage probability for the assigned D2D pairs at the expense of lower cell spectral efficiency.

5.6 Summary

This chapter investigated the multiple RBs assignment problem by developing algorithms that identify several suitable D2D pairs allowed to share RBs scheduled for any number of CTs within a cell. Considering the different RBs, it was observed that depending on the CT to which they are scheduled, the RBs' capabilities of being shared with several D2D pairs also varied. The developed algorithms demonstrated improvements in network performance when applied to an isolated cell. Specifically, it was observed that:

1. the cell spectral efficiency increased significantly owing to the multiplexing gain availed by more sharing opportunities presented to the D2D pairs through the more CTs resources to be shared in the network. The selection process was terminated whenever the given RB's interference margin was reached.

2. several D2D pairs were allowed to share a given CT's RB. This alleviated the capacity demands of massive device numbers that require services in a fully loaded cellular network.

3. most UTs (i.e. CTs and DTs) sharing RBs were able to attain their threshold SINRs with minimal outage probabilities. This provides the required reliability for the applications run by the different communicating users.

The algorithms' performance in realistic network scenarios (i.e. multi-cell environment) indicated deterioration of some objectives, with the UTs' (especially assigned D2D pairs) achieved SINRs being the most negatively impacted. This justified the need for enhancements of the algorithms to ensure that all users sharing RBs met their

performance objectives. The enhancements, that incorporated increased stringency in D2D pairs selection, exhibited better users' SINR performance albeit with reduced number of assigned D2D pairs and cell spectral efficiency. Subsequently, there is a trade-off between maximizing cell spectral efficiency and minimizing UTs' outage probability in the multi-cell environment.

CHAPTER 6

Conclusion and Future Work

Contents

Finally, this chapter attempts to offer readers a concise summary of all the achieved work in this thesis. Section 6.1 starts the chapter with a short overview on the investigated topic, i.e. D2D resource reuse in cellular networks, followed by the major contributions and findings of the completed studies. Lastly, section 6.2 provides an outlook of some new future research engagements (enhancements) that could be explored with this work acting as an initial base. These should serve as food-for-thought in furtherance of the presented ideas to optimize the performance of future cellular networks in the wake of the anticipated massive number of devices.

6.1 Contributions

The thesis has examined the capacity deficit problem of future cellular networks amidst increasing number of devices and their stringent application requirements. This problem necessitates efficient use of the available spectrum through reuse of resources already scheduled for a CT(s) by several other D2D pairs in the cellular network. Thus, the challenge here was to identify appropriate D2D pairs to share a given CT's resources with the objective of maximizing spectral efficiency while concurrently achieving all users (CTs and D2D pairs) threshold SINRs. All the presented ideas have been evaluated using MATLAB simulations of an LTE network. In the first step, a review of the relevant state of the art focusing of D2D resource sharing approaches was included to provide readers with the fundamental background information on the discussed ideas. Thereafter, the following steps focused on development of simulataneous resource(s) reuse mechanisms by several D2D pairs in the cell.

The major contributions and findings in that regard are therefore categorized into four parts and are described in the following subsections.

6.1.1 Supporting Factors and Constraints for D2D Single Resource Reuse

The thesis started with a comprehensive analytical study of uplink resource reuse by multiple D2D pairs. This provided critical insights on key aspects to consider while sharing resources in a cell. The main findings were:

1. Users transmit power: high CT transmit powers facilitate resource reuse through the established interference margin at the BS. However the D2D pairs' transmit power has to be controlled to ensure the interference margin bounds are not exceeded.

2. Users distribution within the cell: CTs closer to the BS present better resource reuse opportunities due to their higher resilience to the caused interference. Additionally, cell-edge D2D pairs are the preferred candidates for resource reuse since they caused less interference at the BS.

3. D2D separation: D2D pairs whose DTs are in close proximity within 10% of the cell radius are observed to enhance the total spectral efficiency. This close proximity provides a good radio channel between DTs while reusing the CT's resources.

6.1.2 Uniform Interference Power (UIP) for D2D Resource Reuse

Based on the above findings, a UIP scheme was proposed to control the transmit power of all D2D pairs sharing the CT's resources. In this scheme, the allocated D2D pairs' transmit power is such that each pair contributes uniform interference at the BS. The results show improved spectral efficiency with multiple D2D pairs sharing the CT's resources and zero outage probability for the CT. However, nearly half of the D2D pairs sharing resources are not able to achieve their threshold SINR. This observation

indicated the need for selection criteria to identify a subset of D2D pairs allowed to share the CT's resources to concurrently maximize the total call spectral efficiency and achieve their threshold SINRs.

6.1.3 Multiple D2D Pairs Selection for Resource Reuse

A spatial resource-reuse scheme was proposed and validated as an applicable framework for selection of appropriate D2D pairs reusing the cellular network's resources. The framework is based on the examination of the CT and D2D pairs' ILAs and ensuring that no ILA overlap occurs during resource sharing. The ILA sizes are formulated in closed-form solutions and depend on network and/or performance parameters, which included: 1) target SNRs and threshold SINRs, 2) maximum/target UTs transmit power and 3) number of D2D pairs sharing a given CT's resources.

Two algorithms to select suitable D2D pairs to share the CT's resources were developed basing on the formulated ILA sizes. With the objective of maximizing the cell spectral efficiency, one algorithm (AOS) selects D2D pairs farthest from other UTs as the most suitable to share resources while the other algorithm (PRS) randomly selects any D2D pairs to share resources as long as they are outside the ILA regions. The algorithms' performance is evaluated using simulations in a single-cell environment. With both algorithms, two known LTE power control strategies (i.e. FST and CL) were employed in the simulations and the following observations were made:

1. Both selection algorithms present their potential in enhancing spectral efficiency while simultaneously achieving the CT and selected D2D pairs threshold SINRs.

2. There are marginal spectral efficiency performance differences between the two algorithms while employing a specific power control strategy. The differences arise from the D2D pairs selection strategies utilized by the algorithms. The AOS algorithm that selects the farthest D2D pairs (i.e. those causing the least interference) to share resources performs better than the PRS algorithm that randomly selects any D2D pairs outside the ILAs.

6.1.4 D2D Resource Reuse in Realistic Network Scenarios

Considering resources scheduled for multiple CTs within the cellular network, it was observed that there are increased options for candidate D2D pairs assignment to such resources. Accordingly, these various assignment options necessitated advanced algorithms to identify which D2D pairs shared given CT's resource(s) for optimal spectral efficiency performance. Initially, the developed algorithms demonstrated up to 23% multiplexing gain of the spectral efficiency results in a single-cell scenario with increased number of assigned D2D pairs. However, subsequent performance evaluation of the algorithms in a realistic multi-cell network environment, showed a reduction in spectral efficency gains and failure by CTs and most assigned D2D pairs to achieve their threshold SINRs. Further algorithms enhancements employing more stringent selection criteria were then implemented to ensure that the CTs' and DTs' threshold SINRs were attained in the multi-cell scenario. The increased stringency in the selection criteria ensured: 1) to reduce the intra-cell interference among the D2D pairs and the CTs by enforcing higher

separation between the selected D2D pairs, 2) to control ICI by enforcing that the selected D2D pairs in any given cell are not close to the cell edges.

6.2 Future Research Ideas

This work presents opportunities for further research engagements on D2D sharing the cellular network's resources. This section presents a future outlook on new research ideas that can be undertaken from this work. Besides research enhancements regarding resource reuse for D2D use cases, other applications for resource reuse are also proposed, which may not be limited to only D2D communication.

6.2.1 Detailed Link Models

In this thesis, the cell spectral efficiency performance has been studied using the Shannon capacity formula. Here, the measured CTs' and D2D pairs' SINRs from the link-level simulations were used to compute the individual users' spectral efficiencies. These then contributed to the cell spectral efficiency. Some users however achieved significantly higher SINRs than their set threshold. A further study, based on extended system-level simulations, can be undertaken that considers use of link adaptation for different users sharing resources. Additionally, user mobility models can also be included in the study to ascertain the appropriateness of the resources assignment alogorithms in scenarios where users are mobile. The expectation is that users with good radio link conditions (i.e. higher SINRs) would have even higher spectral efficiencies while applying less robust modulation and coding schemes. This would complement the results achieved in this work since the presented techniques are generic with respect to resources assignment and thus applicable to system/network-level simulations.

6.2.2 Multi-cell Resource Reuse Challenges

As discussed under simulation results for the enhanced algorithms, mechanisms to determine the appropriate reuse coefficient, β still remain an open problem. The optimal spectral efficiency performance is expected with different β settings for each scheduled resource. Such settings depend on a good prediction of the interference situation from other users (CTs and D2D pairs) sharing a given resource in all neighbouring cells. Further studies will thus be required to initially include β in the objective functions and thereafter design ways of setting β per resource such that spectral efficiency is optimized. However, it should be noted that β should continously be determnined due to the dynamic cellular network environment.

6.2.3 Hybrid with Overlay D2D Resource Allocation

The resource assignment algorithms are able to determine suitable D2D pairs that share the already scheduled cellular resources to optimize spectral efficiency while achieving all UTs' threshold SINRs. The algorithms work in such a way that selection of some given D2D pairs makes others unsuitable to share the resources. The unsuitability of

such D2D pairs to share resources is based on their close proximity to either the BS, CT or other selected D2D pairs. However, this does not mean these unsuitable D2D pairs do not need resources for their respective communication. Accordingly, in order to serve these unassigned D2D pairs, they need orthogonal resources (i.e. overlay D2D resources assignment) such that they pose no interference to the BS. However, this overlay resource assignment is known to be spectrally inefficient. In order to increase the spectral efficiency of such orthogonally assigned resources, reuse of these resources with other unassigned D2D pairs not in close proximity is proposed. Therefore, this creates a need of overlay-underlay hybrid D2D resources assignment schemes and/or algorithms as proposed in [67] so as to serve all users in the network. However, such schemes should employ good optimization techniques to correctly determine the proportion of resources to be reserved for overlay assignment in order to maximize the cell spectral efficiency. The optimization techniques should take into account the load situation in the cellular network's cells.

6.2.4 Resource Reuse for Other Applications

The resource reuse method is not limited to only D2D communication, but can also be applied to several factory automation or traffic management system applications when integrated into the cellular networks.

In factory automation, robots and/or machines exchange process control information directly with each other, e.g. by means of Machine-to-Machine (M2M) communication. These robots/machines typically operate within confined spaces in a factory environment and thus the separation between them is known. The spatial resource reuse may comfortably be applied in such an environment by ensuring that robots/machines sharing the same resources meet the reuse distance requirements. Therefore, such resource assignment to robots/machine would facilitate the integration of factory automation applications into cellular networks.

In a similar manner, traffic management systems e.g. traffic control at crossroads can also benefit from the spatial resource reuse techniques in the cellular network. The predictable separation of vehicles queued up at crossroads may aid the identification of candidate vehicles that can reuse resources during their exchange of traffic control information.

List of Acronyms

5G	Fifth Generation
3GPP	Third Generation Partnership Project
AOS	Adaptive Opportunistic Selection
BAC	Blind Admission Control
BLER	Block Error Rate
BS	Base Station
CDF	Cumulative Distribution Function
CL	Closed Loop power control
CP	Cyclic Prefix
CQI	Channel Quality Indicator
CT	Cellular user Terminal
D2D	Device-to-Device communication
dB	decibel
DFT	Discrete Fourier Transform
DFTS-OFDM	DFT-spread OFDM
DL	Downlink
DM-RS	Demodulation Reference Signals
DPS	Differentiated Pricing Scheme
DT	D2D user Terminal
$\mathbf{DT_{Rx}}$	DT receiver
$\mathbf{DT_{Tx}}$	DT transmitter
EPC	Evolved Packet Core
eNB	evolved NodeB
E-UTRA	Evolved Universal Terrestrial Radio Access
eMBB	enhanced Mobile BroadBand
FDD	Frequency Division Duplex

FFR	Fractional Frequency Reuse
FST	Fixed SNR Target
GAP	Generalized Assignment Problem
GPS	Global Positioning System
ICI	Inter-Cell Interference
ID	Identifier
ICIC	Inter-Cell Interference Coordination
ILA	Interference Limited Area
InH-NLOS	Indoor Hotspot Non Line-Of-Sight
IoT	Internet of Things
ITS	Intelligent Transport Systems
LTE	Long Term Evolution
LTE-A	LTE-Advanced
M2M	Machine-to-Machine
MAC	Media Access Control
MCC	Mission Critical Communication
mIoT	massive Internet of Things
ms	milliseconds
MTC	Machine Type Communication
MU-O	Multi-User Opportunistic
eMU-O	enhanced MU-O
MU-R	Multi-User Random
eMU-R	enhanced MU-R
NFC	Near-Field Communication
OFDM	Orthogonal Frequency Division Multiplexing
OFPC	Open Loop Fractional Power Control
PDF	Probability Density Function
PL	Pathloss
ProSe	Proximity-based Services
PRS	Partial Random Selection
PSO	Particle Swarm Optimization
PSBCH	physical sidelink broadcast channel
PSCCH	physical sidelink control channel
PSDCH	physical sidelink discovery channel
PSSCH	physical sidelink shared channel
QoS	Quality of Service
QoE	Quality of Experience
RB	Resource Blocks
RE	Resource Element
RRM	Radio Resource Management
RSS	Received Signal Strength
SBCCH	sidelink broadcast control channel

SL-BCH sidelink broadcast channel
SC-FDMA Single Carrier Frequency Division Multiple Access
SCI sidelink control information
SINR Signal to Interference plus Noise Ratio
SL-DCH sidelink discovery channel
SLI sidelink identity
SL-SCH sidelink shared channel
SLSS sidelink synchronization signals
SNR Signal to Noise Ratio
STCH sidelink traffic channel
TDD Time Division Duplex
UIP Uniform Interference Power
UL Uplink
UMi-NLOS Urban Micro hexagonal cell Non Line-Of-Sight
URLLC Ultra-Reliable and Low Latency Communications
UT User Terminal
UTs User Terminals
V2V Vehicle-to-Vehicle
V2X Vehicle-to-Everything

Bibliography

[1] International Interconnect Forum for Services over IP (i3 Forum), "Internet of Things Whitepaper (Release 1.0), April 2017." [Online]. Available: www.http://i3forum.org/wp-content/uploads/2017/05/i3forum-IoT-Whitepaper-draft-v1.0.pdf

[2] Ericsson, "Mobility Report, Internet of Things forecast, August 2018." [Online]. Available: www.ericsson.com/en/mobility-report/internet-of-things-forecast

[3] P. Newman, "IoT Report: How Internet of Things Technology is now reaching mainstream companies and consumers," *Business Insider*, July 2018. [Online]. Available: https://www.businessinsider.de/internet-of-things-report?r=US&IR=T

[4] C. MacGillivary and D. Reinsel, "Worldwide Global DataSphere IoT Device and Data Forecast, 2019-2023," *IDC Market Forecast*, May 2019. [Online]. Available: https://www.idc.com/getdoc.jsp?containerId=US45066919

[5] L. Lei, Z. Zhong, C. Lin, and X. Shen, "Operator controlled device-to-device communications in lte-advanced networks," *IEEE Wireless Communications*, vol. 19, no. 3, pp. 96–104, June 2012.

[6] L. Al-Kanj, H. V. Poor, and Z. Dawy, "Optimal cellular offloading via device-to-device communication networks with fairness constraints," *IEEE Transactions on Wireless Communications*, vol. 13, no. 8, pp. 4628–4643, August 2014.

[7] S. Wen, X. Zhu, Y. Lin, Z. Lin, X. Zhang, and D. Yang, "Achievable transmission capacity of relay-assisted device-to-device (d2d) communication underlay cellular networks," in *2013 IEEE 78th Vehicular Technology Conference (VTC Fall)*, September. 2013, pp. 1–5.

[8] G. Piro, A. Orsino, C. Campolo, G. Araniti, G. Boggia, and A. Molinaro, "D2d in lte vehicular networking: System model and upper bound performance," in *2015 7th International Congress on Ultra Modern Telecommunications and Control Systems and Workshops (ICUMT)*, October 2015, pp. 281–286.

[9] K. P. Sharmila, V. Mohan, C. Ramesh, and S. P. Munda, "Proximity services based device-to-device framework design for direct discovery," in *2016 2nd International*

Conference on Advances in Electrical, Electronics, Information, Communication and Bio-Informatics (AEEICB), February 2016, pp. 499–502.

[10] 3rd Generation Partnership Project (3GPP), "TR 21.915 Technical Specification Group Services and System Aspects; Release 15 Description; Summary of Rel-15 Work Items (Release 15)," March 2019.

[11] P. Schulz, A. Wolf, G. Fettweis, A. M. Waswa, D. Mohammad Soleymani, A. Mitschele-Thiel, T. Dudda, M. Dod, M. Rehme, J. Voigt, I. Riedel, T. Wankhede, W. Nitzold, and B. Almeroth, "Network architectures for demanding 5g performance requirements: Tailored toward specific needs of efficiency and flexibility," *IEEE Vehicular Technology Magazine*, vol. 14, no. 2, pp. 33–43, June 2019.

[12] NGMN Alliance, "NGMN 5G White Paper," *Next Generation Mobile Networks, White Paper*, February 2015.

[13] G. Fodor, E. Dahlman, G. Mildh, S. Parkvall, N. Reider, G. Miklós, and Z. Turányi, "Design aspects of network assisted device-to-device communications," *IEEE Communications Magazine*, vol. 50, no. 3, pp. 170–177, March 2012.

[14] 3rd Generation Partnership Project (3GPP), "3GPP TR 36.843: Study on LTE Device to Device Proximity Services; Radio Aspects (Release 12)," March 2014.

[15] ——, "3GPP TS 23.303: Technical Specification Group Services and System Aspects; Proximity-based Services (ProSe); Stage 2 (Release 15)," June 2018.

[16] X. Lin, J. G. Andrews, A. Ghosh, and R. Ratasuk, "An overview of 3gpp device-to-device proximity services," *IEEE Communications Magazine*, vol. 52, no. 4, pp. 40–48, April 2014.

[17] B. Kaufman and B. Aazhang, "Cellular networks with an overlaid device to device network," in *2008 42nd Asilomar Conference on Signals, Systems and Computers*, October 2008, pp. 1537–1541.

[18] A. M. Waswa, D. M. Soleymani, S. Mwanje, J. Mueckenheim, and A. Mitschele-Thiel, "Multiple resource reuse for d2d communication with uniform interference in 5g cellular networks," in *2017 IEEE 28th Annual International Symposium on Personal, Indoor, and Mobile Radio Communications (PIMRC 2017)*, October 2017, pp. 1–7.

[19] A. M. Waswa, S. Mwanje, J. Mueckenheim, and A. Mitschele-Thiel, "Opportunistic and partial random resource reuse for multiple d2d communication in cellular networks," in *2018 10th International Congress on Ultra Modern Telecommunications and Control Systems and Workshops (ICUMT)*, November 2018, pp. 1–7.

[20] ——, "Qos-aware spectrum sharing for d2d communication in cellular networks," in *2020 29th European Conference on Networks and Communications (EuCNC)*, June 2020, pp. 114–119.

[21] J. Liu, Y. Kawamoto, H. Nishiyama, N. Kato, and N. Kadowaki, "Device-to-device communications achieve efficient load balancing in lte-advanced networks," *IEEE Wireless Communications*, vol. 21, no. 2, pp. 57–65, April 2014.

[22] 3rd Generation Partnership Project (3GPP), "3GPP TR 23.703: Technical Specification Group Services and System Aspects; Study on architecture enhancements to supoort Proximity-based Services (ProSe) (Release 12)," February 2014.

[23] P. V. Latha and P. Durgaprasad, "Device to Device Communication in LTE." [Online]. Available: https://www.sasken.com/sites/default/files/Sasken_Whitepaper_Device_to_Device_LTE_Communication.pdf

[24] D. Panaitopol, C. Mouton, B. Lecroart, Y. Lair, and P. Delahaye, "Recent Advances in 3GPP Rel-12 Standardization related to D2D and Public Safety Communications." [Online]. Available: https://pdfs.semanticscholar.org/f179/1396a8d9852fc7667ebf32b9ef0d66f47e2a.pdf

[25] 3rd Generation Partnership Project (3GPP), "3GPP TS 36.300: Technical Specification Group Radio Access Network; Evolved Universal Terresterial Radio Access (E-UTRA) and Evolved Universal Terresterial Radio Access Network (E-UTRAN); Overall description (Release 15)," September 2019.

[26] E. Dahlman, S. Parkvall, and J. Skold, *4G, LTE-Advanced Pro and the Road to 5G*. Academic Press, 2016.

[27] J. Schlienz and A. Roessler, "Device to device communication in lte whitepaper," *ROHDE & SCHWARZ: Munich, Germany*, 2015.

[28] D. Feng, L. Lu, Y. Yuan-Wu, G. Y. Li, S. Li, and G. Feng, "Device-to-device communications in cellular networks," *IEEE Communications Magazine*, vol. 52, no. 4, pp. 49–55, April 2014.

[29] M. Sheybani, M. Mehrjoo, and M. Kazeminia, "Proximity mode selection method in device to device communications," in *2018 8th International Conference on Computer and Knowledge Engineering (ICCKE)*, October 2018, pp. 69–72.

[30] J. Sun, T. Liu, X. Wang, C. Xing, H. Xiao, A. V. Vasilakos, and Z. Zhang, "Optimal mode selection with uplink data rate maximization for d2d-aided underlaying cellular networks," *IEEE Access*, vol. 4, pp. 8844–8856, December 2016.

[31] Y. Xu and S. Wang, "Mode selection for energy efficient content delivery in cellular networks," *IEEE Communications Letters*, vol. 20, no. 4, pp. 728–731, April 2016.

[32] 3rd Generation Partnership Project (3GPP), "3GPP TS 36.213: Technical Specification Group Radio Access Network; Evolved Universal Terresterial Radio Access (E-UTRA); Physical layer procedures (Release 12)," September 2015.

[33] ——, "3GPP TS 36.213: Technical Specification Group Radio Access Network; Evolved Universal Terresterial Radio Access (E-UTRA); Physical layer procedures (Release 14)," March 2018.

[34] Telesystem Innovations, "LTE in a Nutshell: The Physical Layer," *White Paper*, 2010.

[35] H. Bagheri and M. Katz, "A resource allocation mechanism for enhancing spectral efficiency and throughput of multi-link d2d communications," in *IEEE 25th Annual International Symposium on Personal, Indoor, and Mobile Radio Communication (PIMRC)*, September 2014, pp. 1391–1396.

[36] R. Chen and J. Xu, "Particle swarm optimization based power allocation for d2d underlaying cellular networks," in *2017 IEEE 17th International Conference on Communication Technology (ICCT)*, October 2017, pp. 503–507.

[37] Q. Wang, T. Chen, and H. Liu, "Resource allocation for d2d underlay communication systems using pso," in *2017 13th International Conference on Computational Intelligence and Security (CIS)*, December 2017, pp. 202–206.

[38] J. Lianghai, A. Klein, N. Kuruvatti, and H. D. Schotten, "System capacity optimization algorithm for d2d underlay operation," in *2014 IEEE International Conference on Communications Workshops (ICC)*, June 2014, pp. 85–90.

[39] S. Shalmashi, G. Miao, Z. Han, and S. B. Slimane, "Interference constrained device-to-device communications," in *2014 IEEE International Conference on Communications (ICC)*, June 2014, pp. 5245–5250.

[40] B. Kaufman, J. Lilleberg, and B. Aazhang, "Spectrum sharing scheme between cellular users and ad-hoc device-to-device users," *IEEE Transactions on Wireless Communications*, vol. 12, no. 3, pp. 1038–1049, March 2013.

[41] D. Verenzuela and G. Miao, "Scalable d2d communications for frequency reuse greater than 1 in 5g," *IEEE Transactions on Wireless Communications*, vol. 16, no. 6, pp. 3435–3447, June 2017.

[42] N. Rajkumar, M. Lakshmanan, V. N. Mohammed, and M. Palanivelan, "Distance based uplink resource sharing for device-to-device communication," in *2017 4th International Conference on Electronics and Communication Systems (ICECS)*, February 2017, pp. 74–77.

[43] M. H. Bahonar and M. J. Omidi, "Centralized qos-aware resource allocation for d2d communications with multiple d2d pairs in one resource block," in *Electrical Engineering (ICEE), Iranian Conference on*, May 2018, pp. 643–648.

[44] Gil-Mo Kang and Oh-Soon Shin, "Spectrum sharing between cellular uplink and device-to-device communication systems," in *2013 Fifth International Conference on Ubiquitous and Future Networks (ICUFN)*, July 2013, pp. 129–130.

[45] H. Wang and X. Chu, "Distance-constrained resource-sharing criteria for device-to-device communications underlaying cellular networks," *Electronics Letters*, vol. 48, no. 9, pp. 528–530, April 2012.

[46] H. Min, J. Lee, S. Park, and D. Hong, "Capacity enhancement using an interference limited area for device-to-device uplink underlaying cellular networks," *IEEE Transactions on Wireless Communications*, vol. 10, no. 12, pp. 3995–4000, December 2011.

[47] Q. Duong, Y. Shin, and O. Shin, "Resource allocation scheme for device-to-device communications underlaying cellular networks," in *2013 International Conference on Computing, Management and Telecommunications (ComManTel)*, January 2013, pp. 66–69.

[48] B. Akilesh, V. Sathya, A. Ramamurthy, and B. R. Tamma, "A novel scheduling algorithm to maximize the d2d spatial reuse in lte networks," in *2016 IEEE International Conference on Advanced Networks and Telecommunications Systems (ANTS)*, November 2016, pp. 1–6.

[49] S. Shalmashi, G. Miao, and S. Ben Slimane, "Interference management for multiple device-to-device communications underlaying cellular networks," in *2013 IEEE 24th Annual International Symposium on Personal, Indoor, and Mobile Radio Communications (PIMRC)*, September. 2013, pp. 223–227.

[50] P. Bao, G. Yu, and R. Yin, "Novel frequency reusing scheme for interference mitigation in d2d uplink underlaying networks," in *2013 9th International Wireless Communications and Mobile Computing Conference (IWCMC)*, July 2013, pp. 491–496.

[51] D. D. Ningombam and S. Shin, "Radio resource allocation and power control scheme to mitigate interference in device-to-device communications underlaying lte-a uplink cellular networks," in *2017 International Conference on Information and Communication Technology Convergence (ICTC)*, October 2017, pp. 961–963.

[52] C. Lee, S. Oh, and A. Park, "Interference avoidance resource allocation for d2d communication based on graph-coloring," in *2014 International Conference on Information and Communication Technology Convergence (ICTC)*, October 2014, pp. 895–896.

[53] D. Feng, L. Lu, Y. Yuan-Wu, G. Y. Li, G. Feng, and S. Li, "Device-to-device communications underlaying cellular networks," *IEEE Transactions on Communications*, vol. 61, no. 8, pp. 3541–3551, August 2013.

[54] C. Xia, S. Xu, and K. S. Kwak, "Resource allocation for device-to-device communication in lte-a network: A stackelberg game approach," in *2014 IEEE 80th Vehicular Technology Conference (VTC2014-Fall)*, September. 2014, pp. 1–5.

[55] Y. Liu, R. Wang, and Z. Han, "Interference-constrained pricing for d2d networks," *IEEE Transactions on Wireless Communications*, vol. 16, no. 1, pp. 475–486, January 2017.

[56] 3rd Generation Partnership Project (3GPP), "3GPP TS 36.101: Evolved Universal Terrestrial Radio Access (E-UTRA); User Equipment (UE) radio transmission and reception (Release 16)," June 2019.

[57] ——, "3GPP TR 36.814: Evolved Universal Terrestrial Radio Access (E-UTRA); Further advancements for E-UTRA physical layer aspects (Release 9)," December 2016.

[58] ——, "3GPP TS 36.877: LTE Device to Device (D2D) Proximity Services (ProSe); User Equipment (UE) radio transmission and reception (Release 12)," March 2015.

[59] A. F. Molisch and F. Tufvesson, "Propagation channel models for next-generation wireless communications systems," *IEICE Transactions on Communications*, vol. E97.B, no. 10, pp. 2022–2034, October 2014.

[60] A. M. Mathai, *An Introduction to Geometrical Probability: Distributional Aspects with Applications*. CRC Press, 1999, vol. 1.

[61] E. Roth-Mandutz, A. M. Waswa, and A. Mitschele-Thiel, "Capacity optimization for ultra-reliable low-latency communication in 5g — the son perspective," in *2017 13th International Conference on Network and Service Management (CNSM)*, November 2017, pp. 1–8.

[62] G. Fodor, D. D. Penda, M. Belleschi, M. Johansson, and A. Abrardo, "A comparative study of power control approaches for device-to-device communications," in *2013 IEEE International Conference on Communications (ICC)*, June 2013, pp. 6008–6013.

[63] E. Dahlman, S. Parkvall, and S. Johan, *4G LTE/LTE-Advanced for Mobile Broadband*. Academic Press, 2011.

[64] S. Xiong, Y. Yang, and K. Huai, "A new model of generalized assignment problem and its method," in *2017 IEEE 2nd Advanced Information Technology, Electronic and Automation Control Conference (IAEAC)*, March 2017, pp. 2379–2384.

[65] W. Wu, M. Iori, S. Martello, and M. Yagiura, "Algorithms for the min-max regret generalized assignment problem with interval data," in *2014 IEEE International Conference on Industrial Engineering and Engineering Management*, December 2014, pp. 734–738.

[66] D. Pentico, "Assignment problems: A golden anniversary survey," *European Journal of Operational Research*, vol. 176, pp. 774–793, January 2007.

[67] J. Mueckenheim, A. Puschmann, D. Mohammad Soleymani, E. Roth-Mandutz, A. M. Waswa, and A. Mitschele-Thiel, "On D2D-Communication for Resource Efficient Data Transmission of Delay-Critical Services," in *Mobile Communication - Technologies and Applications; 21. ITG-Symposium*, May 2016, pp. 1–7.

Erklärung

Ich versichere, dass ich die vorliegende Arbeit ohne unzulässige Hilfe Dritter und ohne Benutzung anderer als der angegebenen Hilfsmittel angefertigt habe. Die aus anderen Quellen direkt oder indirekt übernommenen Daten und Konzepte sind unter Angabe der Quelle gekennzeichnet.

Weitere Personen waren an der inhaltlich-materiellen Erstellung der vorliegenden Arbeit nicht beteiligt. Insbesondere habe ich hierfür nicht die entgeltliche Hilfe von Vermittlungs- bzw. Beratungsdiensten (Promotionsberater oder anderer Personen) in Anspruch genommen. Niemand hat von mir unmittelbar oder mittelbar geldwerte Leistungen für Arbeiten erhalten, die im Zusammenhang mit dem Inhalt der vorgelegten Dissertation stehen.

Die Arbeit wurde bisher weder im In- noch im Ausland in gleicher oder ähnlicher Form einer Prüfungsbehörde vorgelegt.

Ich bin darauf hingewiesen worden, dass die Unrichtigkeit der vorstehenden Erklärung als Täuschungsversuch bewertet wird und gemäß § 7 Abs. 10 der Promotionsordnung den Abbruch des Promotionsverfahrens zur Folge hat.

Ilmenau, den 28. Februar 2020 Abubaker Matovu Waswa